

Figure 2-346. Finite Element Mesh for the SC-2, Side Impact, 45° Support Structure, Friction 0.2

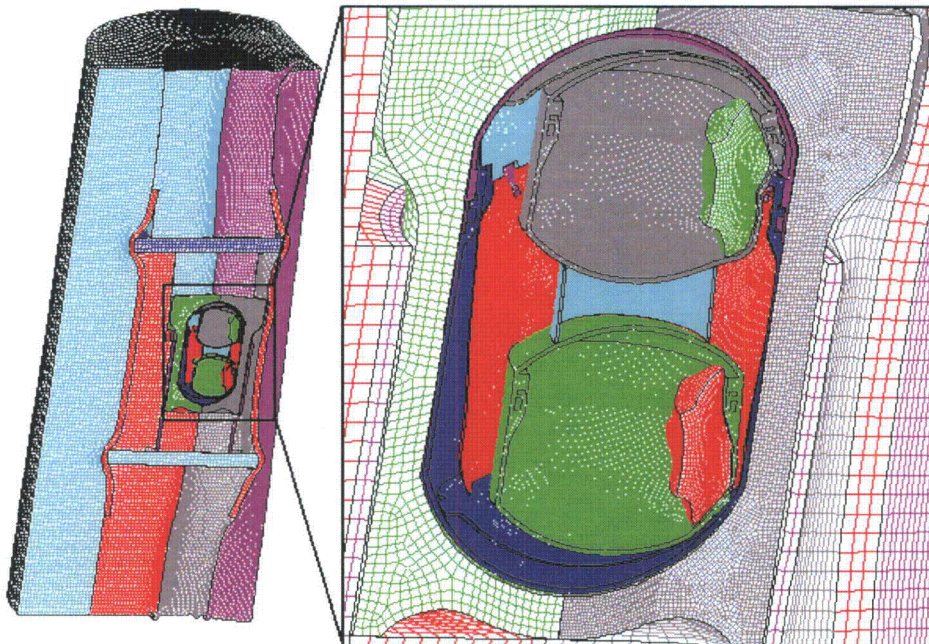


Figure 2-347. Finite Element Mesh for the SC-2, Side Impact, 45° Support Structure, Friction 0.2 – Final Displacement

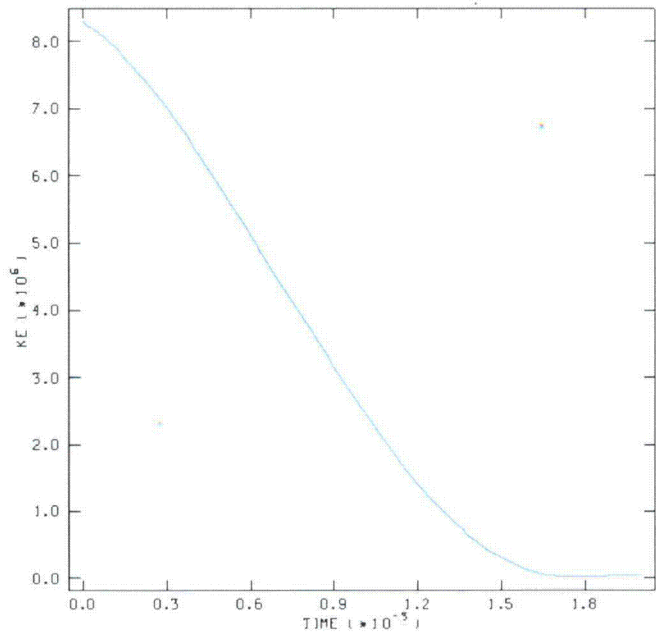


Figure 2-348. Kinetic Energy Time History for the SC-2, Side Impact, 45° Support Structure, Friction 0.2

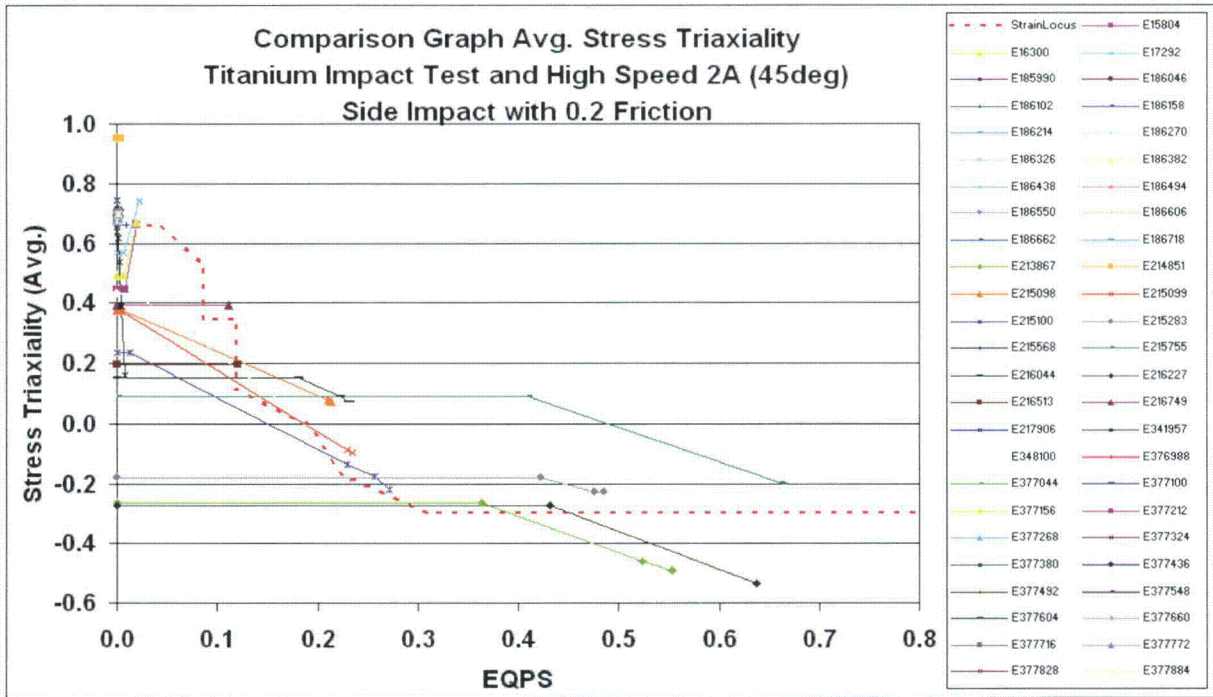
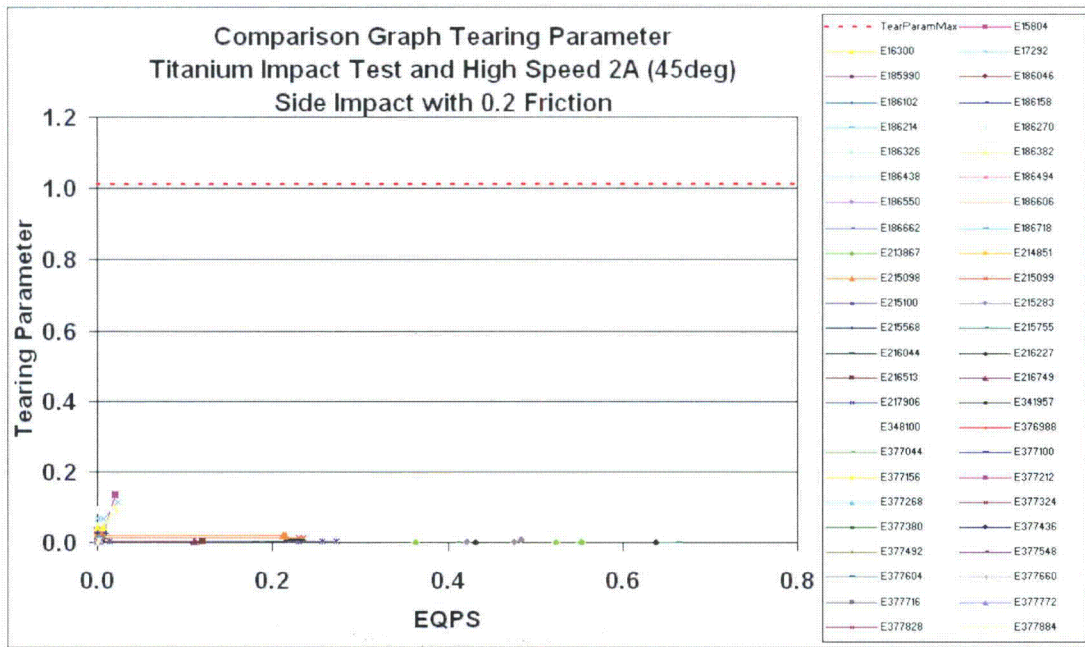
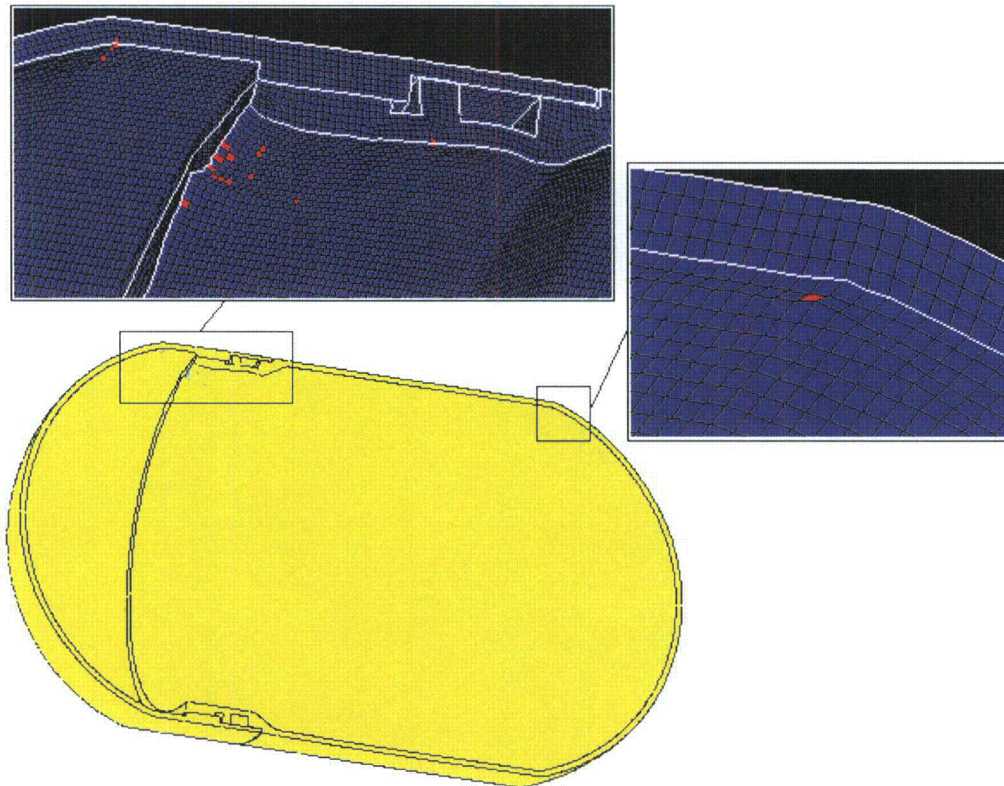


Figure 2-349. Graph of Average Stress Triaxiality versus EQPS of Elements Exceeding the Experimental Strain Locus for the SC-2, Side Impact, 45° Support Structure, Friction 0.2



**Figure 2-350. Graph of Tearing Parameter versus EQPS of Elements Exceeding the Experimental Strain Locus for the SC-2, Side Impact, 45° Support Structure, Friction 0.2**



**Figure 2-351. Plot of Elements Exceeding the Experimental Strain Locus for the SC-2, Side Impact, 45° Support Structure, Friction 0.2**

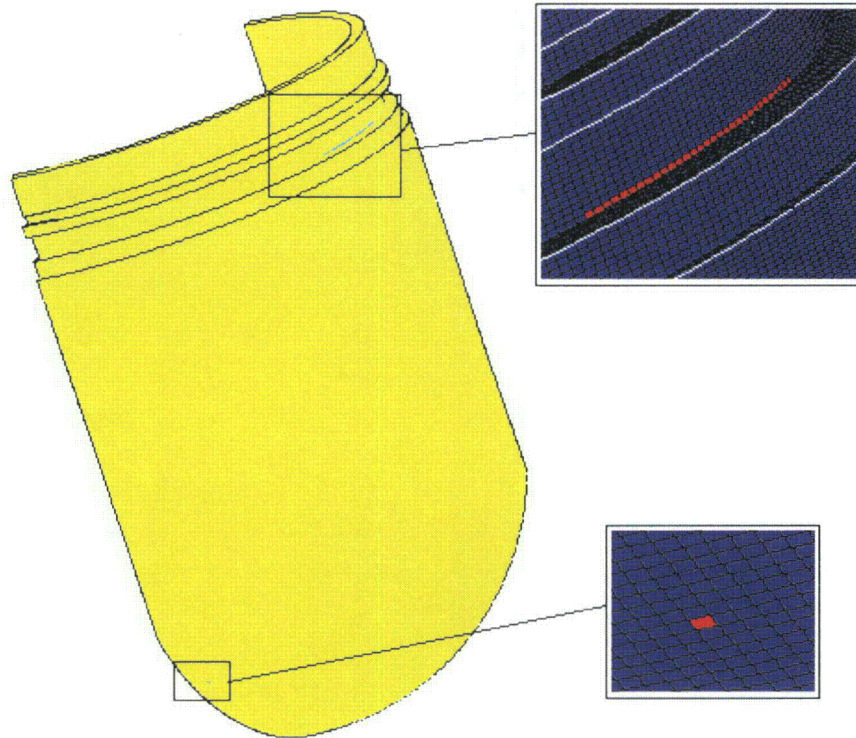


Figure 2-352. Plot of Elements Exceeding the Experimental Strain Locus for the SC-2, Side Impact, 45° Support Structure, Friction 0.2

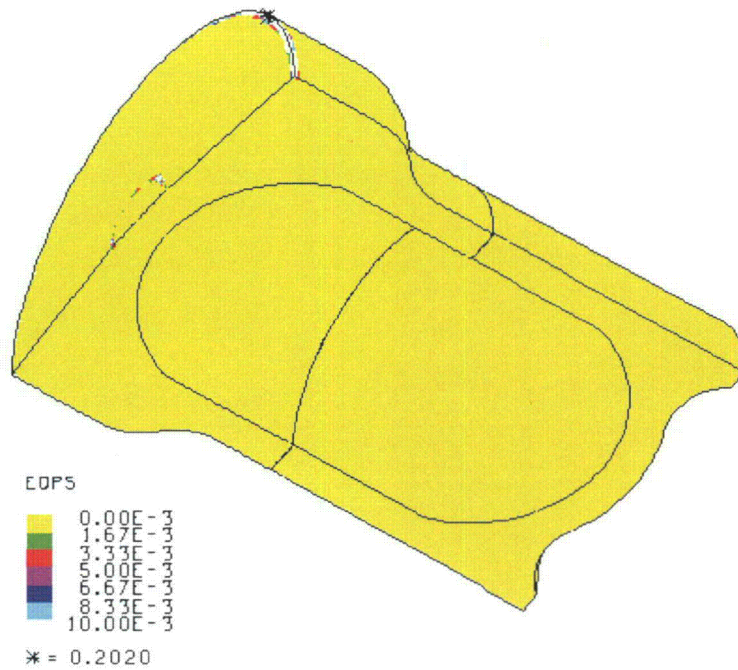


Figure 2-353. Plot of EQPS in the TB-1 for the SC-2, Side Impact, 45° Support Structure, Friction 0.2

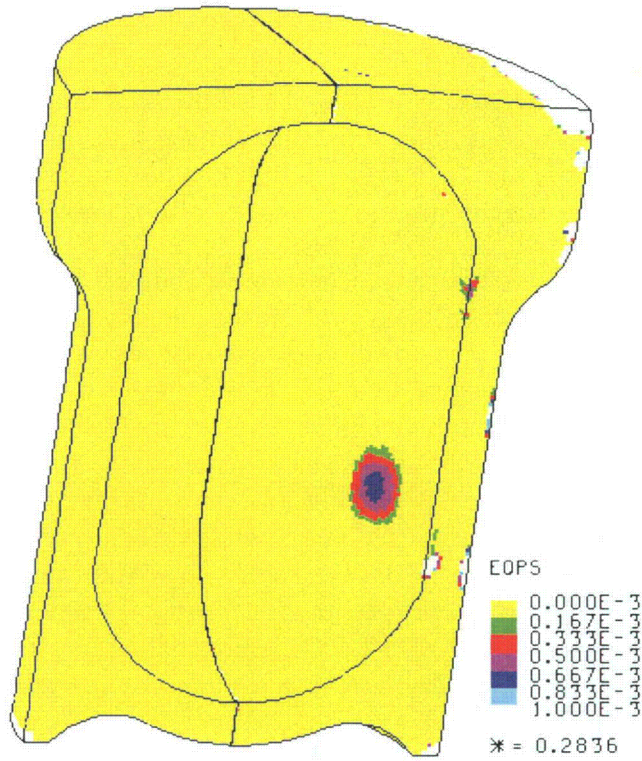


Figure 2-354. Plot of EQPS in the TB-1 for the SC-2, Side Impact, 45° Support Structure, Friction 0.2

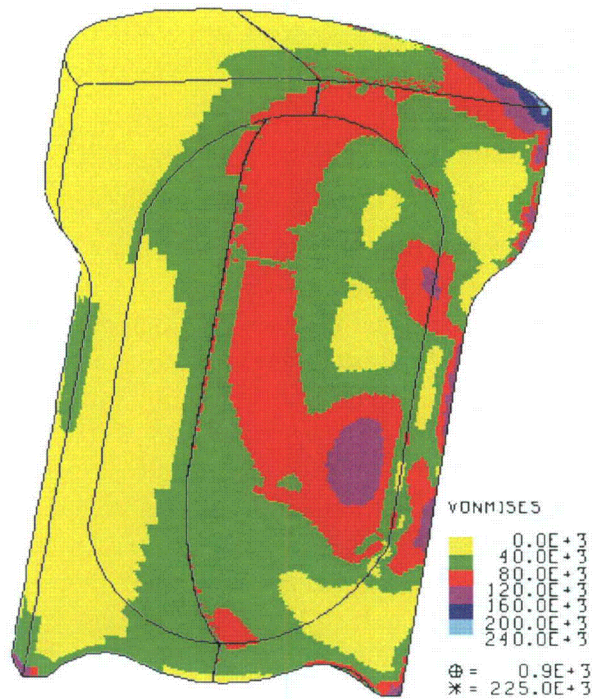


Figure 2-355. Plot of von Mises Stress in the TB-1 for the SC-2, Side Impact, 45° Support Structure, Friction 0.2

#### 2.12.5.5.18 Summary and Conclusion (for High Velocity Impact Analyses)

Although plastic deformation is produced in the T-Ampoule body during the high-speed aircraft accident condition (10 CFR 71.74), using the strain based fracture model developed by Bao and Wierzbicki<sup>5</sup> along with data derived from experimental impact tests, these strains were found not to pose a threat to the integrity of the T-Ampoule body. In addition, stresses in the TB-1 remain virtually elastic and do not threaten the structural integrity of this vessel.

Analyses presented in the high velocity impact section have demonstrated that the PAT-1 package maintains its structural integrity under regulatory 422 ft/sec impacts. Bolt loads, as shown in Figure 2-356 comparing the sum of redwood compression and bolt preload against the under-lid forces from impacting solid metal contents, are minimal and thus lid closure is maintained. Through-thickness stresses in the primary containment vessel, the TB-1, are shown to be below yield values for the S13800 high strength stainless steel material (see Section 2.12.4.9). Only localized minor “denting” occurs in the TB-1, and it would be invisible to the naked eye. And deformations in the T-Ampoule eutectic barrier are shown to be below levels that could initiate a ductile tear, and are largely within the tested locus of stress-triaxiality and plastic strain that precludes failure. Many of the elements with the highest Tearing Parameter values are plotted in stress-triaxiality versus EQPS space in Figure 2-357, demonstrating how close they are to the tested locus, which is not a failure boundary: it is a tested locus of non-failure.

All 27 of the high velocity impact analysis are summarized in Table 2-19, which lists the T-Ampoule contents, overall model and contents orientations, as well as the maximum Tearing Parameter value for all T-Ampoule elements in that particular run or analysis number. The lowest factor of safety against merely *initiating* a ductile tear occurs for a single element in run number 3 with a maximum Tearing Parameter value of 0.6177 (compared to a critical Tearing Parameter value of 1.012 for Ti-6Al-4V, so Factor of Safety =  $1.012/0.6177 = 1.64$ ). This factor of safety pertains to the integrity of the eutectic barrier T-Ampoule, NOT the TB-1 containment boundary, which is has been shown in previous certification tests and the current analyses to fully maintain its integrity (through-thickness stresses below yield), as well.

The numerous additional conservatisms associated with all of these impact analyses should provide additional confidence that containment (and eutectic barrier integrity) would be maintained, even under severe aircraft accident conditions. Additional conservatisms include: neglecting the tantalum foil packing material which would perform some small load spreading and energy absorbing function; neglecting the rolled lid of the outer package skin in aircraft impacts; always assuming the content location and orientation most damaging to the T-Ampoule, e.g., “strongest” plutonium metal hollow cylinder dimensions to resist buckling; most dense, compact, and sharp shape for the delta Pu and Be composite cylinders; delta Pu contents have higher density of alpha Pu; sharpest orientation for the strong Be cylinders, etc. Also, the material properties for these contents are conservatively assumed to have infinite plasticity, when in fact the alpha Pu is very brittle and the Be has rather limited ductility. The Be cylinders were conservatively assumed to have delta Pu density, thus maximizing their impact velocity (due to smaller size). These conservative assumptions maximize the loading and damage potential to the T-Ampoule (as well as TB-1), yet it retains structural integrity as a eutectic barrier.

**Table 2-19. High Velocity (Aircraft) Impact Analyses Peak Tearing Parameter Values**

<b>Run No.</b>	<b>Component</b>	<b>Model Orientation</b>	<b>Maximum Tearing Parameter (T-Ampoule)</b>
1	831 g Plutonium Metal Hollow Cylinder	Bottom position, top impact	0.0528
2	831 g Plutonium Metal Hollow Cylinder	Bottom position (angled), top impact	0.2115
3	831 g Plutonium Metal Hollow Cylinder	Bottom position (angled), CGOC impact	0.6177
4	831 g Plutonium Metal Hollow Cylinder	Far side position, side impact	0.2896
5	831 g Plutonium Metal Hollow Cylinder	Far side position (angled), side impact	0.2389
6	731 g Plutonium Metal Hollow Cylinder	Bottom position, top impact	0.1507
7	731 g Plutonium Metal Hollow Cylinder	Bottom position (angled), top impact	0.2831
8	731 g Plutonium Metal Hollow Cylinder	Bottom position (angled), CGOC impact	0.3967
9	731 g Plutonium Metal Hollow Cylinder	Far side position, side impact	0.4896
10	731 g Plutonium Metal Hollow Cylinder	Far side position (angled), side impact	0.2842
11	SC-1 – Pu	Bottom position, support structure 0°, top impact	0.0319
12	SC-1 – Pu	Far side position, support structure 0°, side impact	0.2417
13	SC-1 – Pu	Far side position, support structure 45°, side impact	0.1958
14	SC-1 – Pu	Bottom position, support structure 0°, CGOC impact	0.0935
15	SC-1 – Pu	Bottom position, support structure 45°, CGOC impact	0.3061

<b>Table 2-19. High Velocity (Aircraft) Impact Analyses Peak Tearing Parameter Values (Continued)</b>			
<b>Run No.</b>	<b>Component</b>	<b>Model Orientation</b>	<b>Maximum Tearing Parameter (T-Ampoule)</b>
16	SC-2 – Pu	Bottom position, support structure 0°, top impact	0.0132
17	SC-2 – Pu	Far side position, support structure 0°, side impact	0.4788
18	SC-2 – Pu	Far side position, support structure 45°, side impact	0.5137
19	SC-2 – Pu	Bottom position, support structure 0°, CGOC impact	0.0953
20	SC-2 – Pu	Bottom position, support structure 45°, CGOC impact	0.0540
21	SC-1 - Be	Bottom position, angled Be, support structure 0°, top impact	0.0155
22	SC-1 – Be	Far side position, angled Be, support structure 0°, side impact	0.2075
23	SC-1 – Be	Far side position, angled Be, support structure 45°, side impact	0.4970
24	SC-1 – Be	Bottom position, angled Be, support structure 0°, CGOC impact	0.0597
25	SC-1 – Be	Bottom position, angled Be, support structure 45°, CGOC impact	0.1197
26	SC-2 – Pu	Far side position, support structure 45°, side impact, friction 0.4	0.4888
27	SC-2 – Pu	Far side position, support structure 45°, side impact, friction 0.2	0.4673

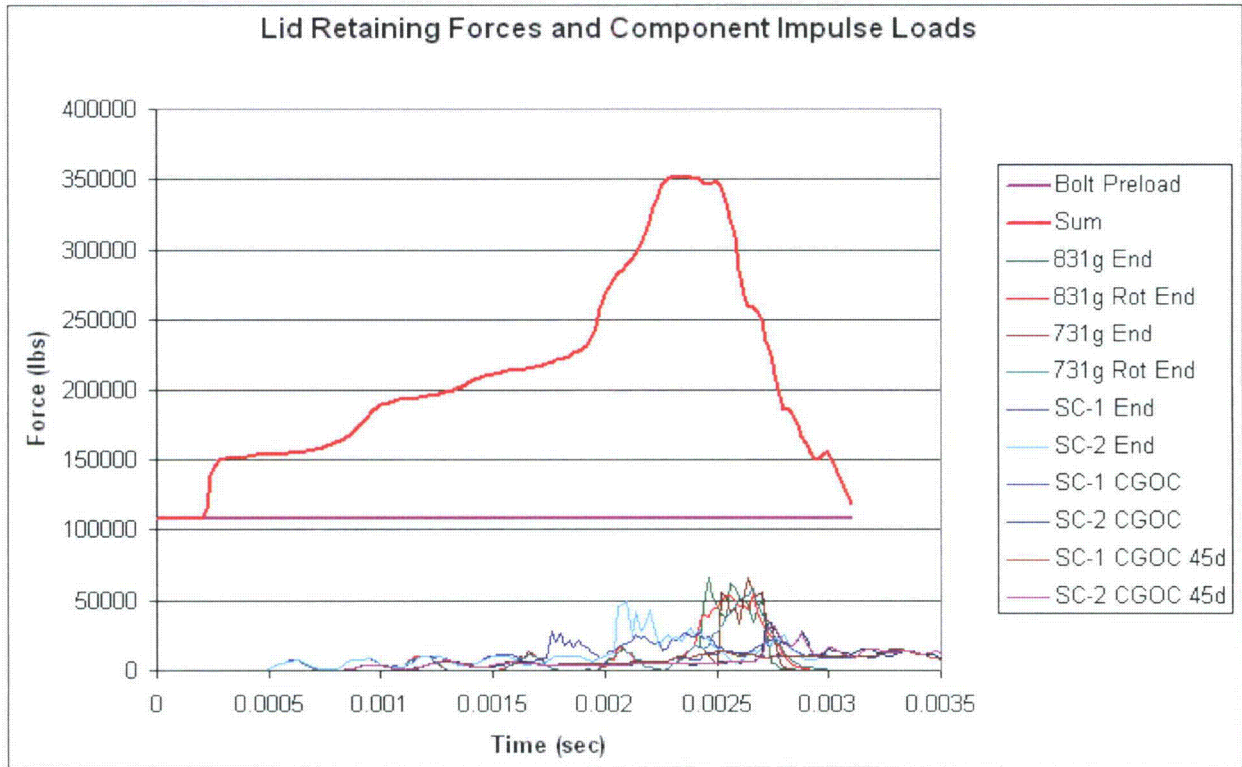


Figure 2-356. Summary Plot of Lid Retaining Forces and Component Impulse Loads

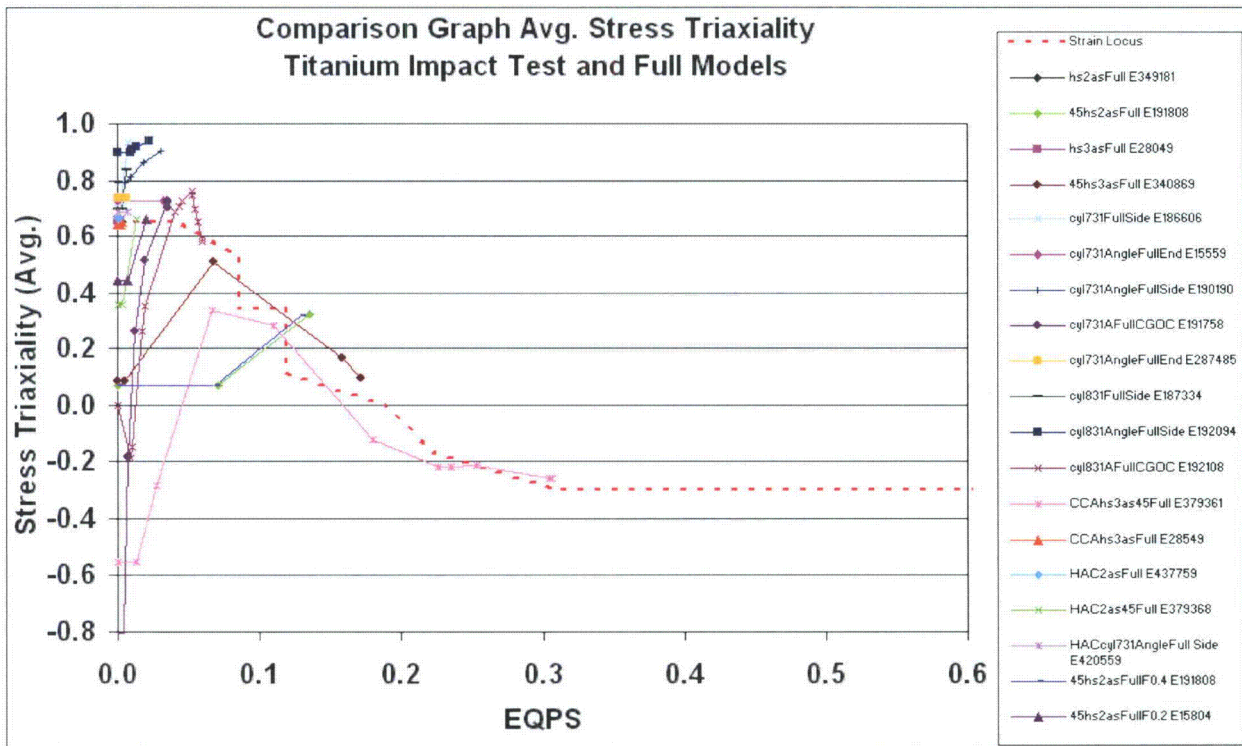


Figure 2-357. Summary Plot of Plastic Stress Triaxiality for Selected Runs

### 2.12.5.6 HAC – Dynamic Crush Analysis Results

In addition to the high-speed aircraft accident analyses, twenty analyses were performed to explore the HAC dynamic crush event described in 10 CFR 71.73. A description of these analyses is provided in Table 2-20. In all of these models, the 1100-lb plate was given an initial velocity of 528 in/s (which corresponds to a 30 ft drop), and was positioned within 0.12 in (3 mm) of the overpack. The overpack and contents had an initial velocity of 0, and gravity was included to ensure proper contact between the contents and the T-Ampoule. The material properties used for each analysis are the same as for the high-speed aircraft impacts and are provided in Section 2.12.4.

The performance of the T-Ampoule for each run was assessed using the same criteria as in the aircraft impact analyses. The maximum Tearing Parameter results for each run are listed in Table 2-20. None of the runs resulted in Tearing Parameters exceeding the maximum allowable Tearing Parameter, termed critical Tearing Parameter ( $TP_{crit} = 1.012$  for Ti-6Al-4V, based on tensile tests to failure). The relatively large 0.44 and 0.22 Tearing Parameter values in run numbers 2 and 3 came from single elements in each analysis associated with a minor localized contact issue, and would otherwise be much smaller or zero (similar to the other analyses listed).

In addition, the stresses in the TB-1 were compared against HAC Reg. Guide 7.6 and ASME B&PV Code stress allowables. None of the runs resulted in through-thickness containment vessel stresses exceeding the ASME limit of 106.6 ksi, shown in Table 2-4. More conservatively, even using the NCT stress intensity limit of 50.8 ksi (see Table 2-4) or 50.0 from Section II, Part D of the ASME Boiler and Pressure Vessel Code for the S13800 material, none of the runs resulted in through-thickness TB-1 stresses exceeding these values in the dynamic crush environment.<sup>8</sup> Nonmandatory Appendix F of the ASME BPVC<sup>9</sup> lists stress intensity limits for inelastic analysis as the greater of  $0.7S_u = 106.6$  ksi or  $S_y + 0.33(S_u - S_y) = 144.8$  ksi for the general primary membrane stress intensity, not to exceed  $0.9S_u = 137.1$  ksi at any location. Conservatively, this limits the peak stress in the dynamic crush events to 137.1 ksi, which is never even approached in any of the HAC analyses, except at the irrelevant regions (due to minor contact modeling artifacts) on some very localized outer surfaces of the TB-1. For example, in Run 3, Section 2.12.5.6.3 for the SC-2 side impact (45-degree rotated) dynamic crush analysis, the through-thickness stress intensity (Tresca stress) is less than 23.5 ksi (Figure 2-382), and the peak stress intensity (excepting the highly localized 226.2 ksi peak due to a contact modeling artifact) was 70.5 ksi where the TB-1 closure diameter necks down to the main body smaller diameter. This 70.5 ksi peak stress intensity is below the Nonmandatory Appendix F peak stress limit of 137.1 ksi.

**Table 2-20. Summary of Hypothetical Accident Condition (HAC) Dynamic Crush Analyses (20), Components, and Orientations**

<b>Run No.</b>	<b>Component</b>	<b>Submodel Orientation</b>	<b>Maximum Tearing Parameter</b>
1	2 SC-2 Sample Containers, delta Pu	Lid end impact	0
2	2 SC-2 Sample Containers, delta Pu	Side impact	0.4464
3	2 SC-2 Sample Containers, delta Pu	Side impact, 45-degree-rotated	0.2288
4	2 SC-2 Sample Containers, delta Pu	CGOC impact	2.78e-3
5	2 SC-2 Sample Containers, delta Pu	CGOC impact, 45-degree-rotated	0
6	3 SC-1 Sample Containers, delta Pu	Lid end impact	0
7	3 SC-1 Sample Containers, delta Pu	Side impact	3.03e-5
8	3 SC-1 Sample Containers, delta Pu	Side impact, 45-degree-rotated	1.6e-2
9	3 SC-1 Sample Containers, delta Pu	CGOC impact	0
10	3 SC-1 Sample Containers, delta Pu	CGOC impact, 45-degree-rotated	0
11	831 g Plutonium Metal Hollow Cylinder, alpha Pu	Lid end impact	0
12	831 g Plutonium Metal Hollow Cylinder, alpha Pu	Side impact	2.94e-6
13	831 g Plutonium Metal Hollow Cylinder, alpha Pu	Lid end impact, angled cylinder	0
14	831 g Plutonium Metal Hollow Cylinder, alpha Pu	Side impact, angled cylinder	2.01e-2
15	831 g Plutonium Metal Hollow Cylinder, alpha Pu	CGOC impact, angled cylinder	0
16	731 g Plutonium Metal Hollow Cylinder, alpha Pu	Lid end impact	0
17	731 g Plutonium Metal Hollow Cylinder, alpha Pu	Side impact	0
18	731 g Plutonium Metal Hollow Cylinder, alpha Pu	Lid end impact, angled cylinder	0
19	731 g Plutonium Metal Hollow Cylinder, alpha Pu	Side impact, angled cylinder	5.09e-2
20	731 g Plutonium Metal Hollow Cylinder, alpha Pu	CGOC impact, angled cylinder	0

#### 2.12.5.6.1 HAC – Run 1, SC-2, End Impact

The dynamic crush end impact HAC analysis for the 2 SC-2 sample container run uses the same model as that used for the 4-ft-drop, but the flange is added to both ends so that it is available to deform where impacted by the plate and the rigid surface upon which it is resting. The finite element mesh and initial position of the model is shown in Figure 2-358. The Pu contents and support structure within the T-Ampoule are positioned at the bottom of the model because it was considered to be at rest.

The post-impact deformation is shown in Figure 2-359 and its kinetic energy history in Figure 2-360. The flanges on the overpack deform, and the contents bounce due to the impact of the plate, but there is no plastic deformation in the T-Ampoule or the TB-1.

Figures 2-361 and 2-362 are plots of the Tresca stresses within the TB-1. The maximum Tresca stress (stress intensity) in the TB-1 is 137.9 ksi due again to a contact modeling artifact), but there are no through thickness stresses exceeding the limit of 106.6 ksi, which can be seen clearly in Figure 2-362. Figure 2-363 is a plot of the Tresca stresses at the time when all of the kinetic energy of the plate has been transferred to the package, just as the plate begins to rebound. The maximum through thickness stress at this time is below 16.7 ksi, below the allowable through thickness stress of 106.6 ksi, as seen in the figure.

As in the high velocity impact analyses, there is a minor modeling artifact occurring due to slight contact over closure between the redwood and the ring of TB-1 top surface elements which is causing this very slight non-realistic localized plasticity.

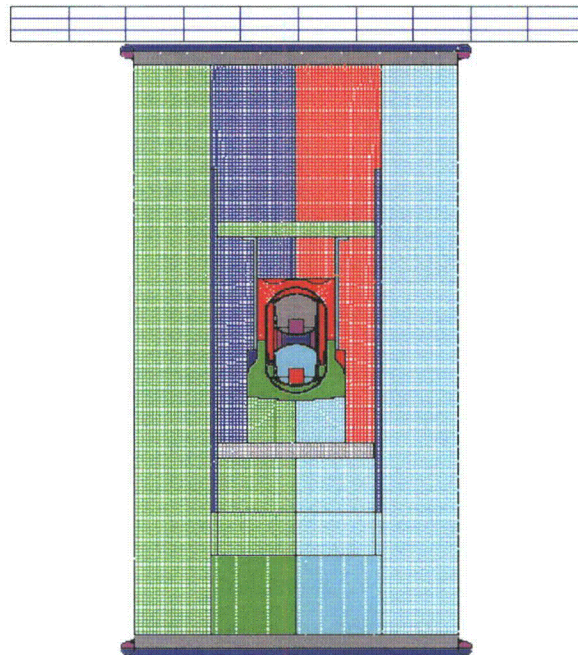


**Figure 2-358. Finite Element Mesh for HAC Run 1, SC-2, End Impact**

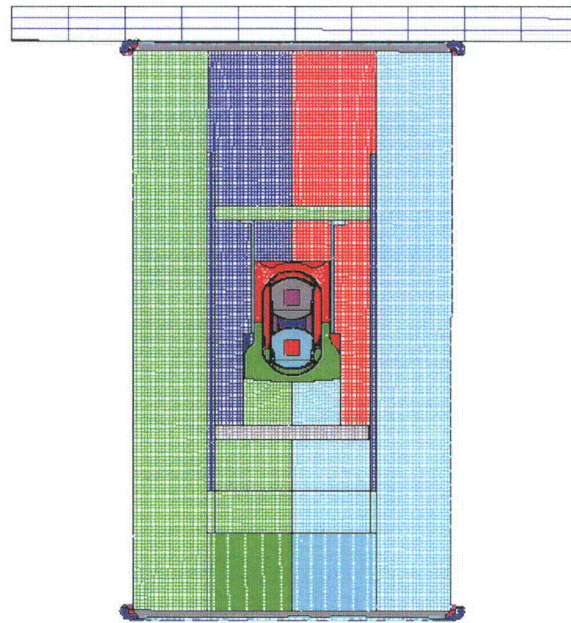


**Figure 2-359. Finite Element Mesh for HAC Run 1, SC-2, End Impact – Final Displacement**

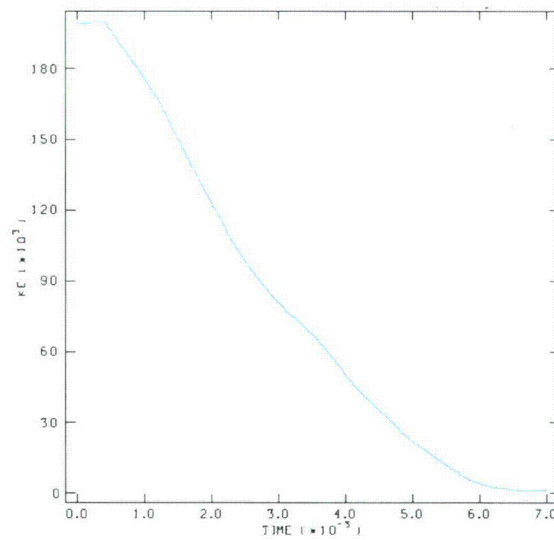


**Figure 2-360. Kinetic Energy Time History for HAC Run 1, SC-2, End Impact**

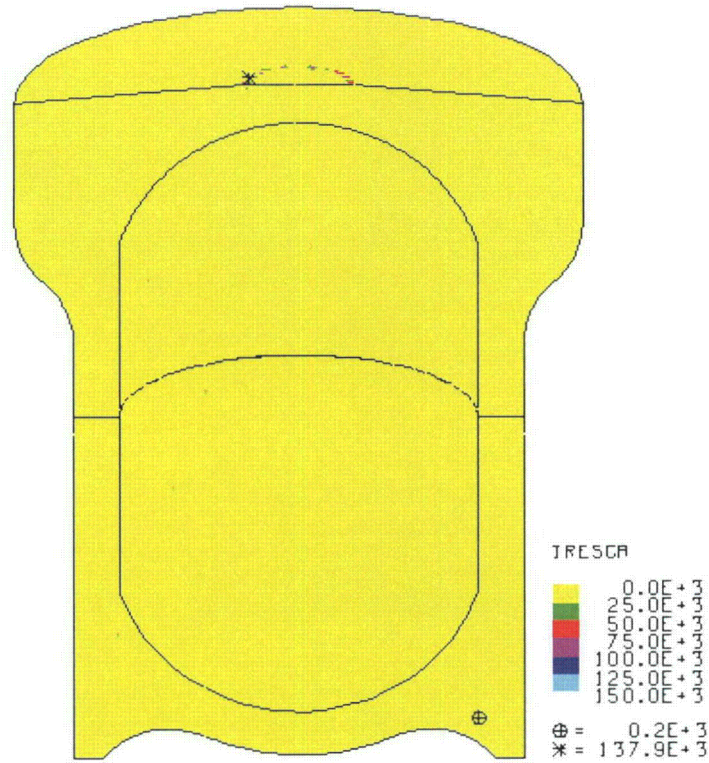


Figure 2-361. Tresca Stress in TB-1 for HAC Run 1, SC-2, End Impact

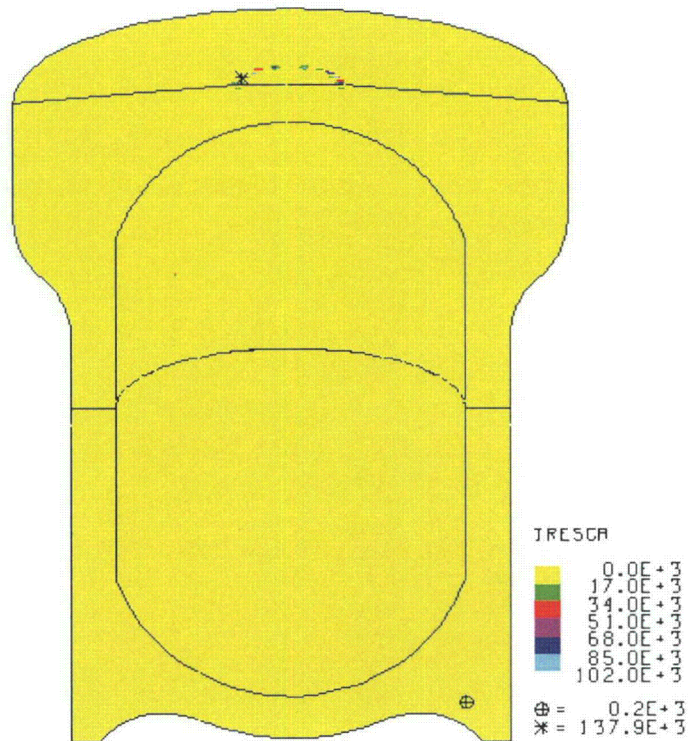
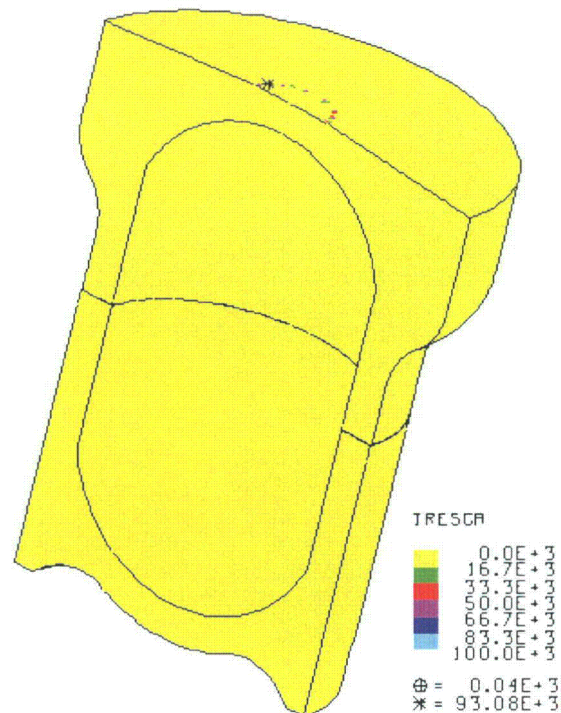


Figure 2-362. Tresca Stress of TB-1 for HAC Run 1, SC-2, End Impact



**Figure 2-363. Tresca Stress of TB-1 for HAC Run 1, SC-2, End Impact when Plate Velocity Reaches Zero**

#### 2.12.5.6.2 HAC- Run 2, SC-2, Side Impact, Support Structure 0°

The dynamic crush end impact HAC analysis for the 2 SC-2 sample container runs uses the same model as that used for the 4-ft-drop, but the flange is added to both ends so that it is available to deform where impacted by the plate and the rigid surface upon which it is resting. The finite element mesh and initial position of the model are shown in Figure 2-364. The Pu contents and support structure within the T-Ampoule are positioned at the bottom of the model because it was considered to be at rest. The plate was positioned between the flanges to be most damaging to the TB-1 and contents by preventing the flanges from absorbing energy and slowing down the plate before it hits the overpack.

The post-impact deformation is shown in Figure 2-365 and its kinetic energy history in Figure 2-366. The flanges on the overpack deform, and the contents bounce due to the impact of the plate. Average stress-triaxiality versus EQPS is shown in Figures 2-367 and 2-368 for the one element extending beyond the tested Bao-Wierzbicki strain locus. This element is at high stress triaxiality and low EQPS. The Tearing Parameter values for this same element are shown in Figure 2-369, and are below the critical Tearing Parameter value of 1.012 for Ti-6Al-4V. This element is highlighted in red Figure 2-370, but note that this element is below the initiation of a ductile tear, thus T-Ampoule integrity is maintained.

Peak EQPS in the TB-1 vessel is shown in Figure 2-371 to be 28.31e-3, and is localized in the outer contact regions with the redwood overpack. Figure 2-372 is a plot of the Tresca stresses within the TB-1. The maximum Tresca stress in the TB-1 is 172.3 ksi, but there are no through thickness stresses exceeding the limit of 106.6 ksi, which can be seen clearly in the figure.

Figure 2-373 is a plot of the Tresca stresses at the time when all of the kinetic energy of the plate has been transferred to the package, just as the plate begins to rebound. The maximum through thickness stress at this time is below 26.7 ksi, below the allowable through thickness stress of 106.6 ksi, as seen in the figure.

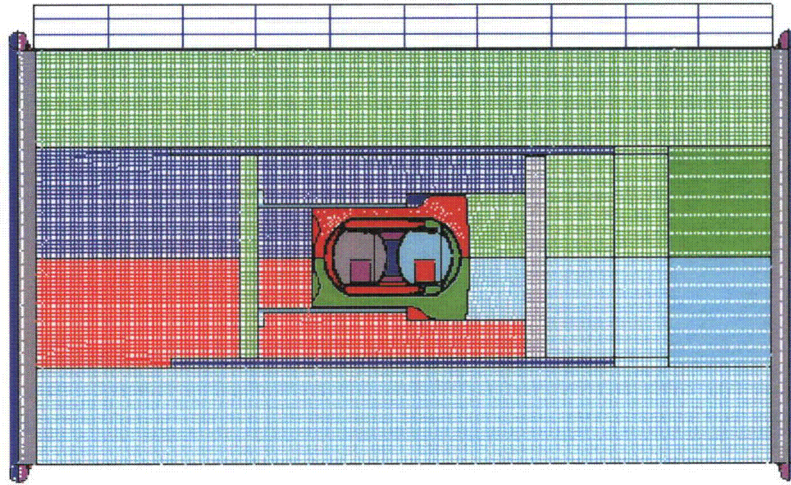


**Figure 2-364. Finite Element Mesh for HAC Run 2, SC-2, Side Impact, Support Structure 0°**

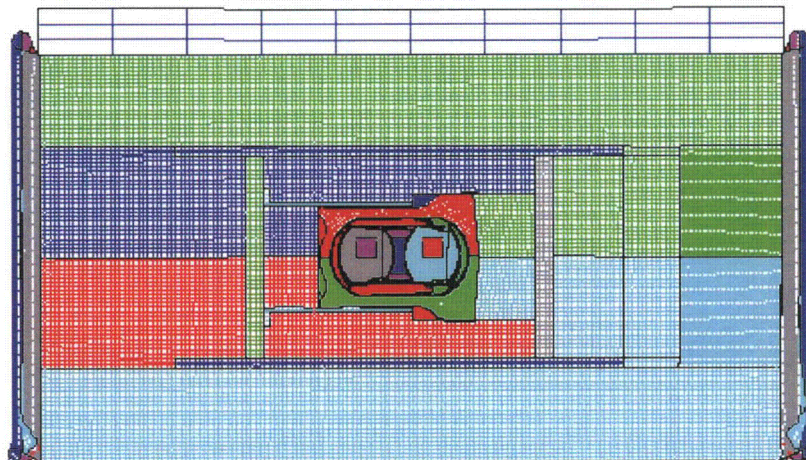


**Figure 2-365. Finite Element Mesh for HAC Run 2, SC-2, Side Impact, Support Structure 0° - Final Displacement**

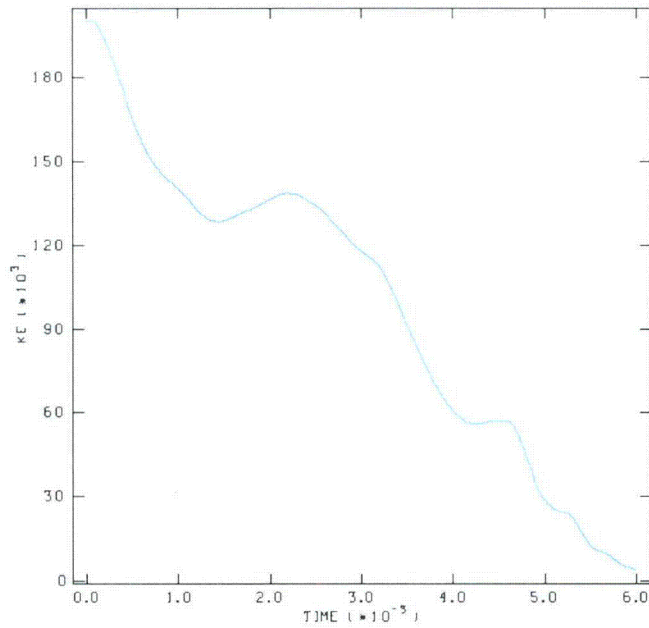


**Figure 2-366. Kinetic Energy Time History for HAC Run 2, SC-2, Side Impact, Support Structure 0°**

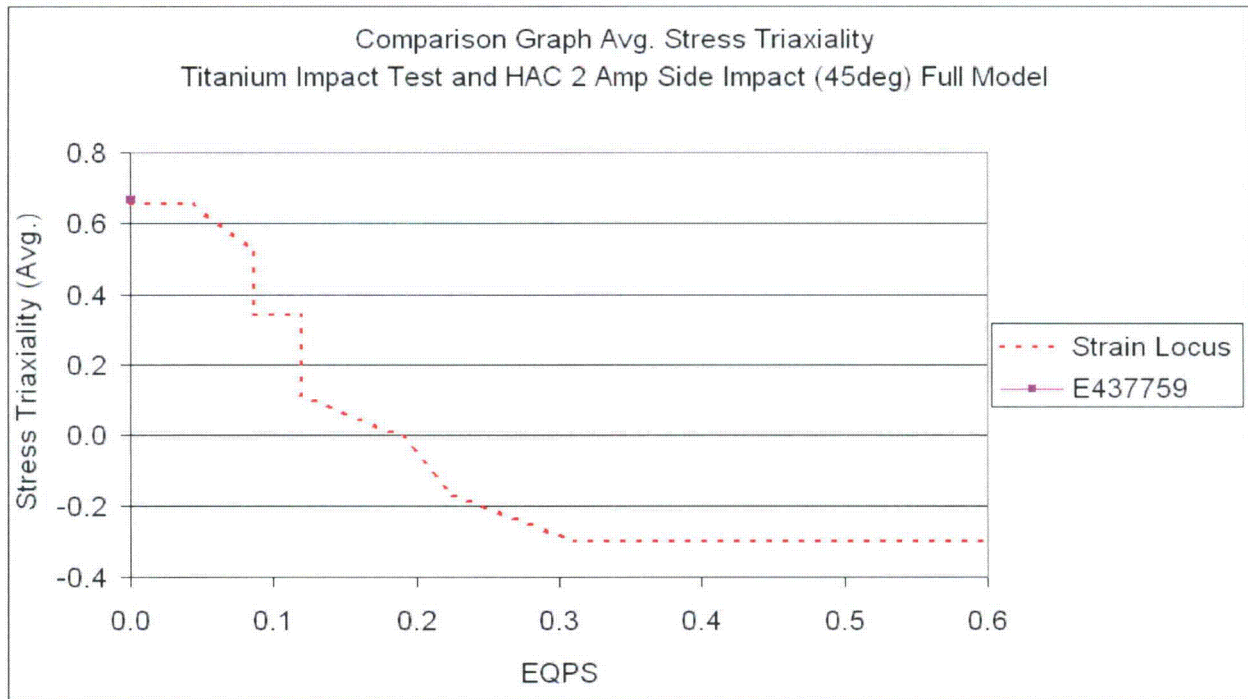


**Figure 2-367. Graph of Average Stress Triaxiality versus EQPS for Element Exceeding Experimental Strain Locus for HAC Run 2, SC-2, Side Impact, Support Structure 0°**

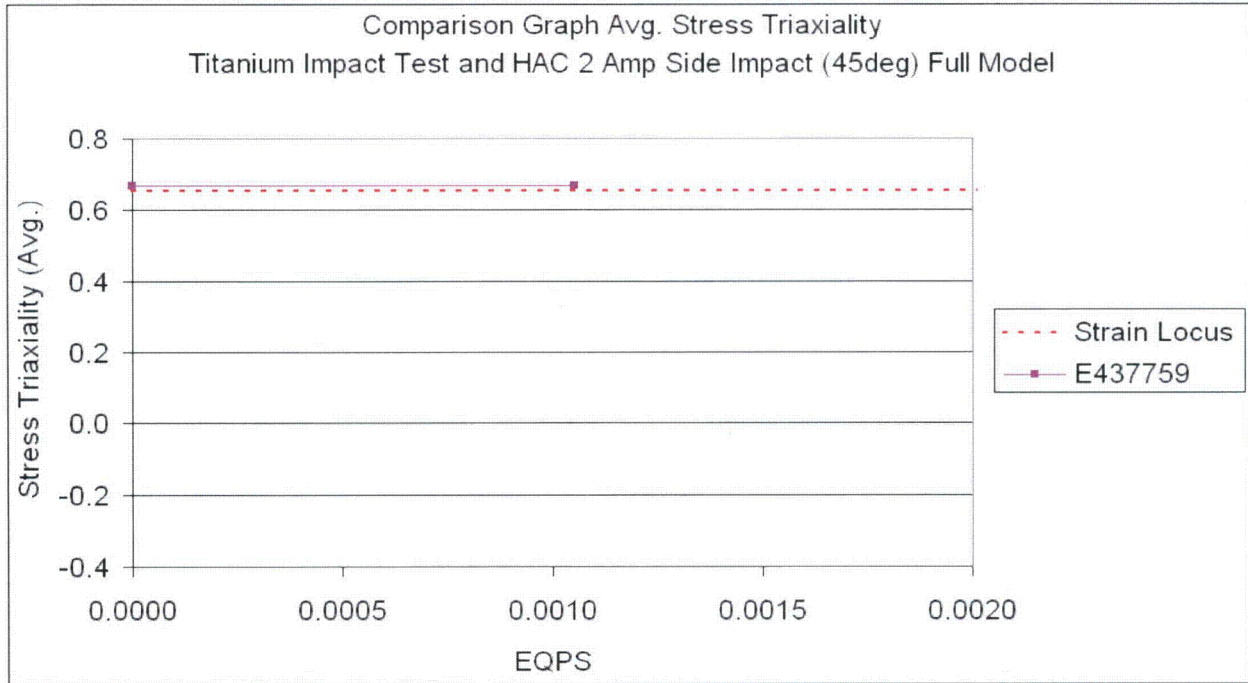


**Figure 2-368. Graph of Average Stress Triaxiality versus EQPS for Element Exceeding Experimental Strain Locus (Zoomed In) for HAC Run 2, SC-2, Side Impact, Support Structure 0°**

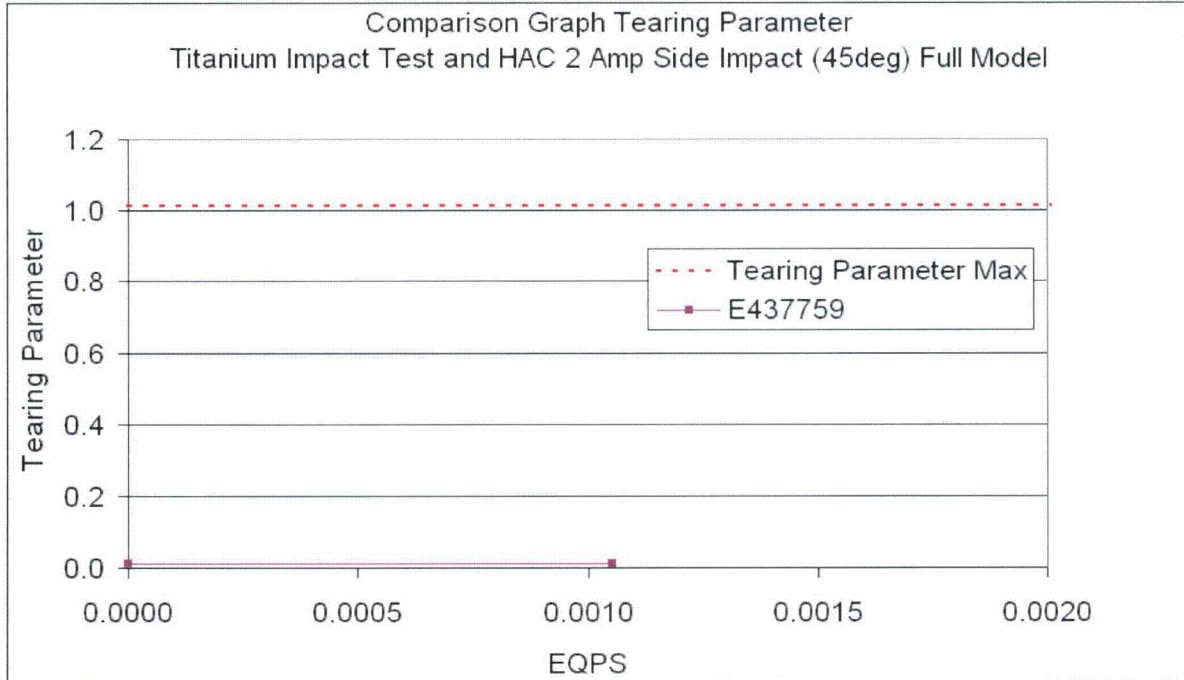


**Figure 2-369. Graph of Tearing Parameter versus EQPS for Element Exceeding Experimental Strain Locus for HAC Run 2, SC-2, Side Impact, Support Structure 0°**

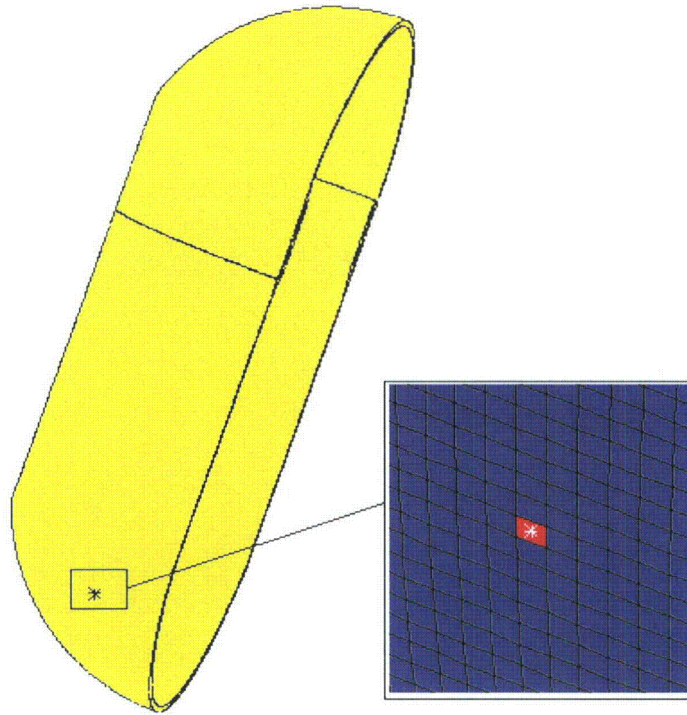


Figure 2-370. Plot of Element Exceeding Experimental Strain Locus for HAC Run 2, SC-2, Side Impact, Support Structure 0°

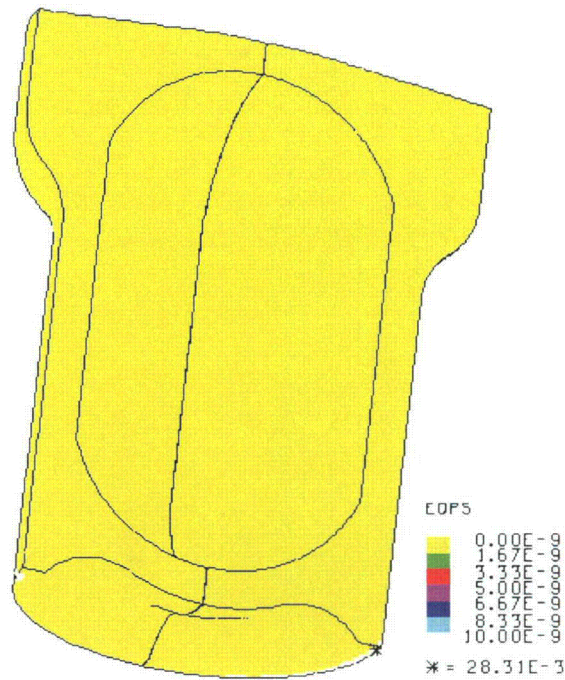


Figure 2-371. Graph of EQPS in the TB-1 for HAC Run 2, SC-2, Side Impact, Support Structure 0°

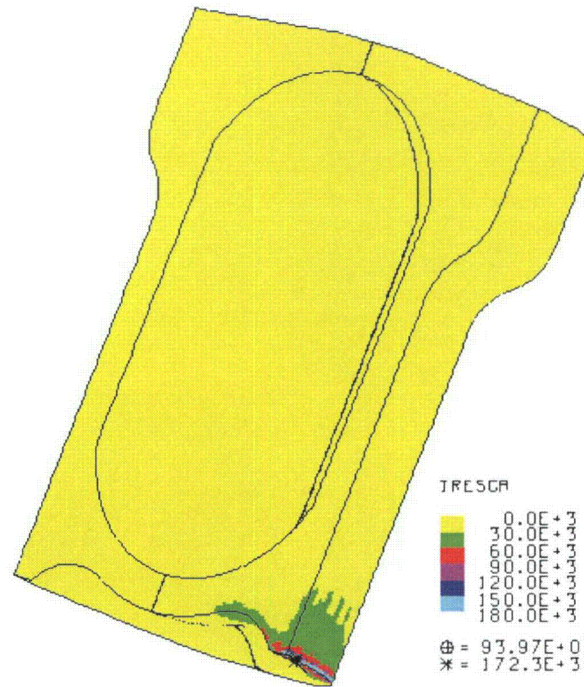


Figure 2-372. Plot of Tresca Stress in the TB-1 for HAC Run 2, SC-2, Side Impact, Support Structure 0°

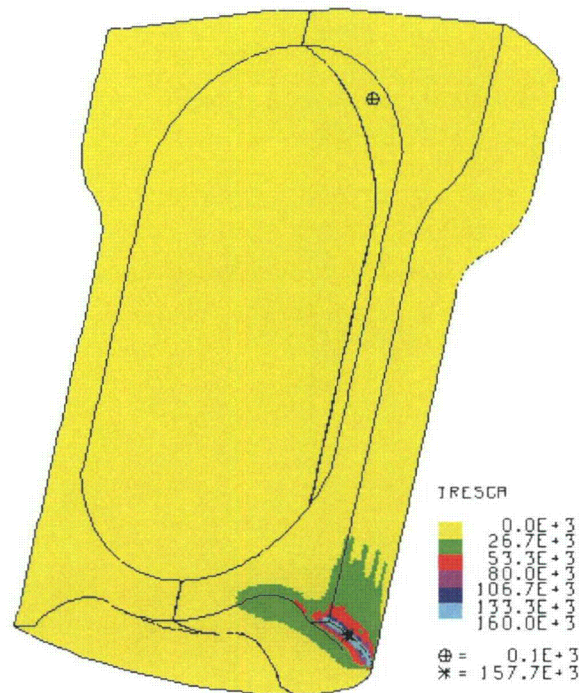


Figure 2-373. Plot of Tresca Stress in the TB-1 for HAC Run 2, SC-2, Side Impact, Support Structure 0° when Plate Velocity Reaches Zero

### 2.12.5.6.3 HAC- Run 3, SC-2, Side Impact, Support Structure 45°

The dynamic crush side impact HAC analysis run for the 2 SC-2 sample container with its support structure rotated 45° uses the same model as that used for the 4-ft-drop, but the flange is added to both ends so that it is available to deform where impacted by the plate and the rigid surface upon which it is resting. The finite element mesh and initial position of the model are shown in Figure 2-374. The Pu contents and support structure within the T-Ampoule are positioned at the bottom of the model because it was considered to be at rest at the time of impact. The plate was positioned between the flanges to be most damaging to the TB-1 and contents by preventing the flanges from absorbing energy and slowing down the plate before it hits the overpack.

The post-impact deformation is shown in Figure 2-375 and its kinetic energy history in Figure 2-376. The flanges on the overpack deform, and the contents bounce due to the impact of the plate. Average stress-triaxiality versus EQPS is shown in Figure 2-377 for the one element extending beyond the tested Bao-Wierzbicki strain locus. This element is at high stress triaxiality and low EQPS. The Tearing Parameter value for this same element is shown in Figure 2-378 and is below the critical Tearing Parameter value of 1.012 for Ti-6Al-4V. This element is highlighted in red Figure 2-379, but note that this element is below the initiation of a ductile tear, thus T-Ampoule integrity is maintained.

Peak EQPS in the TB-1 vessel is shown in Figure 2-380 to be 0.21, and is localized in the outer contact regions with the redwood overpack. Figures 2-381 and 2-382 are plots of the Tresca stresses within the TB-1. The maximum Tresca stress in the TB-1 is 226.7 ksi, but there are no through thickness stresses exceeding the limit of 106.6 ksi, which can be seen clearly in the figures. Figure 2-383 is a plot of the Tresca stresses at the time when all of the kinetic energy of the plate has been transferred to the package, just as the plate begins to rebound. The maximum through thickness stress at this time is below 16.7 ksi, below the allowable through thickness stress of 106.6 ksi, as seen in the figure.

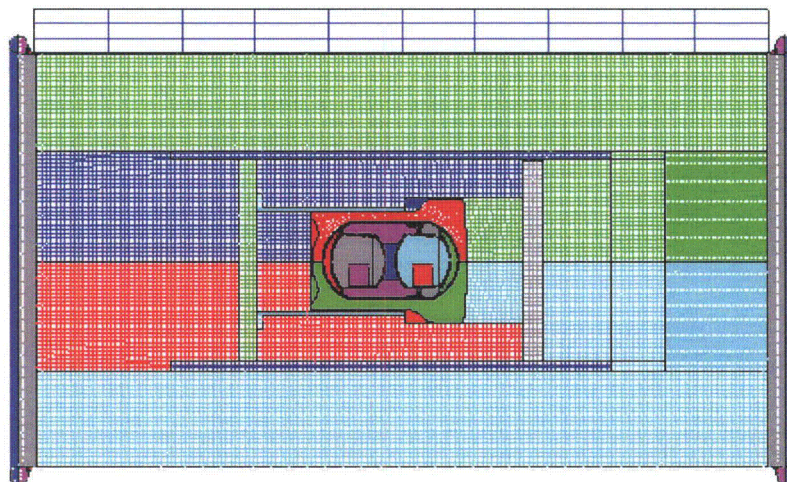


**Figure 2-374. Finite Element Mesh for HAC Run 3, SC-2, Side Impact, Support Structure 45°**

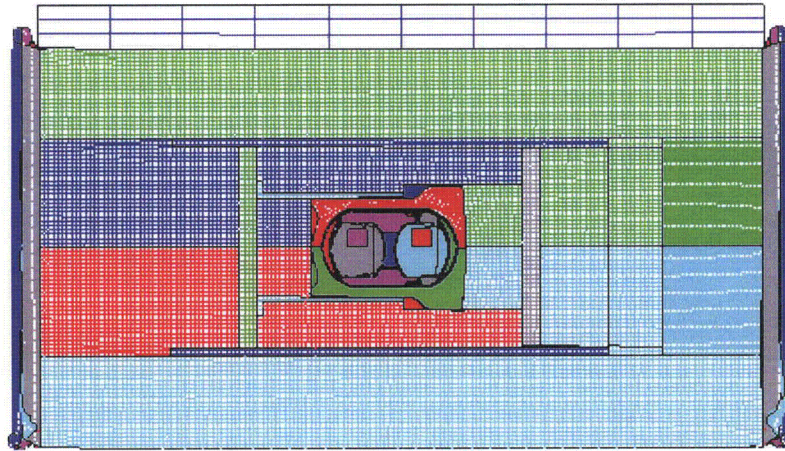


**Figure 2-375. Finite Element Mesh for HAC Run 3, SC-2, Side Impact, Support Structure 45° - Final Displacement**

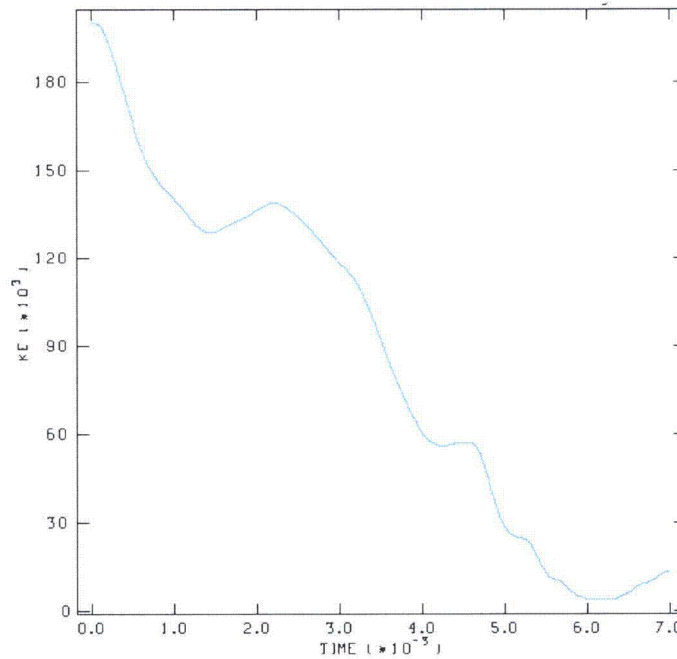


**Figure 2-376. Kinetic Energy Time History for HAC Run 3, SC-2, Side Impact, Support Structure 45°**

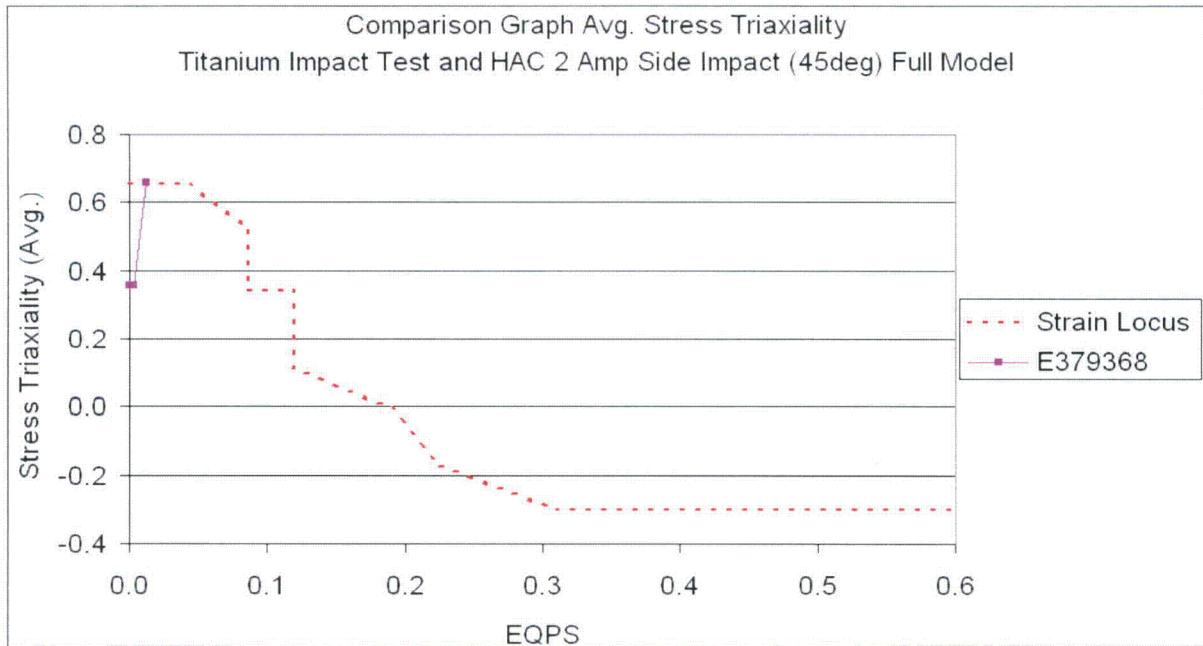


**Figure 2-377. Graph of Average Stress Triaxiality versus EQPS of Element Exceeding Experimental Strain Locus for HAC Run 3, SC-2, Side Impact, Support Structure 45°**

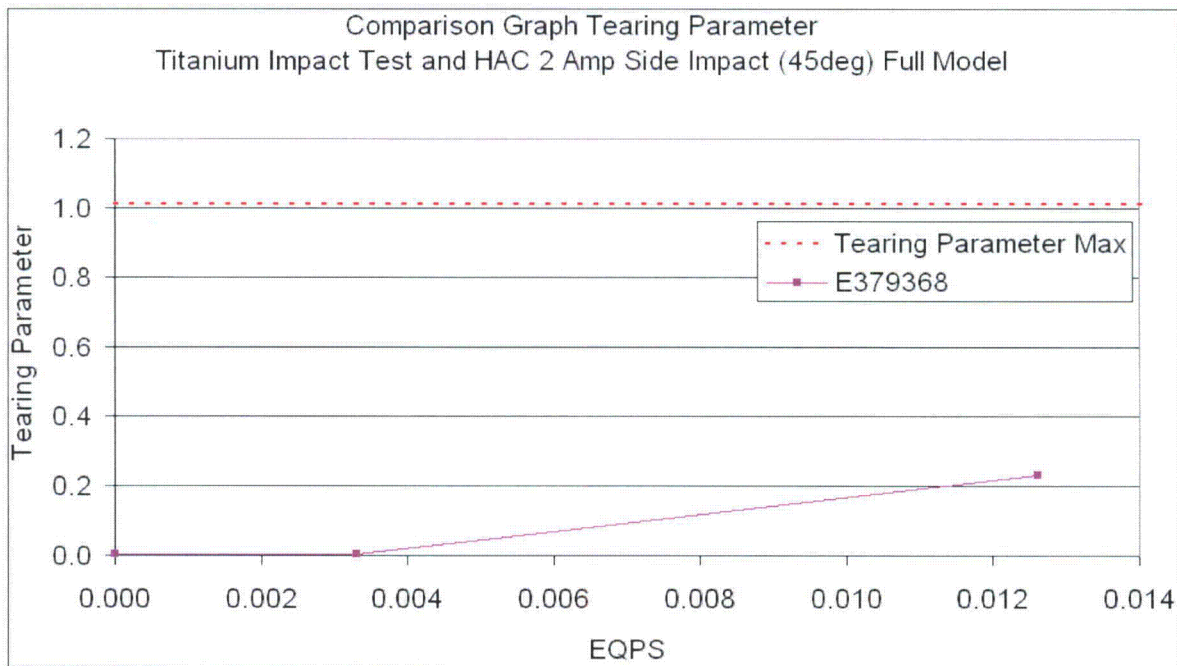


**Figure 2-378. Graph of Tearing Parameter versus EQPS of Element Exceeding Experimental Strain Locus (Zoomed In) for HAC Run 3, SC-2, Side Impact, Support Structure 45°**

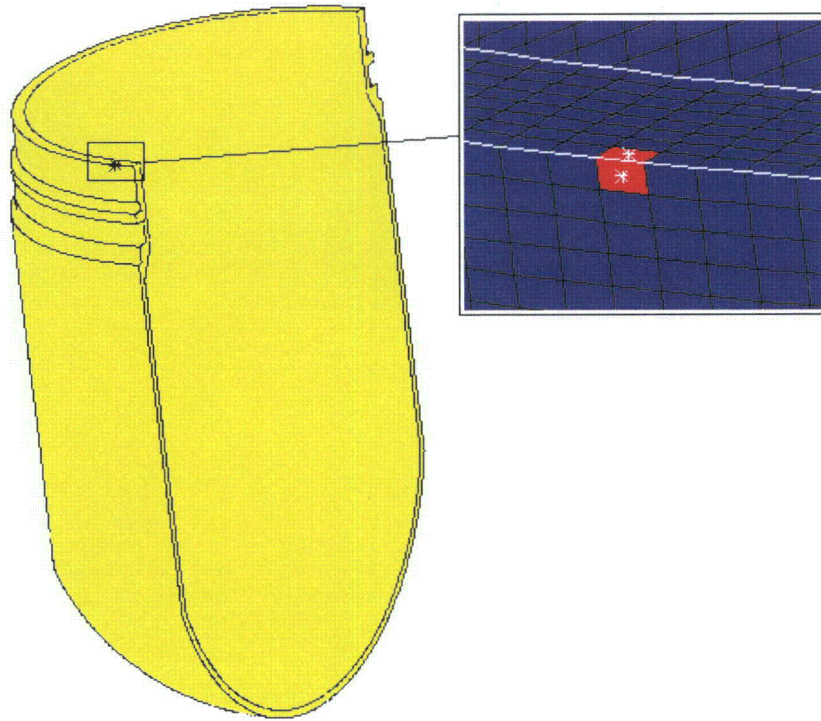


Figure 2-379. Plot of Element Exceeding Experimental Strain Locus for HAC Run 3, SC-2, Side Impact, Support Structure 45°

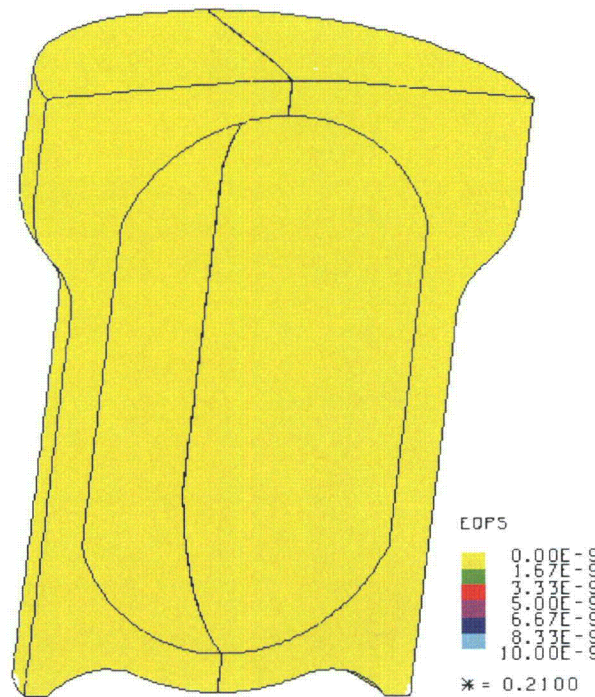


Figure 2-380. Plot of EQPS in the TB-1 for HAC Run 3, SC-2, Side Impact, Support Structure 45°

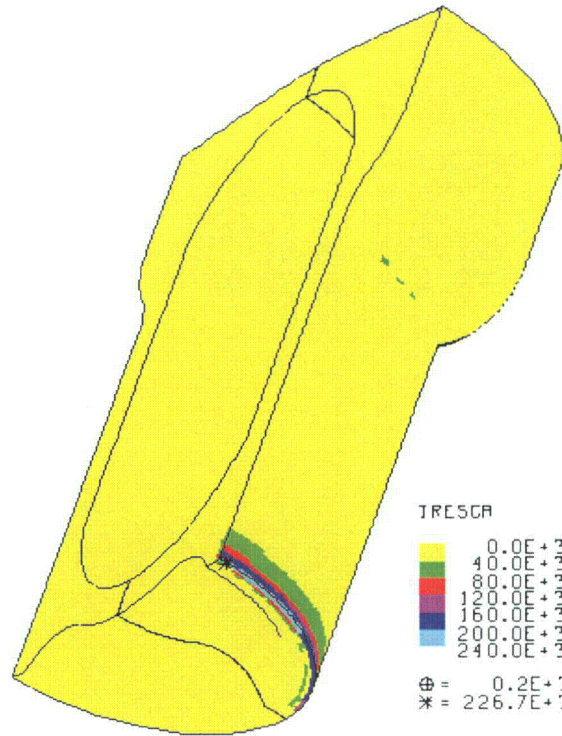


Figure 2-381. Plot of Tresca Stress in the TB-1 for HAC Run 3, SC-2, Side Impact, Support Structure 45°

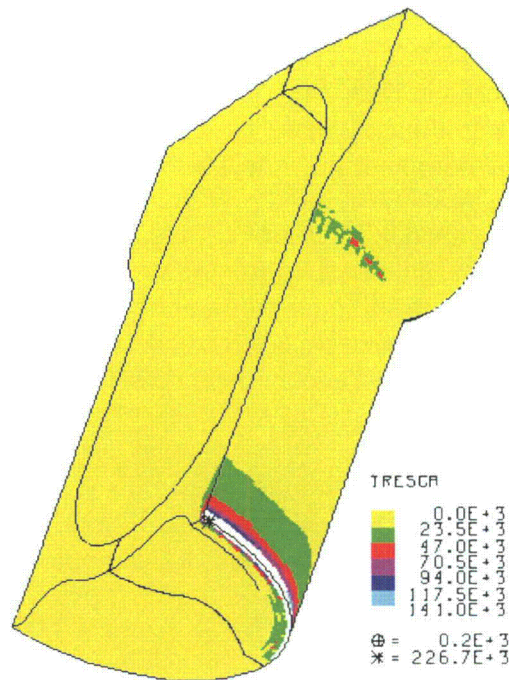
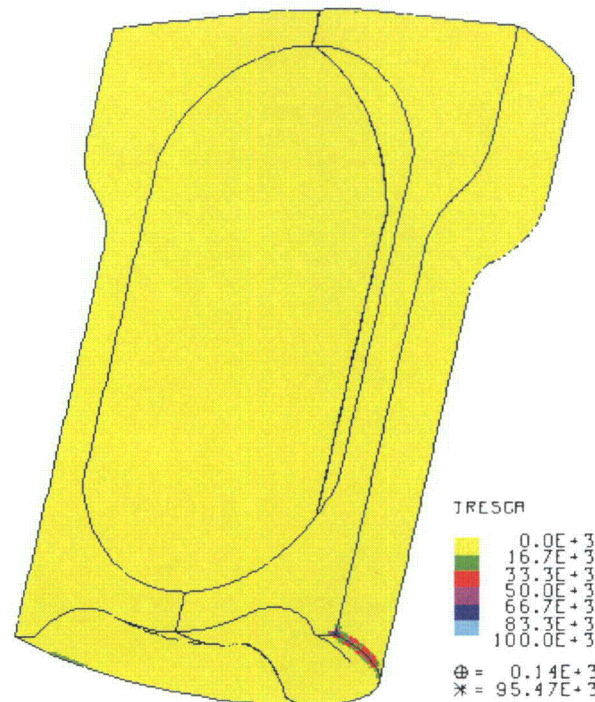


Figure 2-382. Plot of Tresca Stress in the TB-1 for HAC Run 3, SC-2, Side Impact, Support Structure 45°



**Figure 2-383. Plot of Tresca Stress in the TB-1 for HAC Run 3, SC-2, Side Impact, Support Structure 45° when Plate Velocity Reaches Zero**

#### 2.12.5.6.4 HAC- Run 4, SC-2, CGOC Impact, Support Structure 0°

The dynamic crush CGOC impact HAC analysis for the 2 SC-2 sample container run uses the same overpack model as those used in HAC runs 1 through 3. The finite element mesh and initial position of the model are shown in Figure 2-384. The Pu contents and support structure within the T-Ampoule are positioned at the bottom of the model because it was considered to be at rest.

The post-impact deformation is shown in Figure 2-385 and the resulting kinetic energy history is shown in Figure 2-386. The kinetic energy does not drop completely to zero because the plate is still vibrating and internal contents are still in motion. The plutonium cylinders have bounced off of the top and bottom surface of the sample containers, and the plate is now rebounding slowly with the package, ensuring that the highest containment vessel and contents loadings have occurred.

There were no elements that extended beyond the tested Bao-Wierzbicki strain locus. The maximum Tearing Parameter value for this analysis was 2.78e-3, which is below the critical Tearing Parameter value of 1.012 for Ti-6Al-4V, thus T-Ampoule integrity is maintained.

Peak EQPS in the TB-1 vessel is shown in Figure 2-387 to be 1.548e-3, and is localized in the outer contact regions with the redwood overpack. Figures 2-388 and 2-389 are plots of the Tresca stresses within the TB-1. The maximum Tresca stress in the TB-1 is 159.1 ksi, but there are no through thickness stresses exceeding the limit of 106.6 ksi, which can be seen clearly in the figures. Figure 2-389 is a plot of the Tresca stresses at the time when all of the kinetic energy of the plate has been transferred to the package, just as the plate begins to rebound. The

maximum through thickness stress at this time is below 8.33 ksi, below the allowable through thickness stress of 106.6 ksi, as seen in the figure.

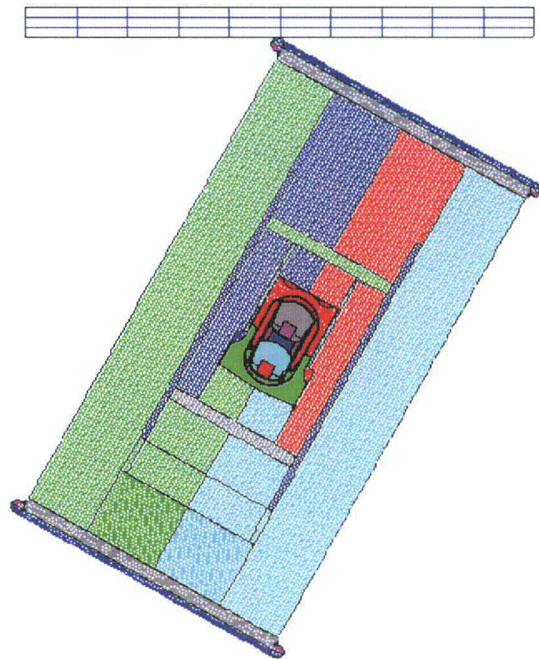


Figure 2-384. Finite Element Mesh for HAC Run 4, SC-2, CGOC Impact, Support Structure 0°

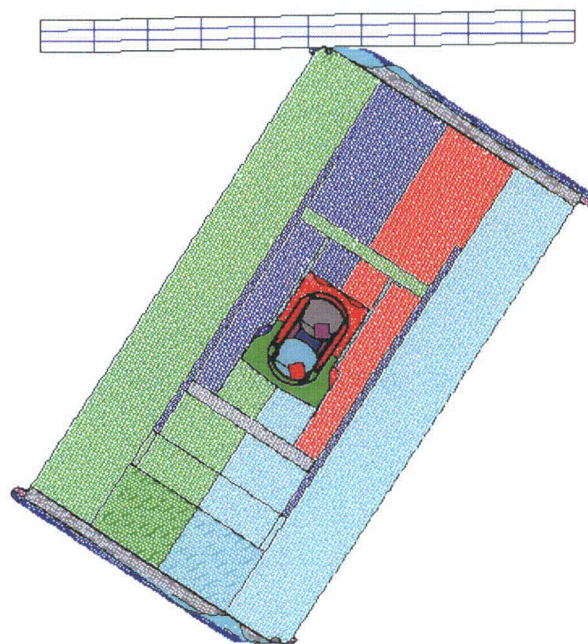


Figure 2-385. Finite Element Mesh for HAC Run 4, SC-2, CGOC Impact, Support Structure 0°, Final Displacement

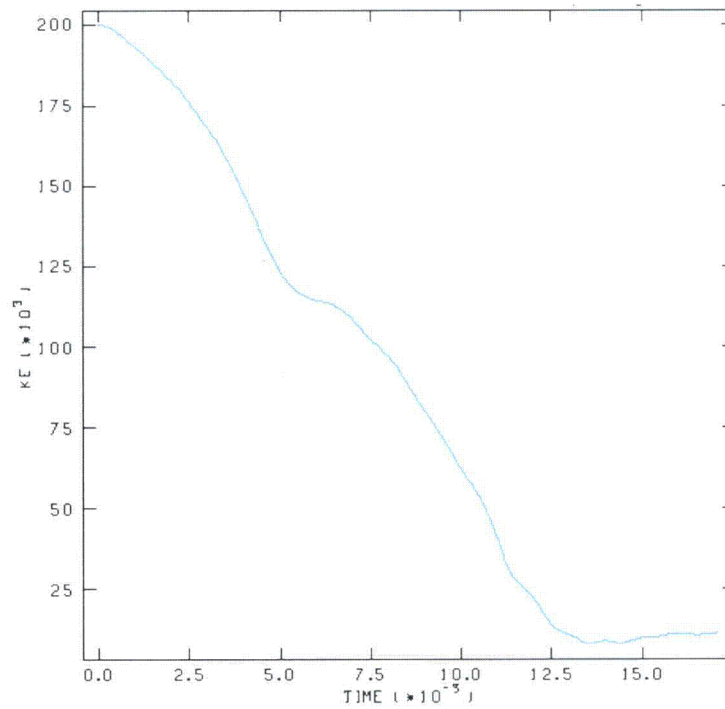


Figure 2-386. Kinetic Energy Time History for HAC Run 4, SC-2, CGOC Impact, Support Structure 0°

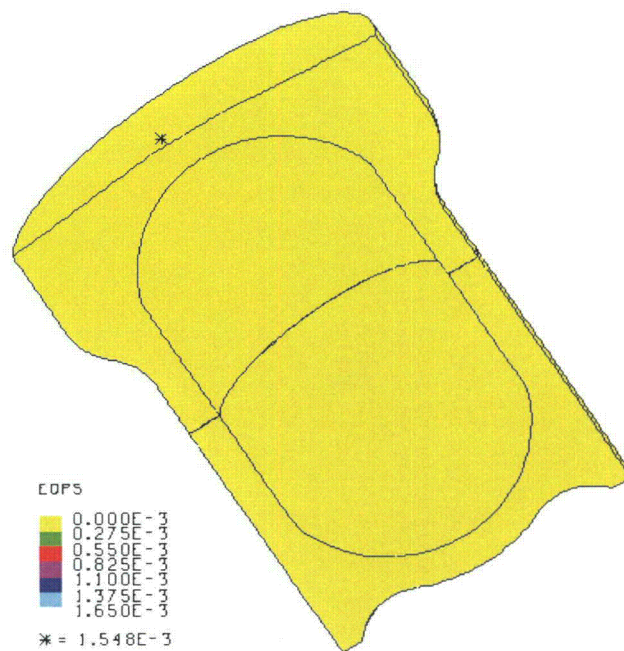


Figure 2-387. Plot of EQPS in TB-1 for HAC Run 4, SC-2, CGOC Impact, Support Structure 0°

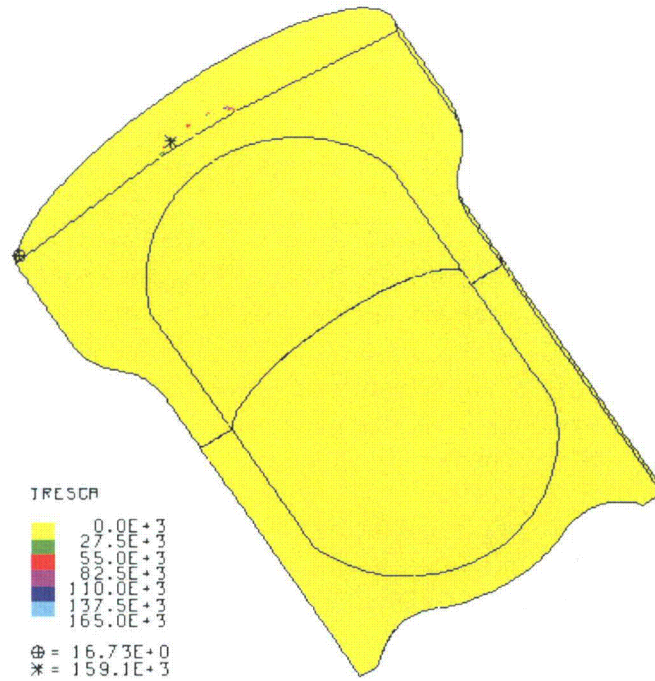


Figure 2-388. Plot of Tresca Stress in TB-1 for HAC Run 4, SC-2, CGOC Impact, Support Structure 0°

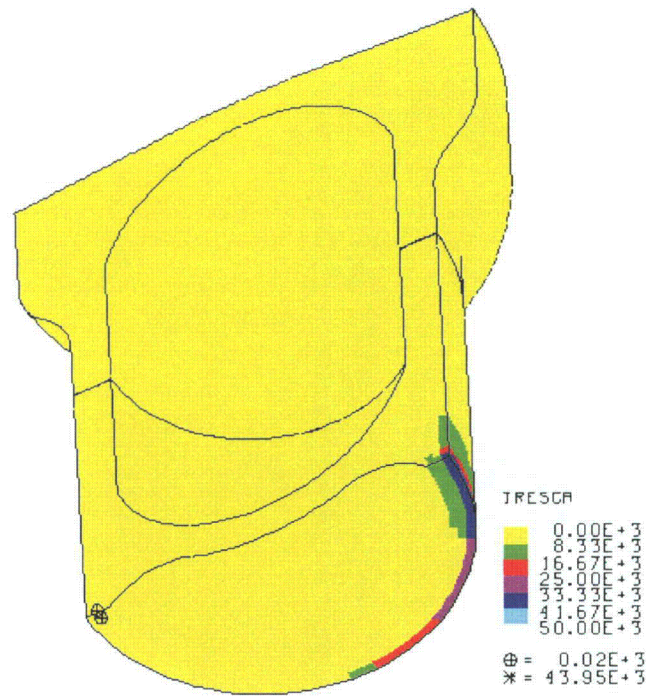


Figure 2-389. Plot of Tresca Stress in the TB-1 for HAC Run 4, SC-2, CGOC Impact, Support Structure 0° when Plate Velocity Reaches Zero

#### 2.12.5.6.5 HAC- Run 5, SC-2, CGOC Impact, Support Structure 45°

The dynamic crush CGOC impact HAC analysis for the 2 SC-2 sample container run uses the same overpack model as those used in HAC runs 1 through 4. The finite element mesh and initial position of the model are shown in Figure 2-390. The Pu contents and support structure within the T-Ampoule are positioned at the bottom of the model because it was considered to be at rest.

The post-impact deformation is shown in Figure 2-391 and its kinetic energy history in Figure 2-392. The flanges on the overpack deform, and the contents bounce due to the impact of the plate. The kinetic energy does not drop completely to zero because the plate is still vibrating and internal contents are still in motion. The plutonium cylinders have bounced off of the top and bottom surface of the sample containers, and the plate is now rebounding slowly with the package, ensuring that the highest containment vessel and contents loadings have occurred.

There was zero EQPS in the T-Ampoule and the TB-1, and the maximum Tearing Parameter was 0. Figure 2-393 is a plot of the Tresca stresses within the TB-1. The maximum Tresca stress in the TB-1 is 157.0 ksi, but there are no through thickness stresses exceeding the limit of 106.6 ksi, which can be seen clearly in the figure. Figure 2-393 is a plot of the Tresca stresses at the time when all of the kinetic energy of the plate has been transferred to the package, just as the plate begins to rebound. The maximum through thickness stress at this time is below 16.7 ksi, below the allowable through thickness stress of 106.6 ksi, as seen in the figure.

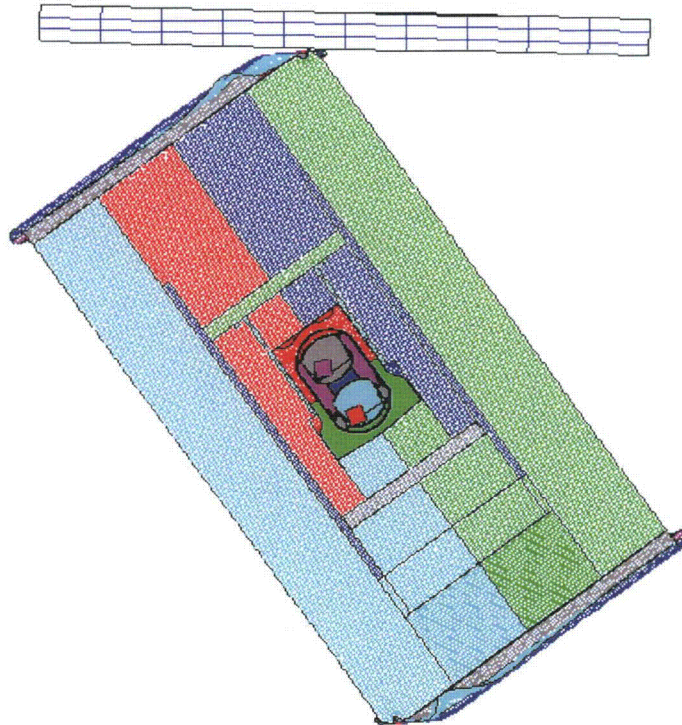


**Figure 2-390. Finite Element Mesh for HAC Run 5, SC-2, CGOC Impact, Support Structure 45°**

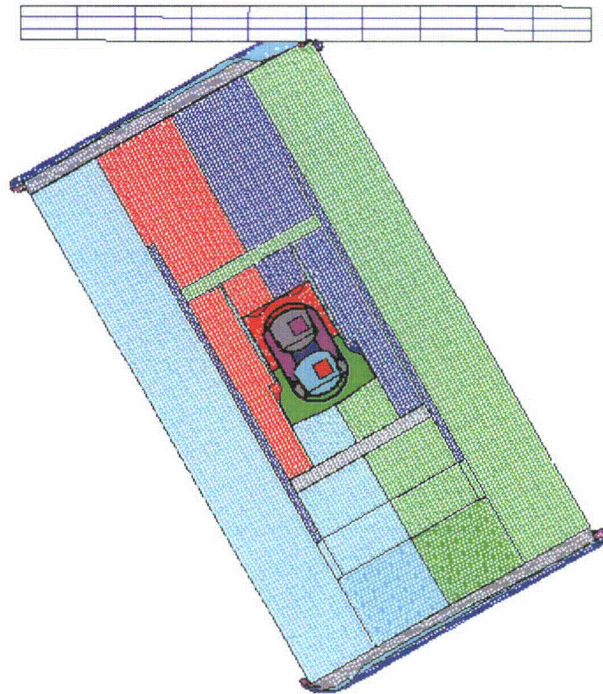


**Figure 2-391. Finite Element Mesh for HAC Run 5, SC-2, CGOC Impact, Support Structure 45° - Final Displacement**

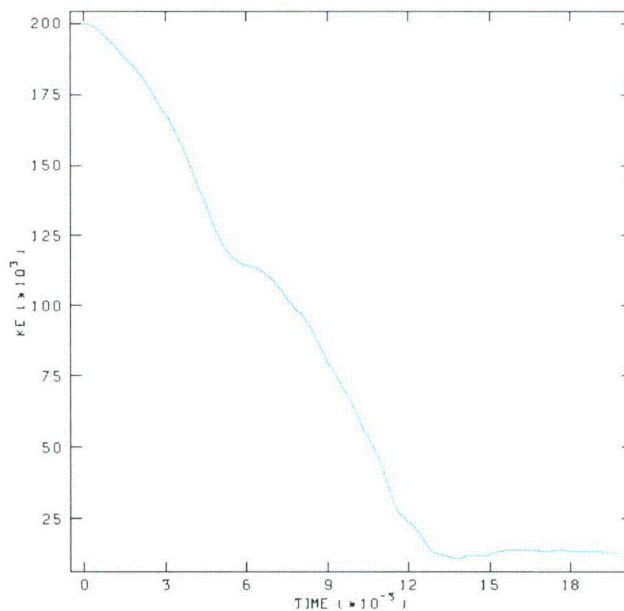


**Figure 2-392. Kinetic Energy Time History for HAC Run 5, SC-2, CGOC Impact, Support Structure 45°**



**Figure 2-393. Plot of Tresca Stress in the TB-1 for HAC Run 5, SC-2, CGOC Impact, Support Structure 45° when Stress is a Maximum**

#### 2.12.5.6.6 HAC- Run 6, SC-1, End Impact

The dynamic crush end impact HAC analysis run for the SC-1 sample container with its support structure rotated 0° uses the same model as that used for the 4-ft-drop, but the flange is added to both ends so that it is available to deform where impacted by the plate and the rigid surface upon which it is resting. The finite element mesh and initial position of the model are shown in Figure 2-394. The Pu contents and support structure within the T-Ampoule are positioned at the bottom of the model because it was considered to be at rest at the time of impact.

The post-impact deformation is shown in Figure 2-395 and its kinetic energy history in Figure 2-396. The flanges on the overpack deform, and the contents bounce due to the impact of the plate. There was zero EQPS in the TB-1, and zero elements extended beyond the tested Bao-Wierzbicki strain locus. The maximum Tearing Parameter was 3.03e-5 in the T-Ampoule, and is below the critical Tearing Parameter value of 1.012 for Ti-6Al-4V, thus T-Ampoule integrity is maintained. Figure 2-397 is a plot of the Tresca stresses within the TB-1. The maximum Tresca stress in the TB-1 is 127.1 ksi, but there are no through thickness stresses exceeding the limit of 106.6 ksi, which can be seen clearly in the figures. Figure 2-398 is a plot of the Tresca stresses at the time when all of the kinetic energy of the plate has been transferred to the package, just as the plate begins to rebound. The maximum through thickness stress at this time is below 8.33 ksi, below the allowable through thickness stress of 106.6 ksi, as seen in the figure.

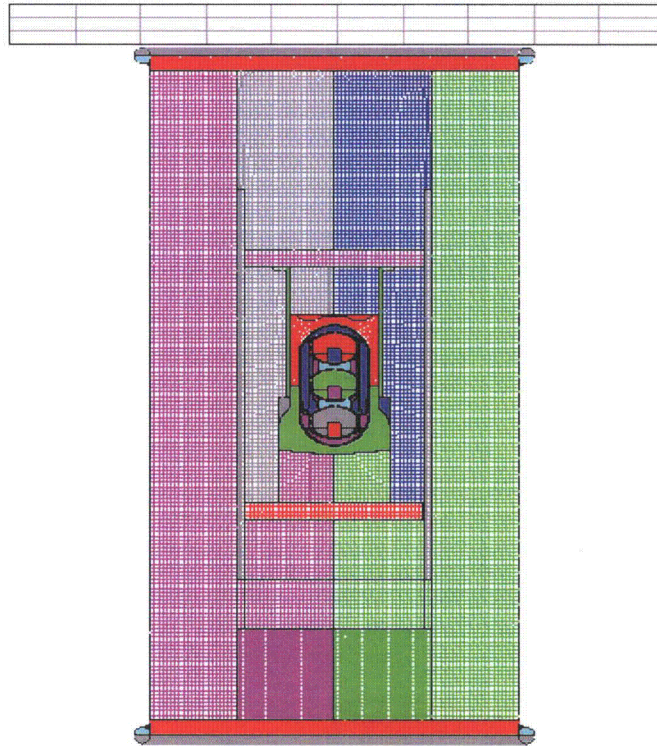


**Figure 2-394. Finite Element Mesh for HAC Run 6, SC-1, End Impact, Support Structure 0°**

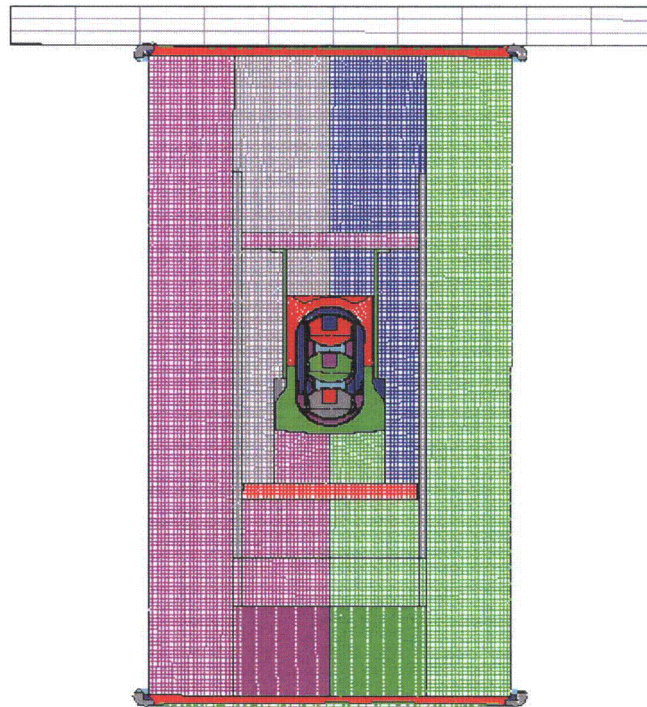


**Figure 2-395. Finite Element Mesh for HAC Run 6, SC-1, End Impact, Support Structure 0° - Final Displacement**

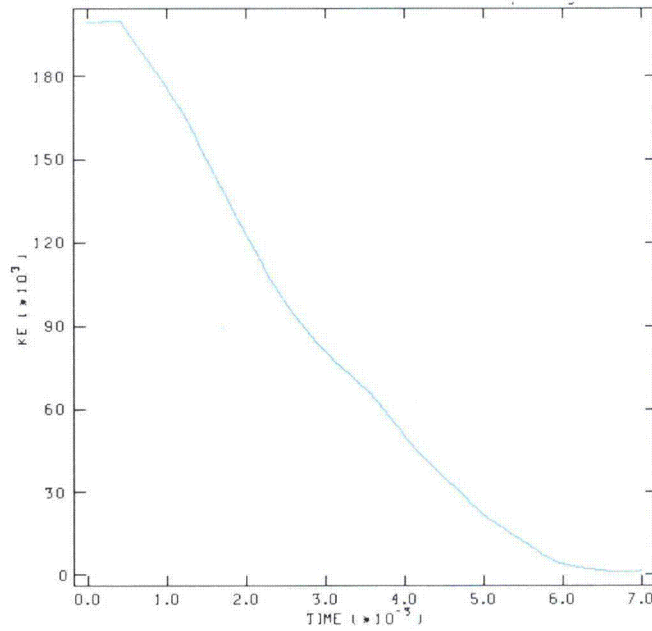


Figure 2-396. Kinetic Energy Time History for HAC Run 6, SC-1, End Impact, Support Structure 0°

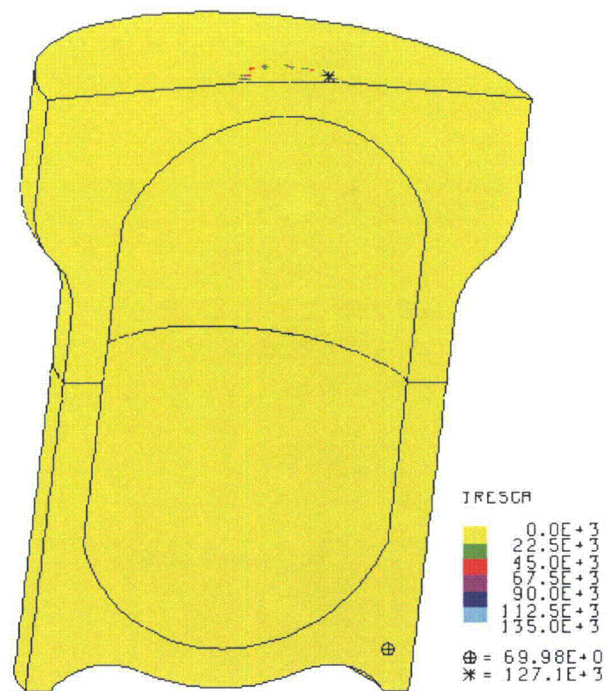
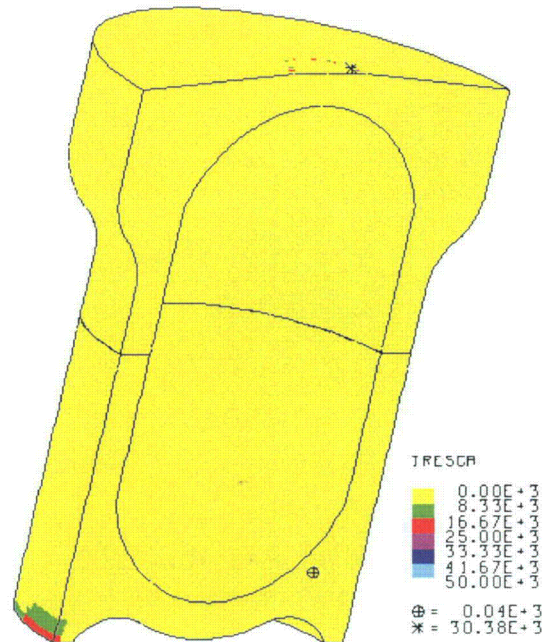


Figure 2-397. Plot of Tresca Stress in the TB-1 for HAC Run 6, SC-1, End Impact, Support Structure 0°



**Figure 2-398. Plot of Tresca Stress in the TB-1 for HAC Run 6, SC-1, End Impact, Support Structure 0° when Plate Velocity Reaches Zero**

#### 2.12.5.6.7 HAC- Run 7, SC-1, Side Impact, Support Structure 0°

The dynamic crush side impact HAC analysis run for the SC-1 sample containers with its support structure rotated 45° uses the same model as that used for the 4-ft-drop, but the flange is added to both ends so that it is available to deform where impacted by the plate and the rigid surface upon which it is resting. The finite element mesh and initial position of the model are shown in Figure 2-399. The Pu contents and support structure within the T-Ampoule are positioned at the bottom of the model because it was considered to be at rest at the time of impact. The plate was positioned between the flanges to be most damaging to the TB-1 and contents by preventing the flanges from absorbing energy and slowing down the plate before it hits the overpack.

The post-impact deformation is shown in Figure 2-400 and its kinetic energy history in Figure 2-401. The flanges on the overpack deform, and the contents bounce due to the impact of the plate. Zero elements extended beyond the tested Bao-Wierzbicki strain locus. The maximum Tearing Parameter value for this analysis was 3.03e-5, and is below the critical Tearing Parameter value of 1.012 for Ti-6Al-4V, thus T-Ampoule integrity is maintained.

Peak EQPS in the TB-1 vessel is shown in Figure 2-402 to be 27.67e-3, and is localized in the outer contact regions with the redwood overpack. Figure 2-403 is a plot of the Tresca stresses within the TB-1. The maximum Tresca stress in the TB-1 is 172.3 ksi, but there are no through thickness stresses exceeding the limit of 106.6 ksi, which can be seen clearly in the figure. Figure 2-404 is a plot of the Tresca stresses at the time when all of the kinetic energy of the plate has been transferred to the package, just as the plate begins to rebound. The maximum through thickness stress at this time is below 25.0 ksi, below the allowable through thickness stress of 106.6 ksi, as seen in the figure.

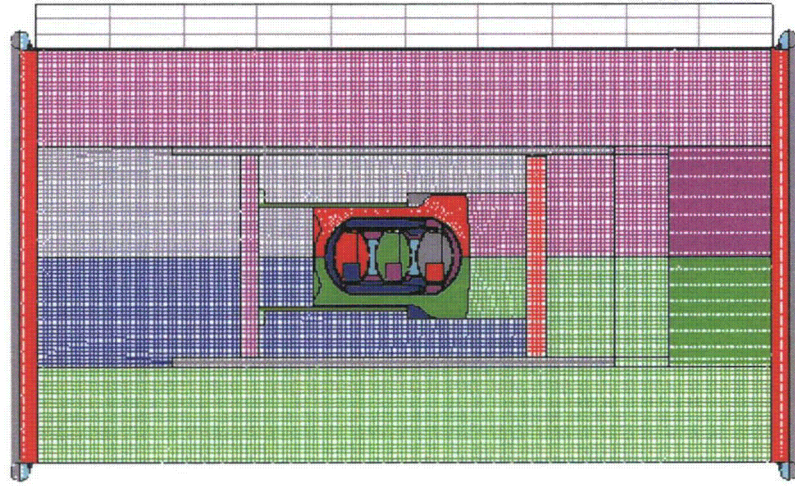


**Figure 2-399. Finite Element Mesh for HAC Run 7, SC-1, Side Impact, Support Structure 0°**

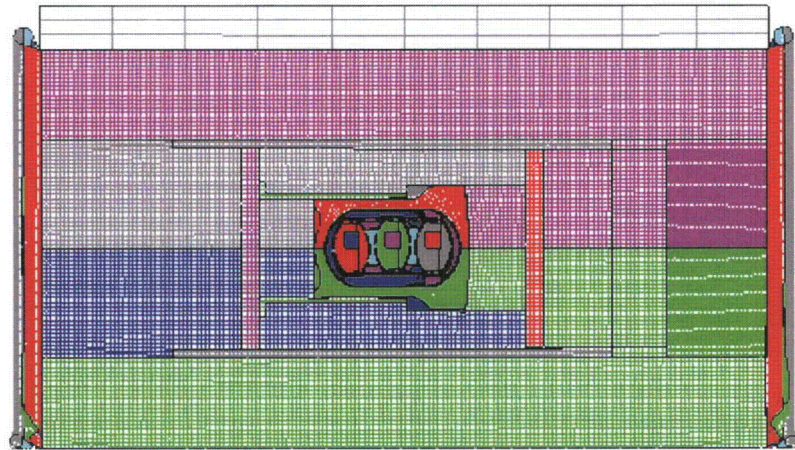


**Figure 2-400. Finite Element Mesh for HAC Run 7, SC-1, Side Impact, Support Structure 0° - Final Displacement**

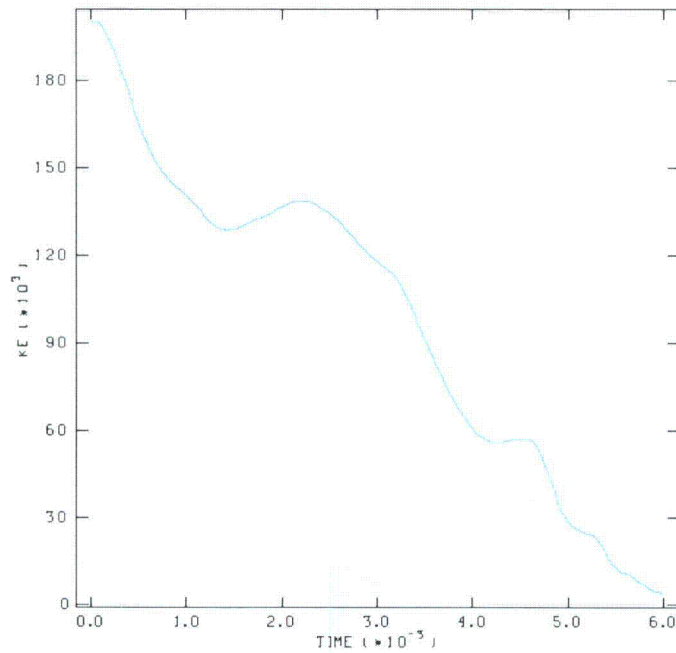


Figure 2-401. Kinetic Energy Time History for HAC Run 7, SC-1, Side Impact, Support Structure 0°

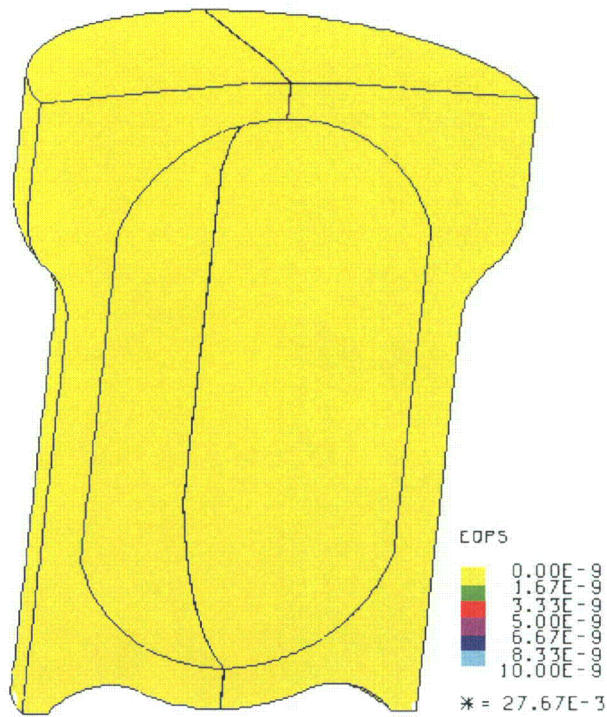


Figure 2-402. Plot of EQPS in TB-1 for HAC Run 7, SC-1, Side Impact, Support Structure 0°

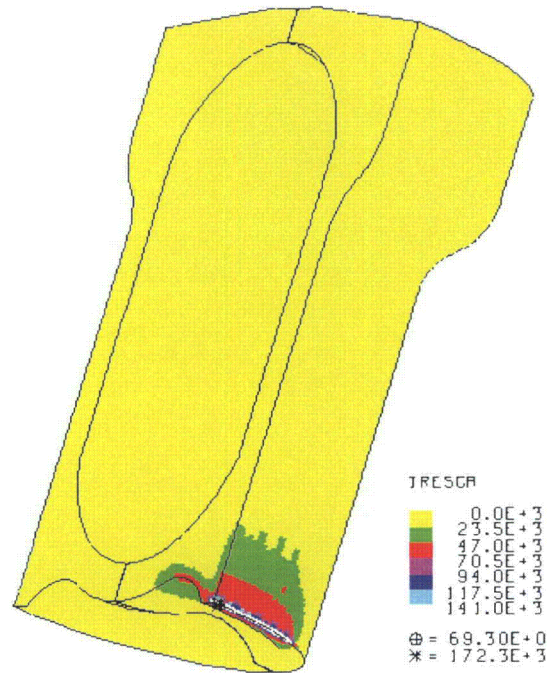


Figure 2-403. Plot of Tresca Stress in the TB-1 for HAC Run 7, SC-1, Side Impact, Support Structure 0°

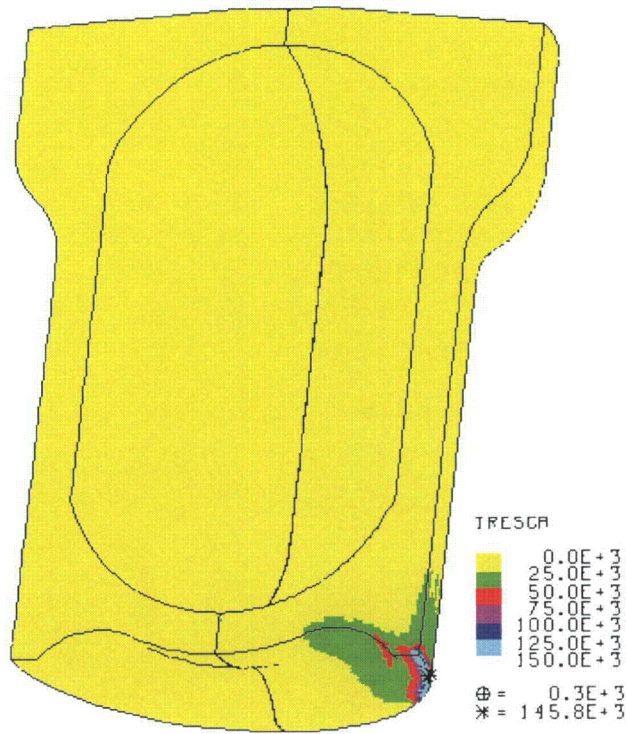


Figure 2-404. Plot of Tresca Stress in the TB-1 for HAC Run 7, SC-1, Side Impact, Support Structure 0° when Plate Velocity Reaches Zero

#### 2.12.5.6.8 HAC- Run 8, SC-1, Side Impact, Support Structure 45°

The dynamic crush side impact HAC analysis run for the SC-1 sample container with its support structure rotated 45° uses the same model as that used for the 4-ft-drop, but the flange is added to both ends so that it is available to deform where impacted by the plate and the rigid surface upon which it is resting. The finite element mesh and initial position of the model are shown in Figure 2-405. The Pu contents and support structure within the T-Ampoule are positioned at the bottom of the model because it was considered to be at rest at the time of impact. The plate was positioned between the flanges to be most damaging to the TB-1 and contents by preventing the flanges from absorbing energy and slowing down the plate before it hits the overpack.

The post-impact deformation is shown in Figure 2-406 and its kinetic energy history in Figure 2-407. The flanges on the overpack deform, and the contents bounce due to the impact of the plate. Zero elements extended beyond the tested Bao-Wierzbicki strain locus. The maximum Tearing Parameter value for this analysis was 1.6e-2, and is below the critical Tearing Parameter value of 1.012 for Ti-6Al-4V, thus T-Ampoule integrity is maintained.

Peak EQPS in the TB-1 vessel is shown in Figure 2-408 to be 0.1829, and is localized in the outer contact regions with the redwood overpack. Figures 2-409 and 2-410 are plots of the Tresca stresses within the TB-1. The maximum Tresca stress in the TB-1 is 225.9 ksi (contact modeling artifact), but there are no through thickness stresses exceeding the limit of 106.6 ksi, which can be seen clearly in the figures. Figure 2-411 is a plot of the Tresca stresses at the time when all of the kinetic energy of the plate has been transferred to the package, just as the plate begins to rebound. The maximum through thickness stress at this time is below 33.3 ksi, below the allowable through thickness stress of 106.6 ksi, as seen in the figure.

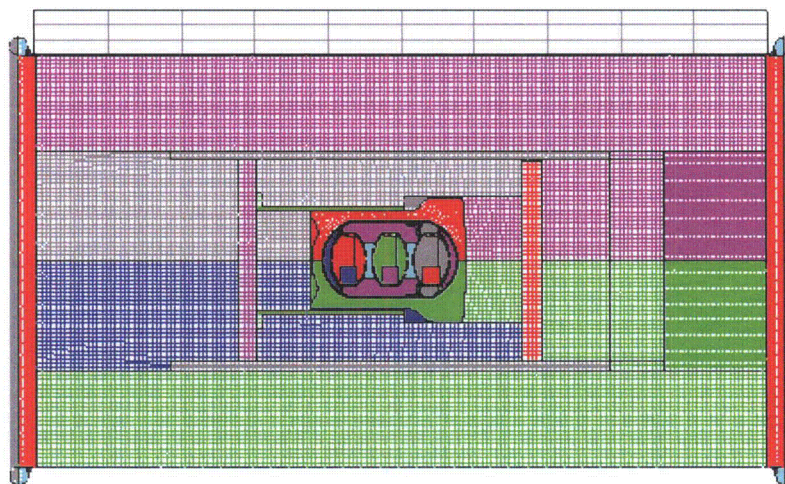
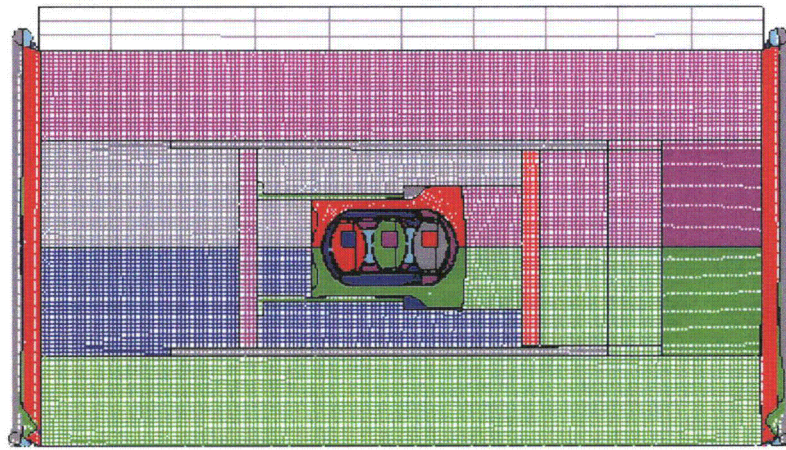
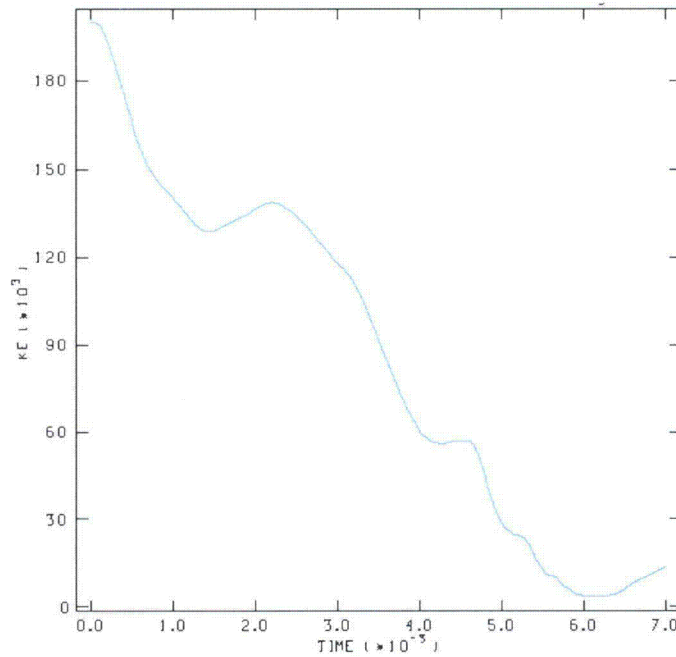


Figure 2-405. Finite Element Mesh for HAC Run 8, SC-1, Side Impact, Support Structure 45°



**Figure 2-406. Finite Element Mesh for HAC Run 8, SC-1, Side Impact, Support Structure 45° - Final Displacement**



**Figure 2-407. Kinetic Energy Time History for HAC Run 8, SC-1, Side Impact, Support Structure 45°**

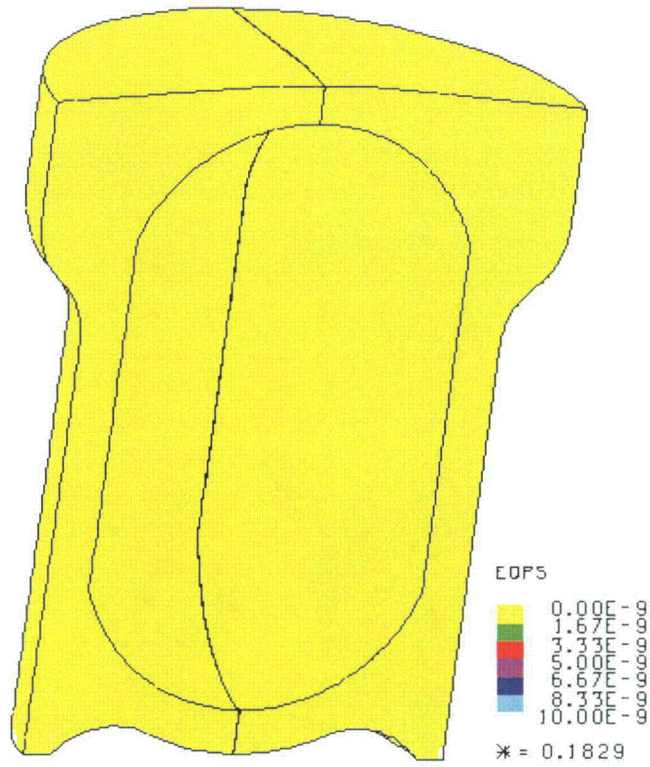


Figure 2-408. Plot of EQPS in TB-1 for HAC Run 8, SC-1, Side Impact, Support Structure 45°

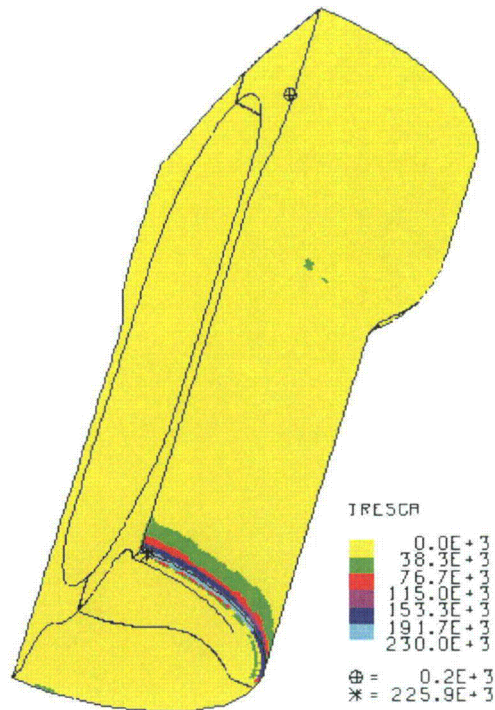


Figure 2-409. Plot of Tresca Stress in TB-1 for HAC Run 8, SC-1, Side Impact, Support Structure 45°

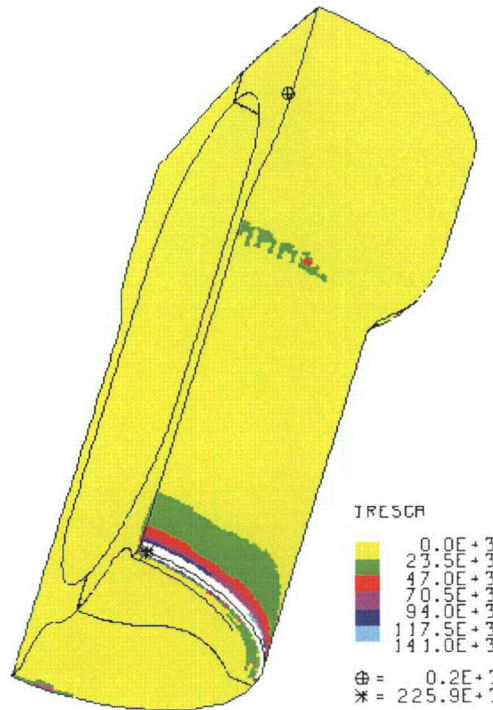


Figure 2-410. Plot of Tresca Stress in TB-1 for HAC Run 8, SC-1, Side Impact, Support Structure 45°

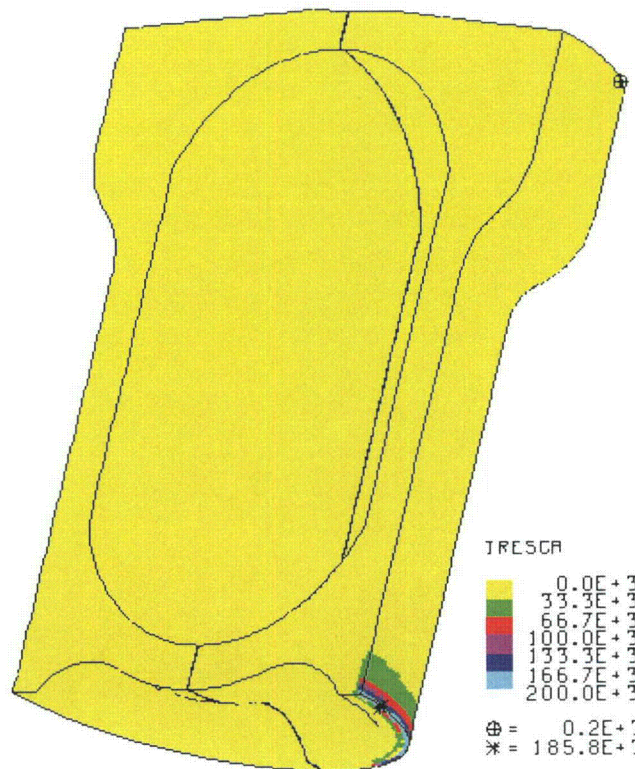


Figure 2-411. Plot of Tresca Stress in TB-1 for HAC Run 8, SC-1, Side Impact, Support Structure 45° when Plate Velocity Reaches Zero

#### 2.12.5.6.9 HAC- Run 9, SC-1, CGOC Impact, Support Structure 0°

The dynamic crush CGOC impact HAC analysis for the SC-1 sample container run uses the same overpack model as those used in HAC runs 1 through 8. The finite element mesh and initial position of the model are shown in Figure 2-412. The Pu contents and support structure within the T-Ampoule are positioned at the bottom of the model because it was considered to be at rest.

The post-impact deformation is shown in Figure 2-413 and its kinetic energy history in Figure 2-414. The flanges on the overpack deform, and the contents bounce due to the impact of the plate. The kinetic energy does not drop completely to zero because the plate is still vibrating and internal contents are still in motion. The plutonium cylinders have bounced off of the top and bottom surface of the sample containers, and the plate is now rebounding slowly with the package, ensuring that the highest containment vessel and contents loadings have occurred.

There was zero EQPS in the T-Ampoule and the TB-1, and the maximum Tearing Parameter was 0. Figure 2-415 is a plot of the Tresca stresses within the TB-1. The maximum Tresca stress in the TB-1 is 146.5 Ksi, but there are no through thickness stresses exceeding the limit of 106.6 ksi, which can be seen clearly in the figure. Figure 2-416 is a plot of the Tresca stresses at the time when all of the kinetic energy of the plate has been transferred to the package, just as the plate begins to rebound. The maximum through thickness stress at this time is below 8.33 ksi, below the allowable through thickness stress of 106.6 ksi, as seen in the figure.

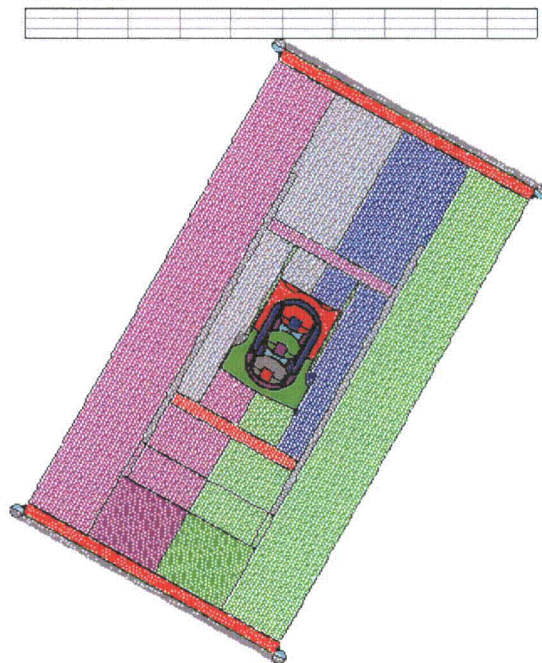


**Figure 2-412. Finite Element Mesh for HAC Run 9, SC-1, CGOC Impact, Support Structure 0°**

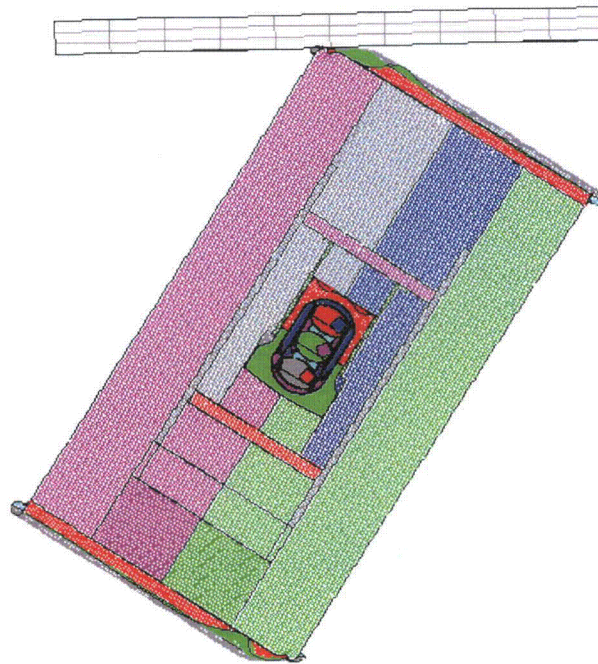


**Figure 2-413. Finite Element Mesh for HAC Run 9, SC-1, CGOC Impact, Support Structure 0° - Final Displacement**

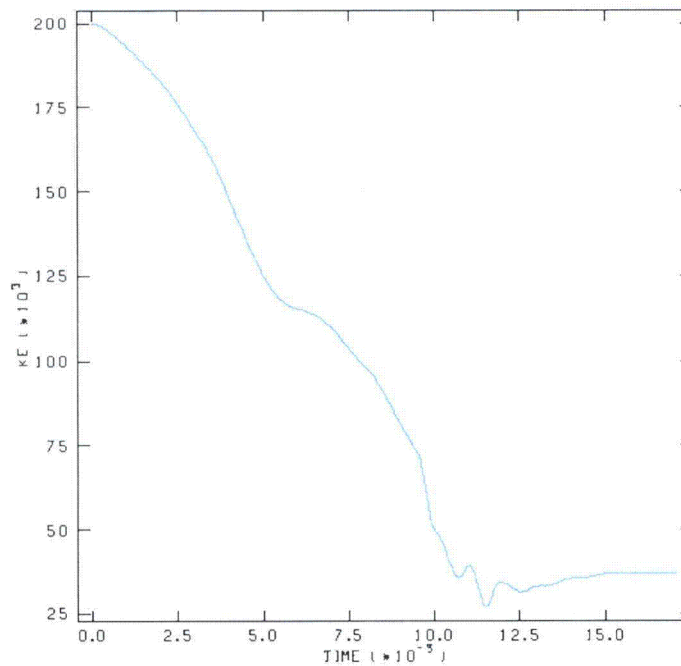


**Figure 2-414. Kinetic Energy Time History for HAC Run 9, SC-1, CGOC Impact, Support Structure 0°**

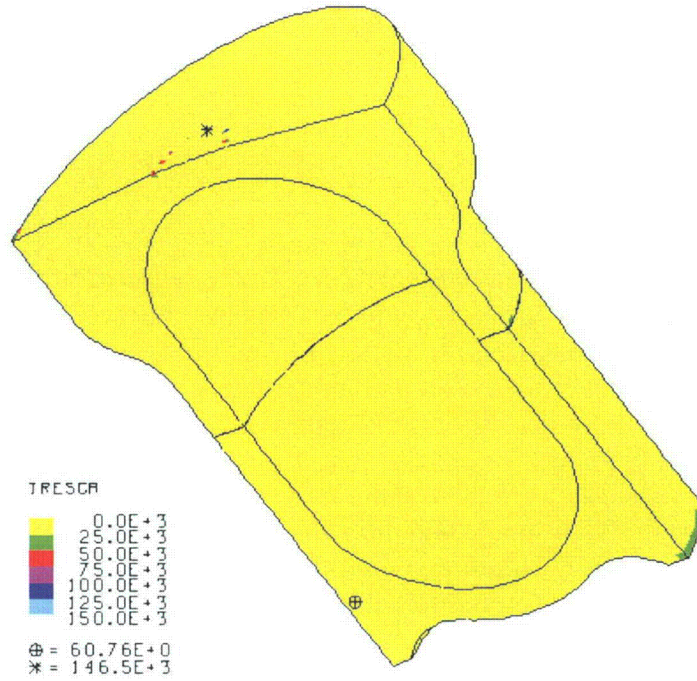


Figure 2-415. Tresca Stress for HAC Run 9, SC-1, CGOC Impact, Support Structure 0°

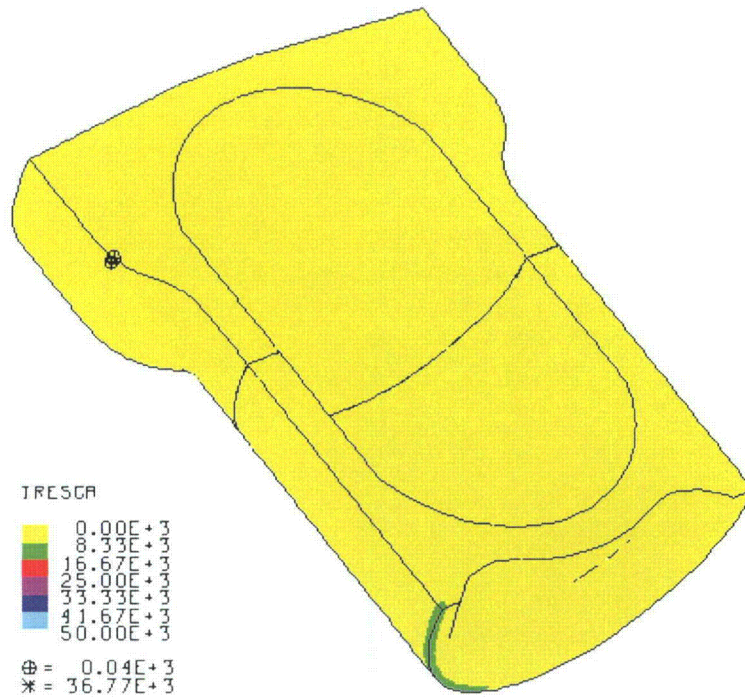


Figure 2-416. Plot of Tresca Stress in the TB-1 for HAC Run 9, SC-1, CGOC Impact, Support Structure 0° when Plate Velocity Reaches Zero

#### 2.12.5.6.10 HAC- Run 10, SC-1, CGOC Impact, Support Structure 45°

The dynamic crush CGOC impact HAC analysis for the SC-1 sample container run uses the same overpack model as those used in HAC runs 1 through 9. The finite element mesh and initial position of the model are shown in Figure 2-417. The Pu contents and support structure within the T-Ampoule are positioned at the bottom of the model because it was considered to be at rest.

The post-impact deformation is shown in Figure 2-418 and its kinetic energy history in Figure 2-419. The flanges on the overpack deform, and the contents bounce due to the impact of the plate. The kinetic energy does not drop completely to zero because the plate is still vibrating and internal contents are still in motion. The plutonium cylinders have bounced off of the top and bottom surface of the sample containers, and the plate is now rebounding slowly with the package, ensuring that the highest containment vessel and contents loadings have occurred.

There was zero EQPS in the T-Ampoule and the TB-1, and the maximum Tearing Parameter was 0. Figure 2-420 is a plot of the Tresca stresses within the TB-1. The maximum Tresca stress in the TB-1 is 158.8 ksi, but there are no through thickness stresses exceeding the limit of 106.6 ksi, which can be seen clearly in the figure. Figure 2-421 is a plot of the Tresca stresses at the time when all of the kinetic energy of the plate has been transferred to the package, just as the plate begins to rebound. The maximum through thickness stress at this time is below 16.7 ksi, below the allowable through thickness stress of 106.6 ksi, as seen in the figure.

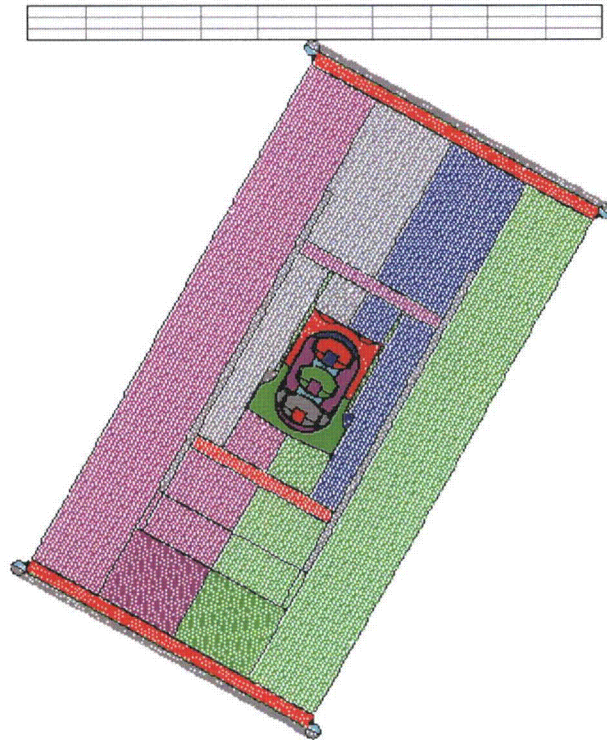


**Figure 2-417. Finite Element Mesh for HAC Run 10, SC-1, CGOC Impact, Support Structure 45°**

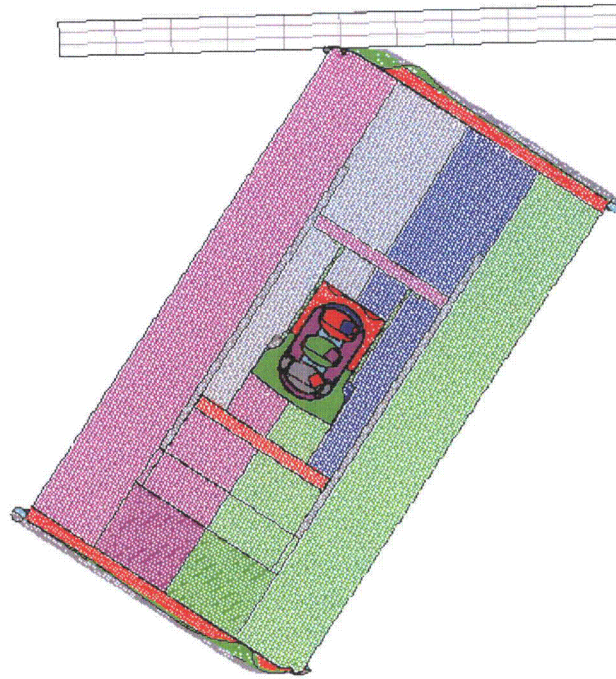


**Figure 2-418. Finite Element Mesh for HAC Run 10, SC-1, CGOC Impact, Support Structure 45° - Final Displacement**

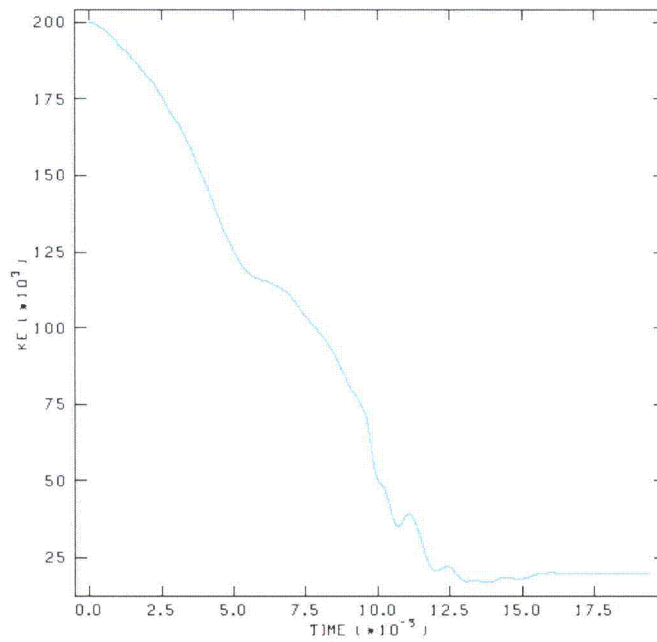


**Figure 2-419. Kinetic Energy Time History for HAC Run 10, SC-1, CGOC Impact, Support Structure 45°**

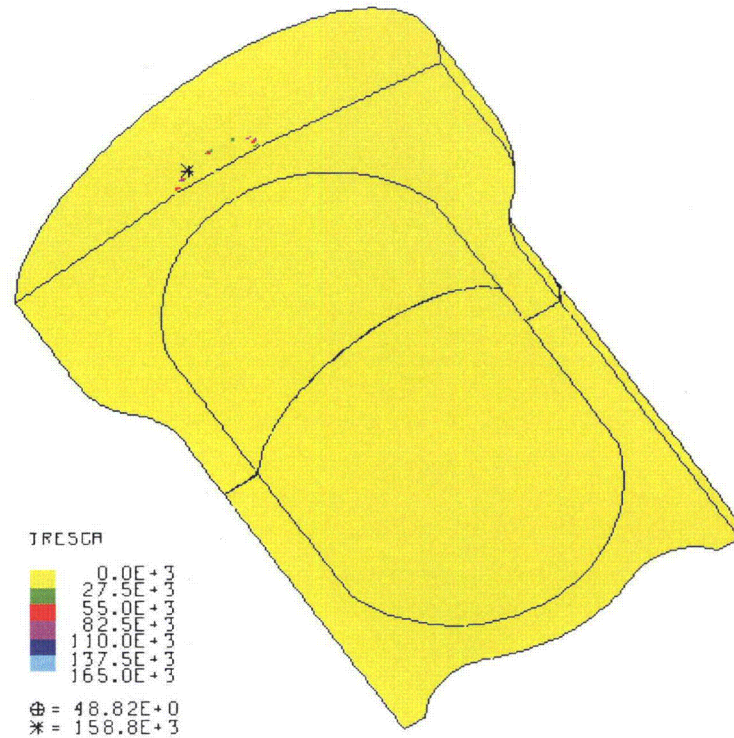


Figure 2-420. Plot of Tresca Stress in the TB-1 for HAC Run 10, SC-1, CGOC Impact, Support Structure 45°

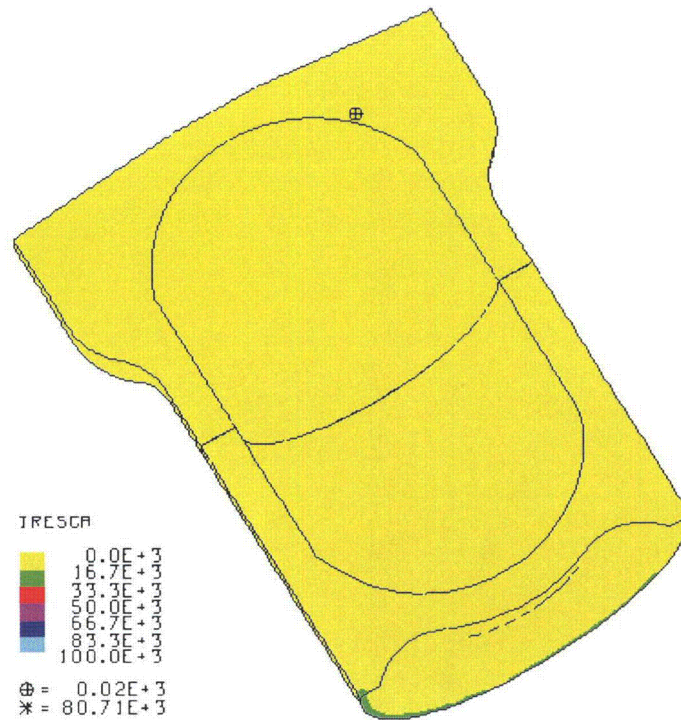


Figure 2-421. Plot of Tresca Stress in the TB-1 for HAC Run 10, SC-1, CGOC Impact, Support Structure 45° when Plate Velocity Reaches Zero

#### 2.12.5.6.11 HAC- Run 11, 831 g Plutonium Metal Hollow Cylinder, End Impact

The dynamic crush end impact HAC analysis run for the 831 g plutonium metal hollow cylinder uses the same model for the overpack as the one used in the previous 10 runs. The TB-1, T-Ampoule, and plutonium metal hollow cylinder are the same model as that used in the aircraft analysis. The finite element mesh and initial position of the model are shown in Figure 2-422. The plutonium metal hollow cylinder within the T-Ampoule is positioned at the bottom of the model because it was considered to be at rest at the time of impact.

The post-impact deformation is shown in Figure 2-423 and its kinetic energy history in Figure 2-424. The flanges on the overpack deform, and the cylinder bounces due to the impact of the plate. Zero elements extended beyond the tested Bao-Wierzbicki strain locus. The maximum Tearing Parameter value for this analysis was 0.

Peak EQPS in the TB-1 vessel is shown in Figure 2-425 to be  $2.68e-3$ , and is localized in the outer contact regions with the redwood overpack. Figure 2-426 plots the Tresca stresses within the TB-1. The maximum Tresca stress in the TB-1 is 156.7 ksi, but there are no through thickness stresses exceeding the limit of 106.6 ksi, which can be seen clearly in the figure. Figure 2-427 is a plot of the Tresca stresses at the time when all of the kinetic energy of the plate has been transferred to the package, just as the plate begins to rebound. The maximum through thickness stress at this time is below 25.0 ksi, below the allowable through thickness stress of 106.6 ksi, as seen in the figure.

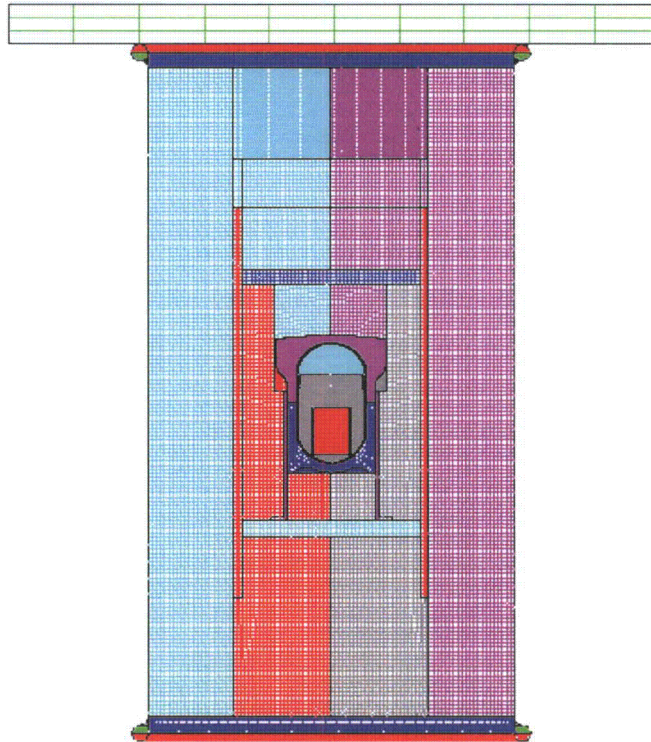
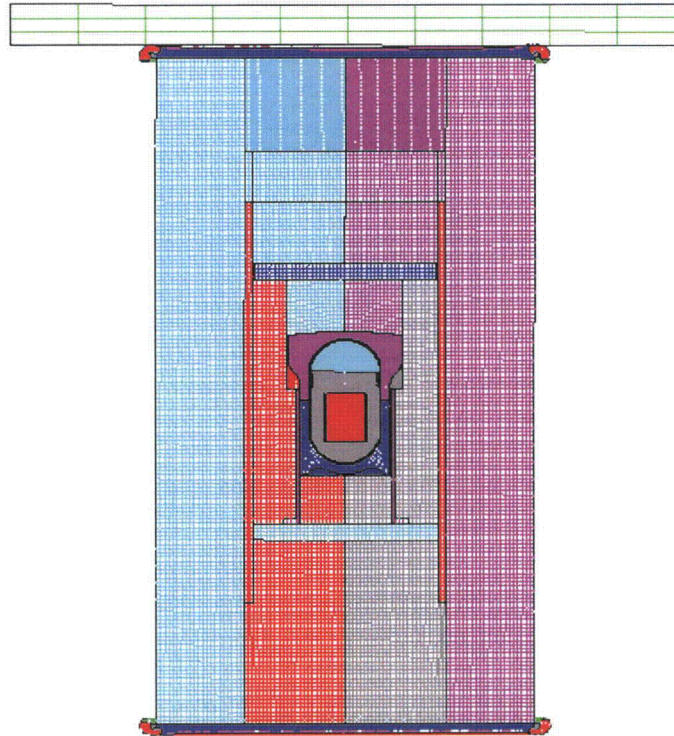
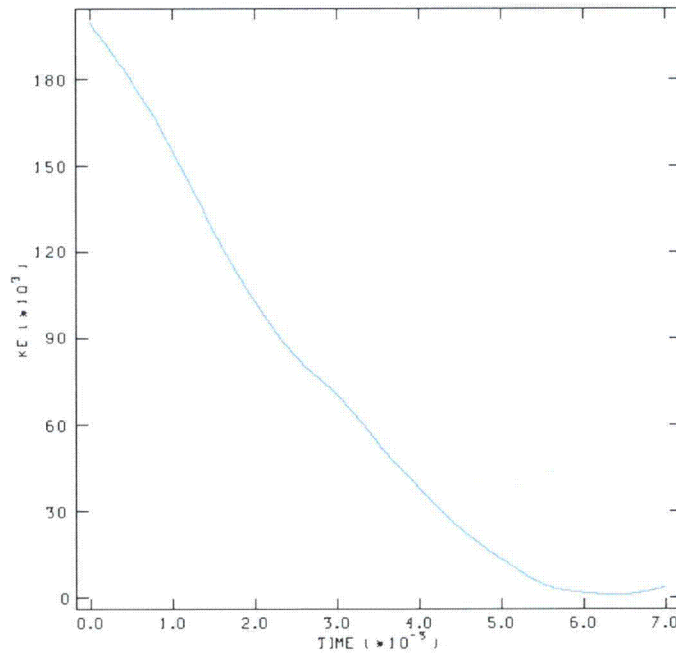


Figure 2-422. Finite Element Mesh for HAC Run 11, 831 g Plutonium Metal Hollow Cylinder, End Impact



**Figure 2-423. Finite Element Mesh for HAC Run 11, 831 g, Plutonium Metal Hollow Cylinder, End Impact – Final Displacement**



**Figure 2-424. Kinetic Energy Time History for HAC Run 11, 831 g, Plutonium Metal Hollow Cylinder, End Impact**

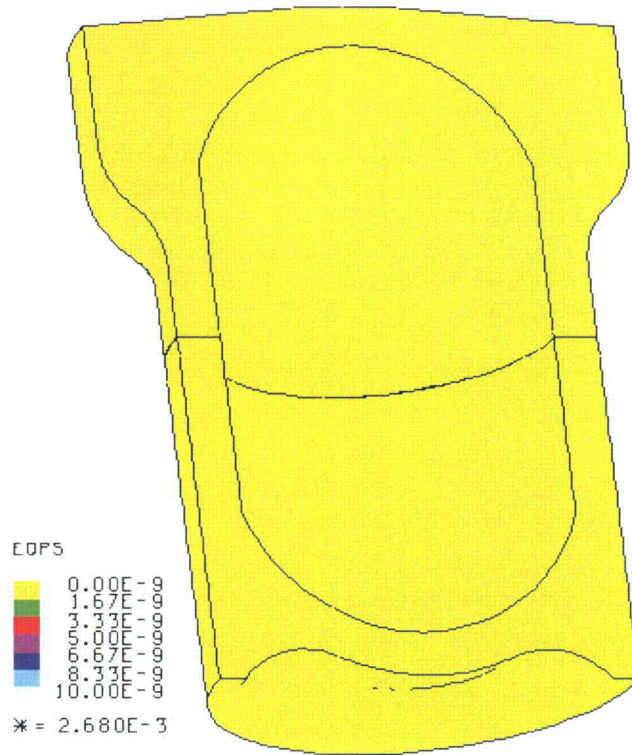


Figure 2-425. Plot of EQPS in the TB-1 for HAC Run 11, 831 g, Plutonium Metal Hollow Cylinder, End Impact

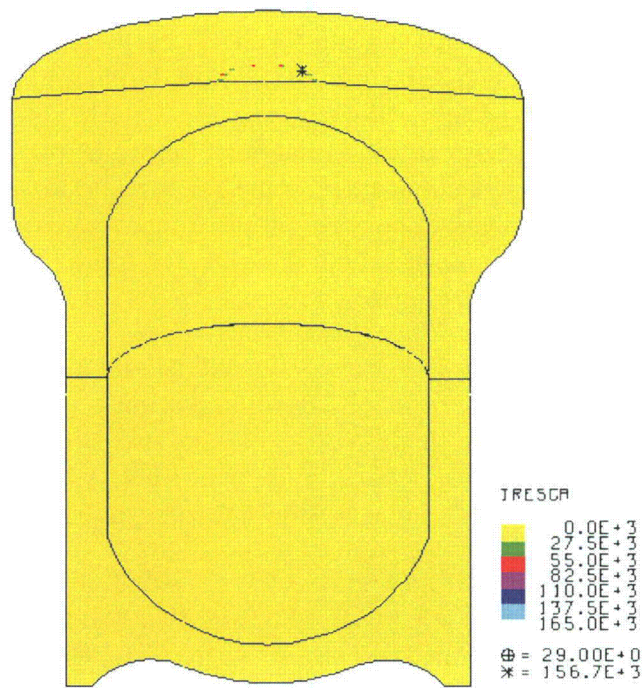
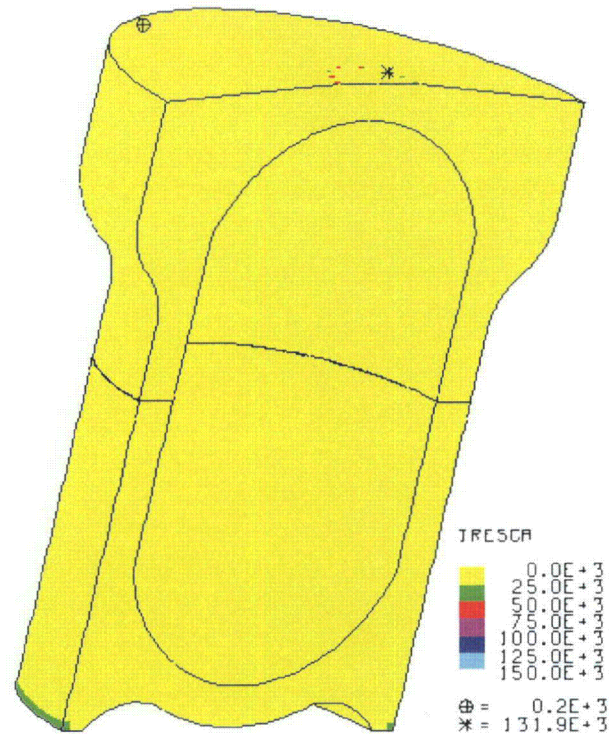


Figure 2-426. Plot of Tresca Stress in the TB-1 for HAC Run 11, 831 g, Plutonium Metal Hollow Cylinder, End Impact



**Figure 2-427. Plot of Tresca Stress in the TB-1 for HAC Run 11, 831 g Plutonium Metal Hollow Cylinder, End Impact when Plate Velocity Reaches Zero**

*2.12.5.6.12 HAC- Run 12, 831 g Plutonium Metal Hollow Cylinder, Side Impact*

The dynamic crush side impact HAC analysis run for the 831 g plutonium metal hollow cylinder uses the same model for the overpack as the one used in the previous 11 runs. The TB-1, T-Ampoule, and plutonium metal hollow cylinder are the same model as that used in the aircraft analysis. The finite element mesh and initial position of the model are shown in Figure 2-428. The plutonium metal hollow cylinder within the T-Ampoule is positioned at the bottom of the model because it was considered to be at rest at the time of impact. The plate was positioned between the flanges to be most damaging to the TB-1 and contents by preventing the flanges from absorbing energy and slowing down the plate before it hits the overpack.

The post-impact deformation is shown in Figure 2-429 and its kinetic energy history in Figure 2-430. The flanges on the overpack deform, and the cylinder bounces due to the impact of the plate. Zero elements extended beyond the tested Bao-Wierzbicki strain locus. The maximum Tearing Parameter value for this analysis was  $2.94\text{e-}6$ , and is below the critical Tearing Parameter value of 1.012 for Ti-6Al-4V, thus T-Ampoule integrity is maintained.

Peak EQPS in the TB-1 vessel is shown in Figure 2-431 to be  $32.78\text{e-}3$ , and is localized in the outer contact regions with the redwood overpack. Figures 2-432 and 2-433 plot the Tresca stresses within the TB-1. The maximum Tresca stress in the TB-1 is 173.8 ksi, but there are no through thickness stresses exceeding the limit of 106.6 ksi, which can be seen clearly in the figure. Figure 2-434 is a plot of the Tresca stresses at the time when all of the kinetic energy of the plate has been transferred to the package, just as the plate begins to rebound. The maximum

through thickness stress at this time is below 20.8 ksi, below the allowable through thickness stress of 106.6 ksi, as seen in the figure.

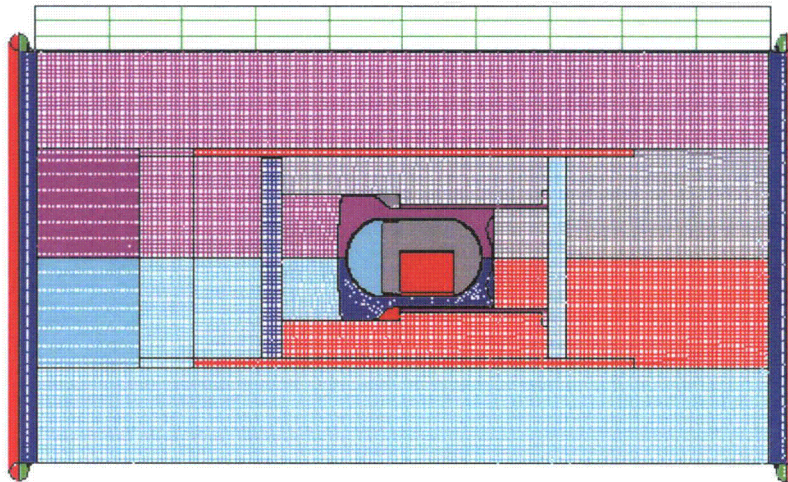


**Figure 2-428. Finite Element Mesh for HAC Run 12, 831 g, Plutonium Metal Hollow Cylinder, Side Impact**

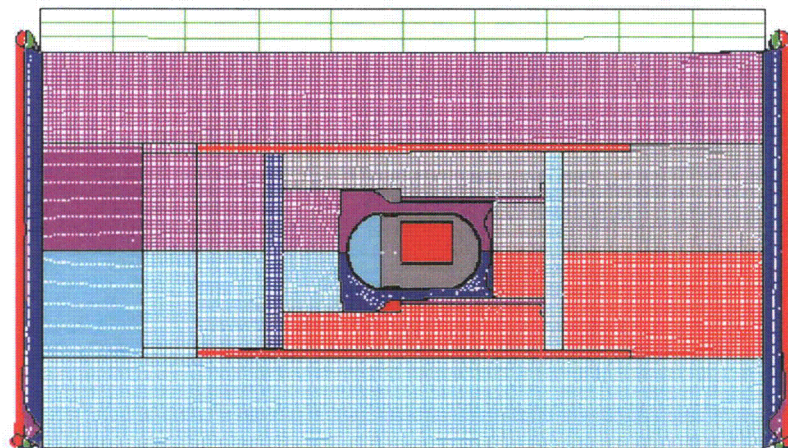


**Figure 2-429. Finite Element Mesh for HAC Run 12, 831 g, Plutonium Metal Hollow Cylinder, Side Impact – Final Displacement**

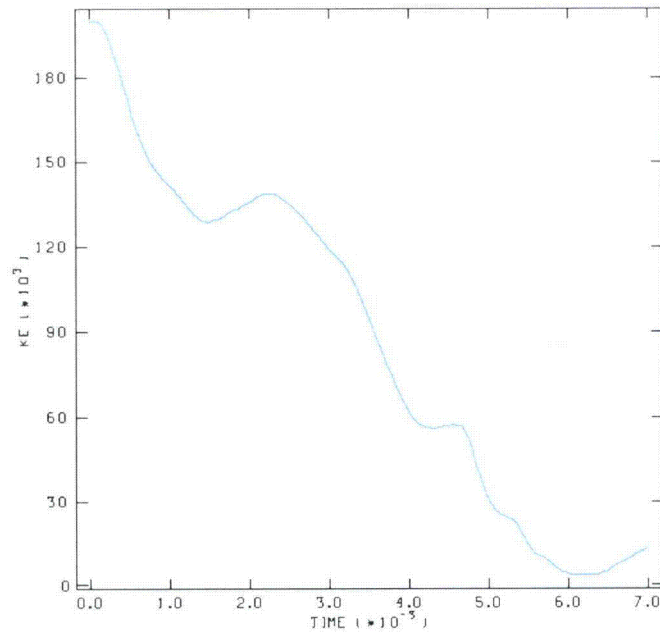


**Figure 2-430. Kinetic Energy Time History for HAC Run 12, 831 g, Plutonium Metal Hollow Cylinder, Side Impact**

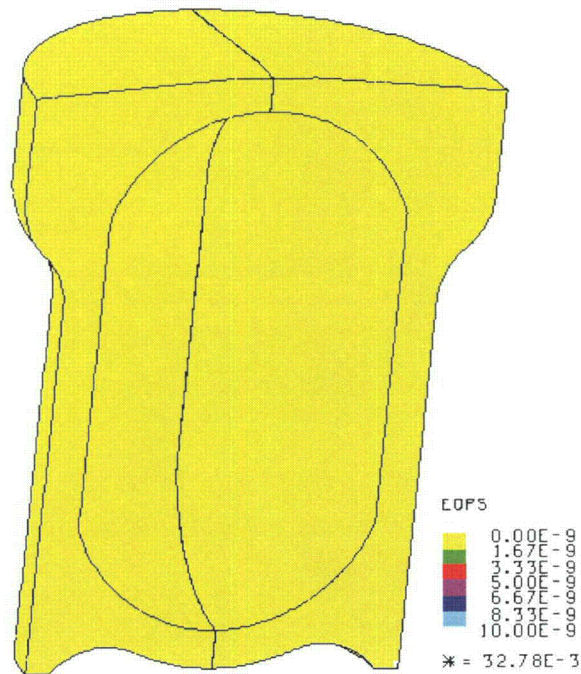


**Figure 2-431. Plot of EQPS in the TB-1 for HAC Run 12, 831 g, Plutonium Metal Hollow Cylinder, Side Impact**

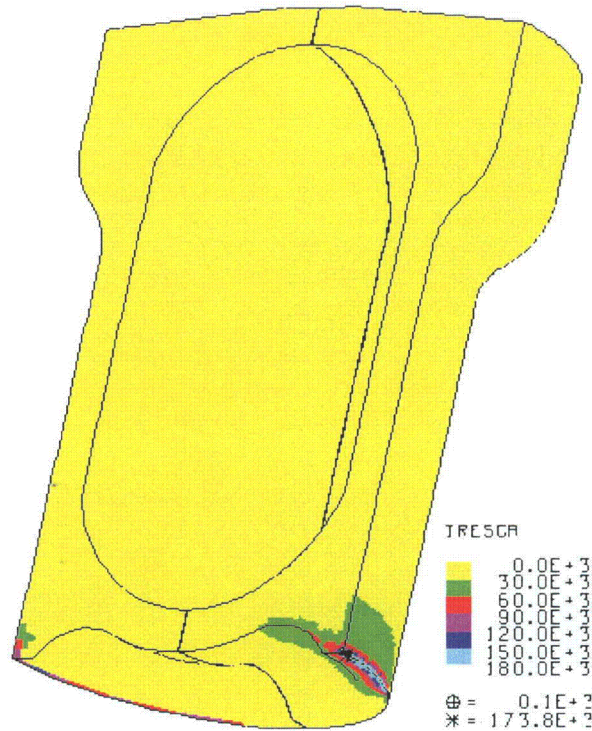


Figure 2-432. Plot of Tresca Stress in the TB-1 for HAC Run 12, 831 g Plutonium Metal Hollow Cylinder, Side Impact

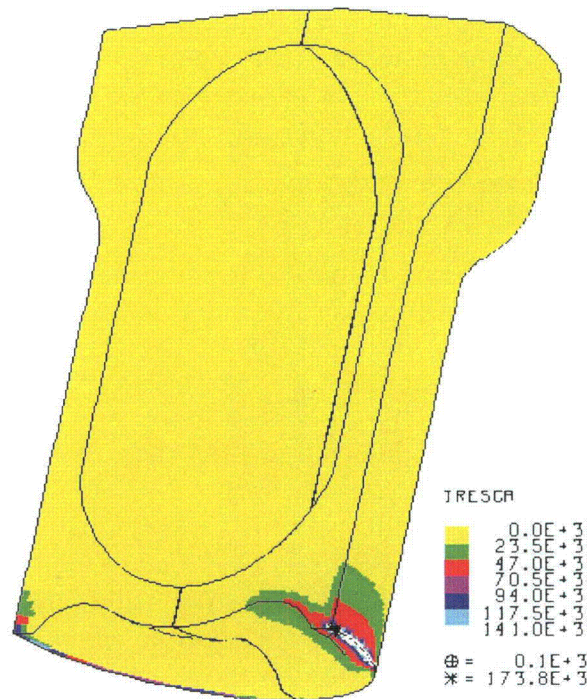
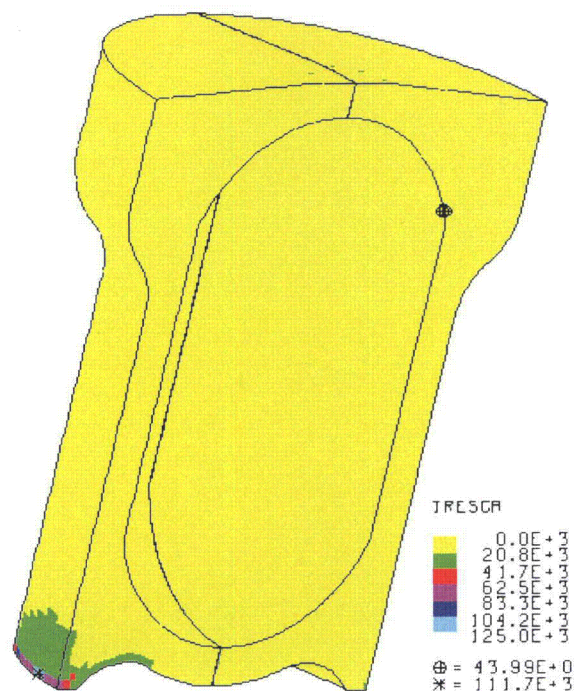


Figure 2-433. Plot of Tresca Stress for HAC Run 12, 831 g Plutonium Metal Hollow Cylinder, Side Impact



**Figure 2-434. Plot of Tresca Stress for HAC Run 12, 831 g Plutonium Metal Hollow Cylinder, Side Impact when Plate Velocity Reaches Zero**

*2.12.5.6.13 HAC- Run 13, 831 g Angled Plutonium Metal Hollow Cylinder, End Impact*

The dynamic crush end impact HAC analysis run for the 831 g angled plutonium metal hollow cylinder uses the same model for the overpack as the one used in the previous 12 runs. The TB-1, T-Ampoule, and plutonium metal hollow cylinder are the same model as that used in the aircraft analysis. The finite element mesh and initial position of the model are shown in Figure 2-435. The plutonium metal hollow cylinder within the T-Ampoule is positioned at the bottom of the model because it was considered to be at rest at the time of impact.

The post-impact deformation is shown in Figure 2-436 and its kinetic energy history in Figure 2-437. The flanges on the overpack deform, and the contents bounce due to the impact of the plate. Zero elements extended beyond the tested Bao-Wierzbicki strain locus. The maximum Tearing Parameter value for this analysis was 0.

Peak EQPS in the TB-1 vessel is shown in Figure 2-438 to be  $2.389\text{e-}3$ , and is localized in the outer contact regions with the redwood overpack. Figure 2-439 plots the Tresca stresses within the TB-1. The maximum Tresca stress in the TB-1 is 155.6 ksi, but there are no through thickness stresses exceeding the limit of 106.6 ksi, which can be seen clearly in the figure. Figure 2-440 is a plot of the Tresca stresses at the time when all of the kinetic energy of the plate has been transferred to the package, just as the plate begins to rebound. The maximum through thickness stress at this time is below 25.0 ksi, below the allowable through thickness stress of 106.6 ksi, as seen in the figure.

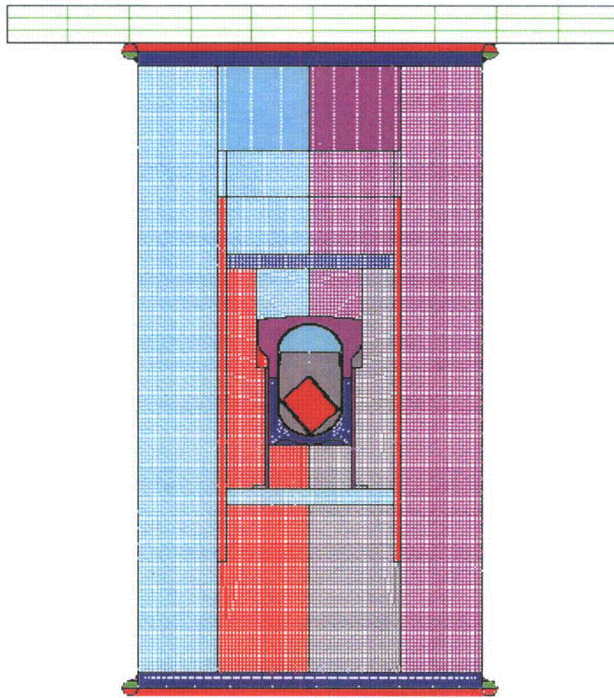


Figure 2-435. Finite Element Mesh for HAC Run 13, 831 g, Angled, Plutonium Metal Hollow Cylinder, End Impact

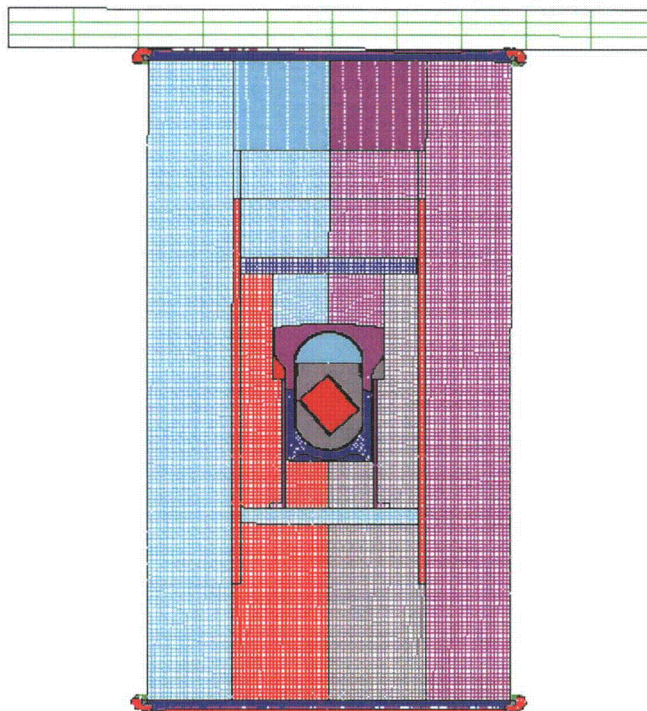
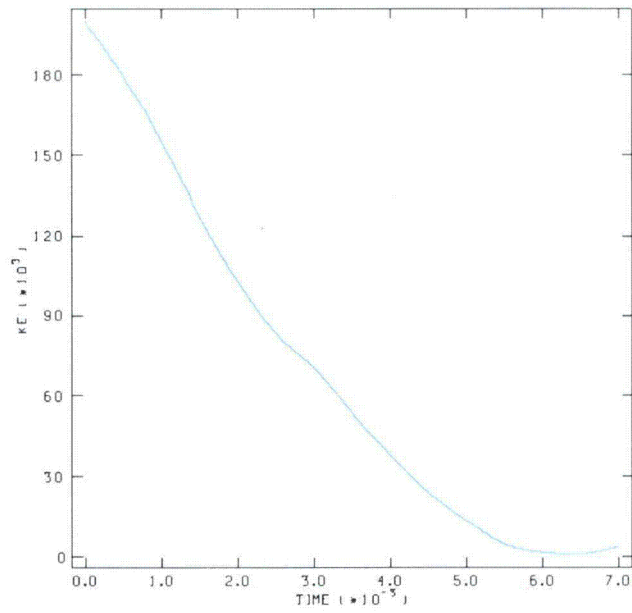
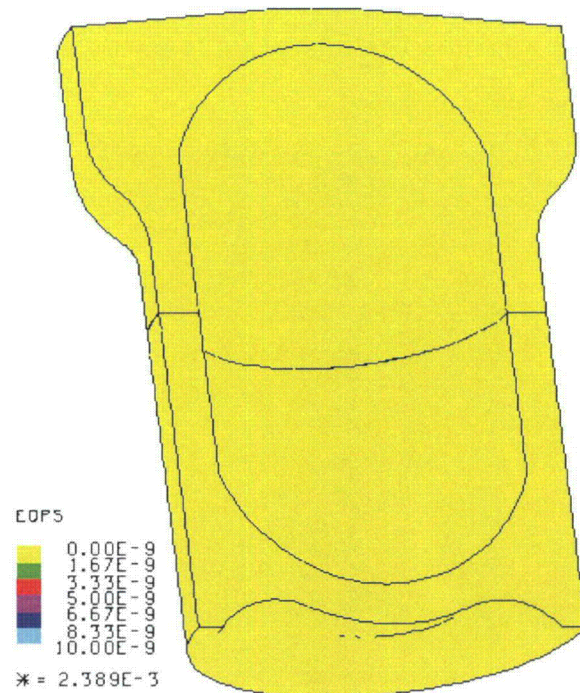


Figure 2-436. Finite Element Mesh for HAC Run 13, 831 g, Angled, Plutonium Metal Hollow Cylinder, End Impact – Final Displacement



**Figure 2-437. Kinetic Energy Time History for HAC Run 13, 831 g, Angled, Plutonium Metal Hollow Cylinder, End Impact**



**Figure 2-438. Plot of EQPS in the TB-1 for HAC Run 13, 831 g, Angled, Plutonium Metal Hollow Cylinder, End Impact**

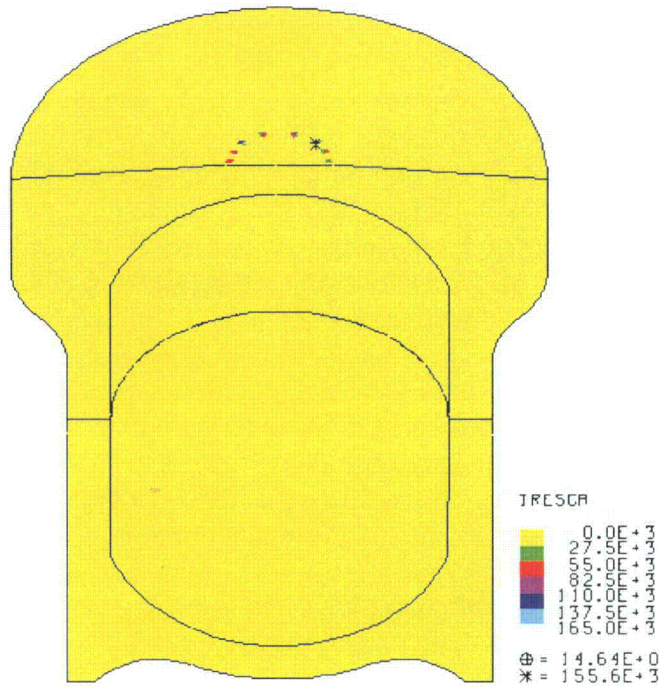


Figure 2-439. Plot of Tresca Stress in the TB-1 for HAC Run 13, 831 g, Angled, Plutonium Metal Hollow Cylinder, End Impact

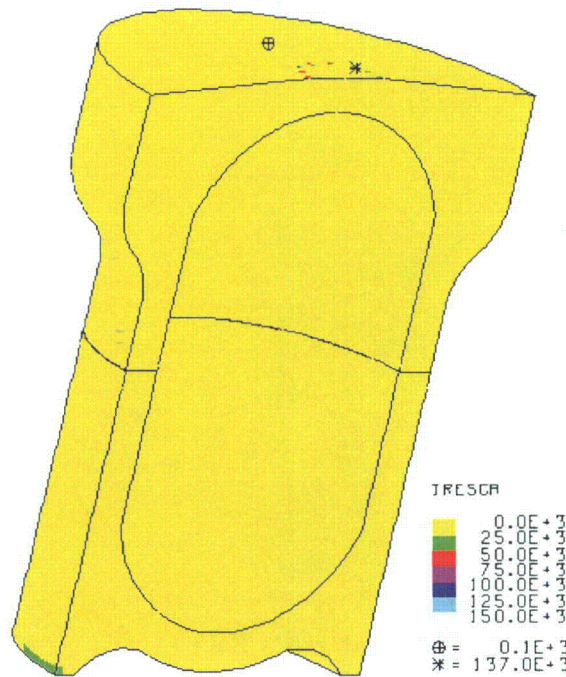


Figure 2-440. Plot of Tresca Stress in the TB-1 for HAC Run 13, 831 g Angled Plutonium Metal Hollow Cylinder, End Impact when Plate Velocity Reaches Zero

#### 2.12.5.6.14 HAC- Run 14, 831 g Angled Plutonium Metal Hollow Cylinder, Side Impact

The dynamic crush side impact HAC analysis run for the 831 g angled plutonium metal hollow cylinder uses the same model for the overpack as the one used in the previous 13 runs. The TB-1, T-Ampoule, and plutonium metal hollow cylinder are the same model as that used in the aircraft analysis. The finite element mesh and initial position of the model are shown in Figure 2-441. The plutonium metal hollow cylinder within the T-Ampoule is positioned at the bottom of the model because it was considered to be at rest at the time of impact. The plate was positioned between the flanges to be most damaging to the TB-1 and contents by preventing the flanges from absorbing energy and slowing down the plate before it hits the overpack.

The post-impact deformation is shown in Figure 2-442 and its kinetic energy history in Figure 2-443. The flanges on the overpack deform, and the cylinder bounces due to the impact of the plate. Zero elements extended beyond the tested Bao-Wierzbicki strain locus. The maximum Tearing Parameter value for this analysis was  $2.01e-2$ , and is below the critical Tearing Parameter value of 1.012 for Ti-6Al-4V, thus T-Ampoule integrity is maintained.

Peak EQPS in the TB-1 vessel is shown in Figure 2-444 to be  $31.46e-3$ , and is localized in the outer contact regions with the redwood overpack. Figure 2-445 plots the Tresca stresses within the TB-1. The maximum Tresca stress in the TB-1 is 172.5 ksi, but there are no through thickness stresses exceeding the limit of 106.6 ksi, which can be seen clearly in the figure. Figure 2-446 is a plot of the Tresca stresses at the time when all of the kinetic energy of the plate has been transferred to the package, just as the plate begins to rebound. The maximum through thickness stress at this time is below 25.0 ksi, below the allowable through thickness stress of 106.6 ksi, as seen in the figure.

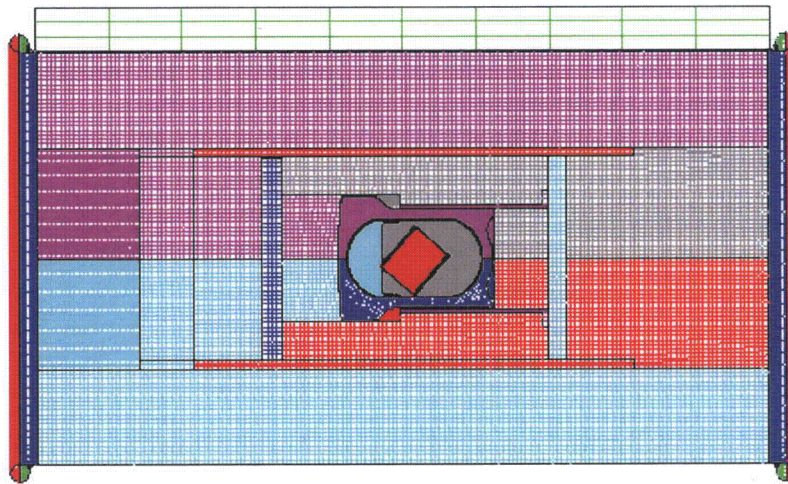


**Figure 2-441. Finite Element Mesh for HAC Run 14, 831 g Angled Plutonium Metal Hollow Cylinder, Side Impact**

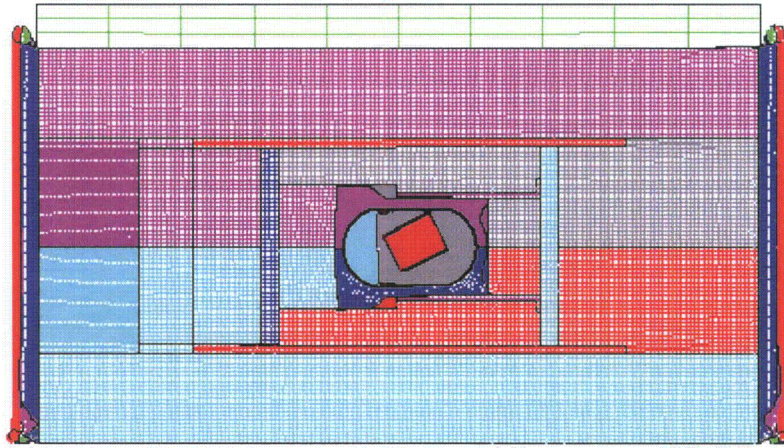


**Figure 2-442. Finite Element Mesh for HAC Run 14, 831 g Angled Plutonium Metal Hollow Cylinder, Side Impact – Final Displacement**

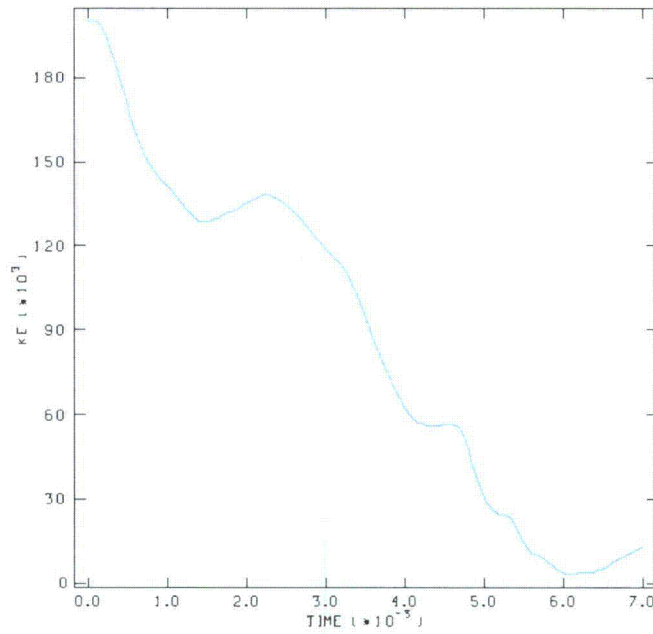


**Figure 2-443. Kinetic Energy Time History for HAC Run 14, 831 g Angled Plutonium Metal Hollow Cylinder, Side Impact**

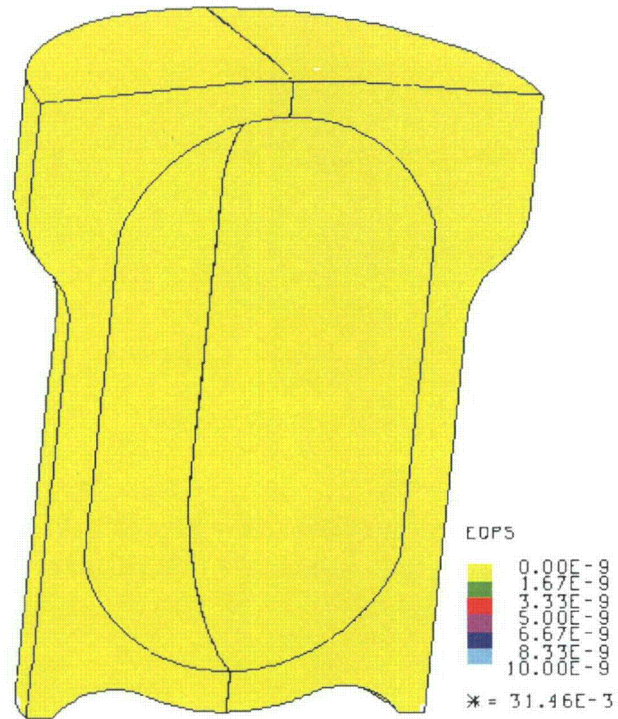


Figure 2-444. Plot of EQPS in the TB-1 for HAC Run 14, 831 g Angled Plutonium Metal Hollow Cylinder, Side Impact

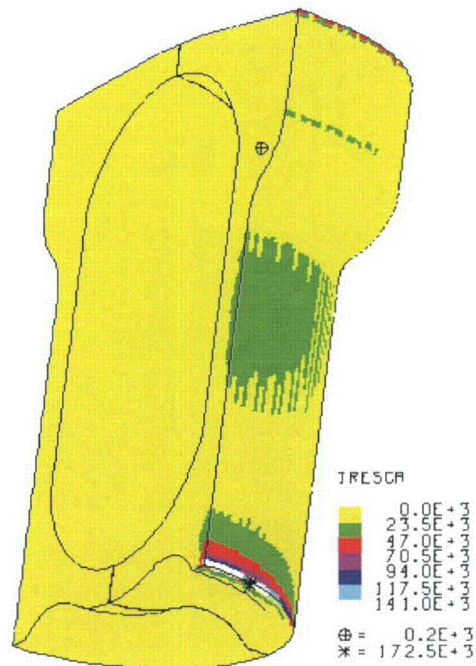
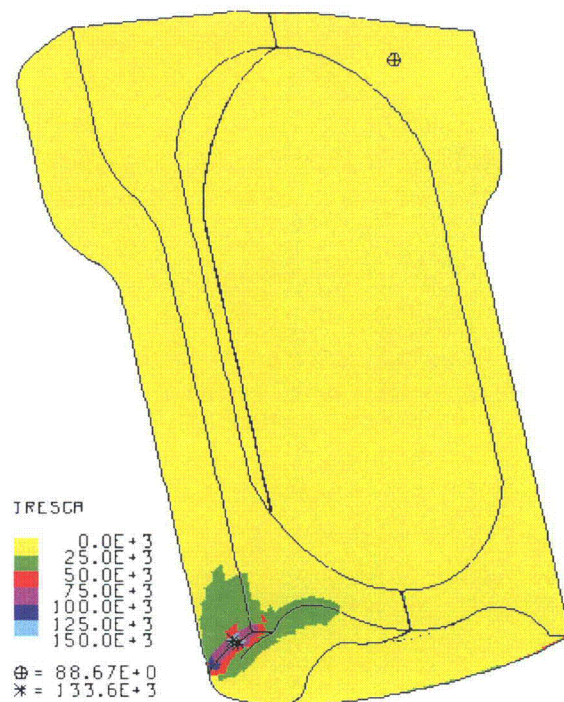


Figure 2-445. Plot of Tresca Stress in the TB-1 for HAC Run 14, 831 g Angled, Plutonium Metal Hollow Cylinder, Side Impact



**Figure 2-446. Plot of Tresca Stress in the TB-1 for HAC Run 14, 831 g Angled Plutonium Metal Hollow Cylinder, Side Impact when Plate Velocity Reaches Zero**

*2.12.5.6.15 HAC- Run 15, 831 g Angled Plutonium Metal Hollow Cylinder, CGOC Impact*

The dynamic crush CGOC impact HAC analysis run for the 831 g angled plutonium metal hollow cylinder uses the same overpack model as those used in HAC runs 1 through 14. The finite element mesh and initial position of the model are shown in Figure 2-447. The plutonium metal hollow cylinder within the T-Ampoule is positioned at the bottom of the model because it was considered to be at rest.

The post-impact deformation is shown in Figure 2-448 and its kinetic energy history in Figure 2-449. The flanges on the overpack deform, and the cylinder bounces due to the impact of the plate. The kinetic energy does not drop completely to zero because the plate is still vibrating and internal contents are still in motion. The plutonium metal hollow cylinder has bounced off of the top and bottom surface of the T-Ampoule, and the plate is now rebounding slowly with the package, ensuring that the highest containment vessel and contents loadings have occurred.

There was zero EQPS in the T-Ampoule and the TB-1, and the maximum Tearing Parameter was 0. Figure 2-450 is a plot of the Tresca stresses within the TB-1. The maximum Tresca stress in the TB-1 is 147.1 ksi, but there are no through thickness stresses exceeding the limit of 106.6 ksi, which can be seen clearly in the figure. Figure 2-451 is a plot of the Tresca stresses at the time when all of the kinetic energy of the plate has been transferred to the package, just as the plate begins to rebound. The maximum through thickness stress at this time is below 16.7 ksi, below the allowable through thickness stress of 106.6 ksi, as seen in the figure.

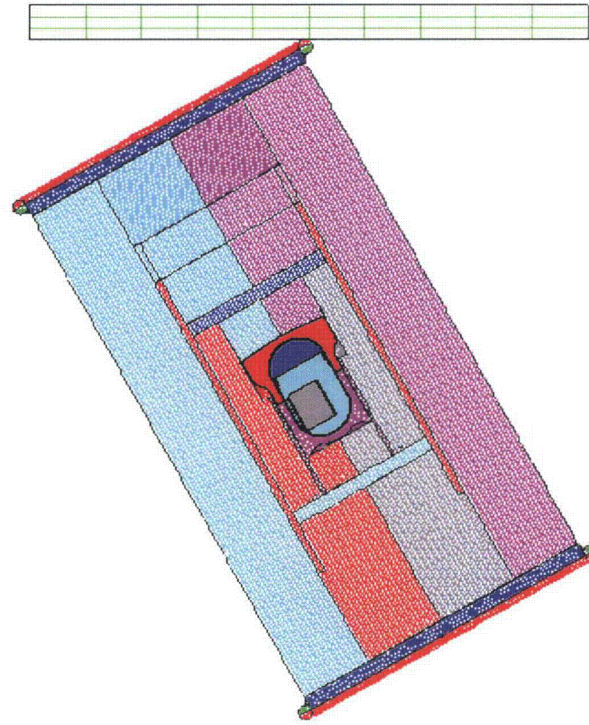


**Figure 2-447. Finite Element Mesh for HAC Run 15, 831 g Angled Plutonium Metal Hollow Cylinder, CGOC Impact**

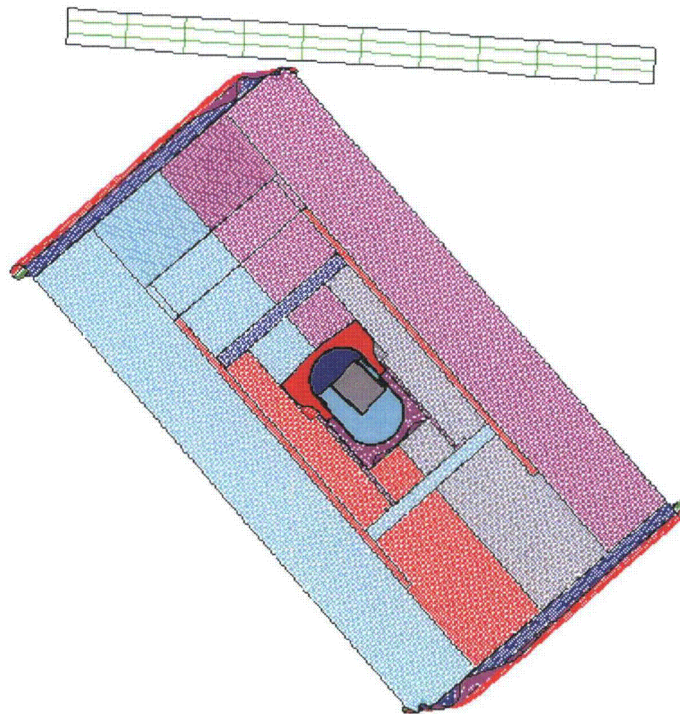


**Figure 2-448. Finite Element Mesh for HAC Run 15, 831 g Angled Plutonium Metal Hollow Cylinder, CGOC Impact – Final Displacement**

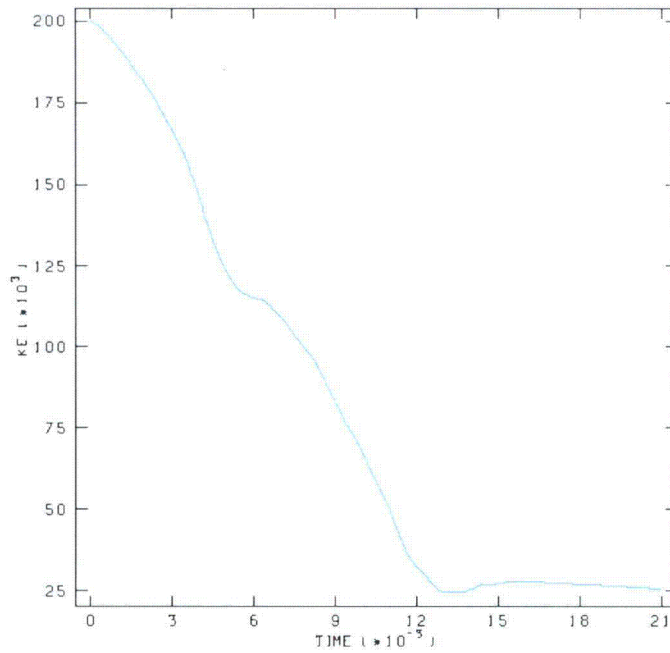


**Figure 2-449. Kinetic Energy Time History for HAC Run 15, 831 g Angled Plutonium Metal Hollow Cylinder, CGOC Impact**



**Figure 2-450. Plot of Tresca Stress in the TB-1 for HAC Run 15, 831 g Angled Plutonium Metal Hollow Cylinder, CGOC Impact**

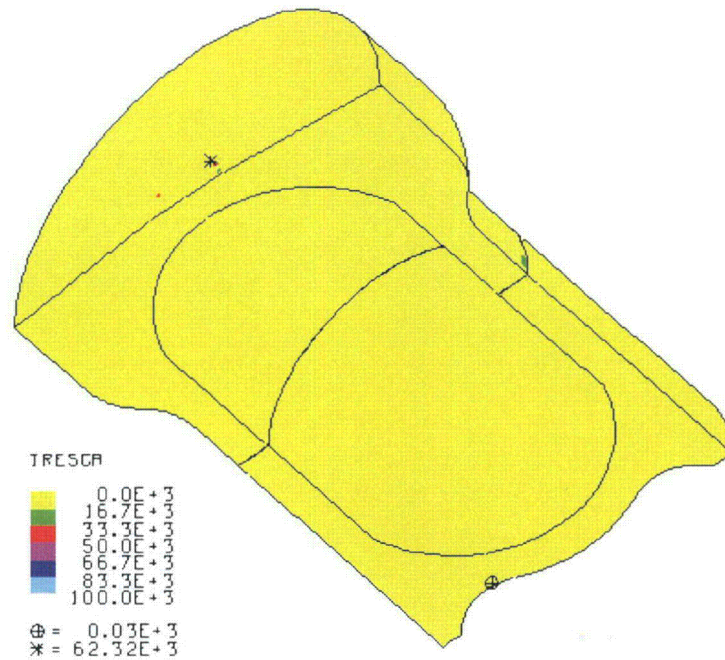


**Figure 2-451. Plot of Tresca Stress in the TB-1 for HAC Run 15, 831 g Angled Plutonium Metal Hollow Cylinder, CGOC Impact when Plate Velocity Reaches Zero**

*2.12.5.6.16 HAC- Run 16, 731 g Plutonium Metal Hollow Cylinder, End Impact*

The dynamic crush end impact HAC analysis run for the 731 g angled plutonium metal hollow cylinder uses the same model for the overpack as the one used in the previous 15 runs. The TB-1, T-Ampoule, and plutonium metal hollow cylinder are the same model as that used in the aircraft analysis. The finite element mesh and initial position of the model are shown in Figure 2-452. The plutonium metal hollow cylinder within the T-Ampoule is positioned at the bottom of the model because it was considered to be at rest at the time of impact.

The post-impact deformation is shown in Figure 2-453 and its kinetic energy history in Figure 2-454. The flanges on the overpack deform, and the cylinder bounces due to the impact of the plate. Zero elements extended beyond the tested Bao-Wierzbicki strain locus. The maximum Tearing Parameter value for this analysis was 0.

Peak EQPS in the TB-1 vessel is shown in Figures 2-455 and 2-456 to be  $2.237 \times 10^{-3}$ , and is localized in the outer contact regions with the redwood overpack. Figure 2-457 plots the Tresca stresses within the TB-1. The maximum Tresca stress in the TB-1 is 157.2 ksi, but there are no through thickness stresses exceeding the limit of 106.6 ksi, which can be seen clearly in the figure. Figure 2-458 is a plot of the Tresca stresses at the time when all of the kinetic energy of the plate has been transferred to the package, just as the plate begins to rebound. The maximum through thickness stress at this time is below 25.0 ksi, below the allowable through thickness stress of 106.6 ksi, as seen in the figure.

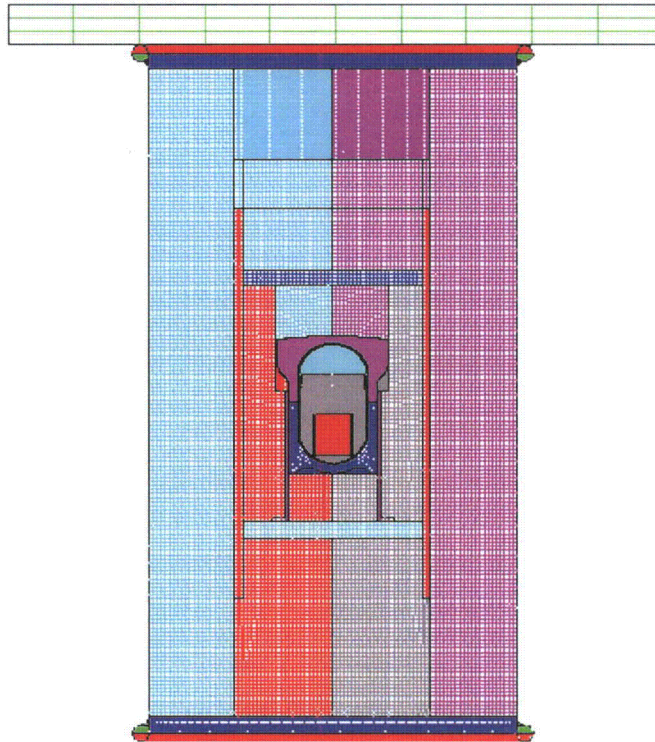


Figure 2-452. Finite Element Mesh for HAC Run 16, 731 g Plutonium Metal Hollow Cylinder, End Impact

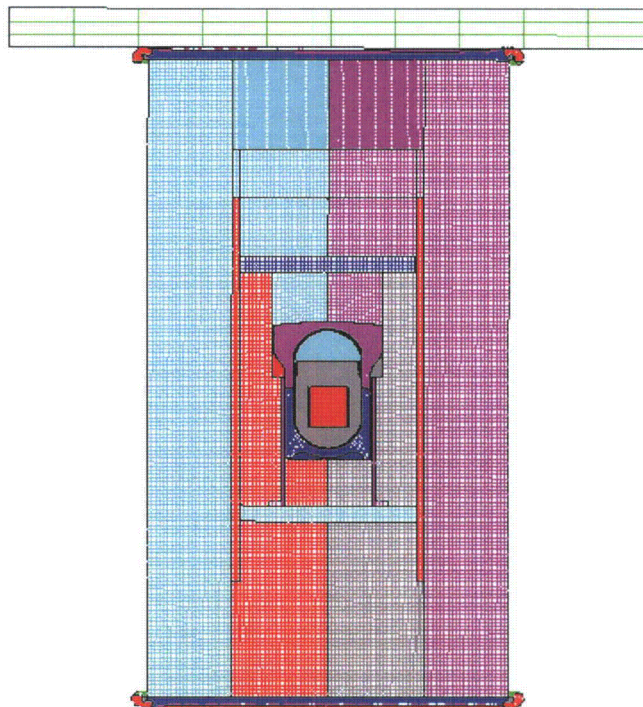
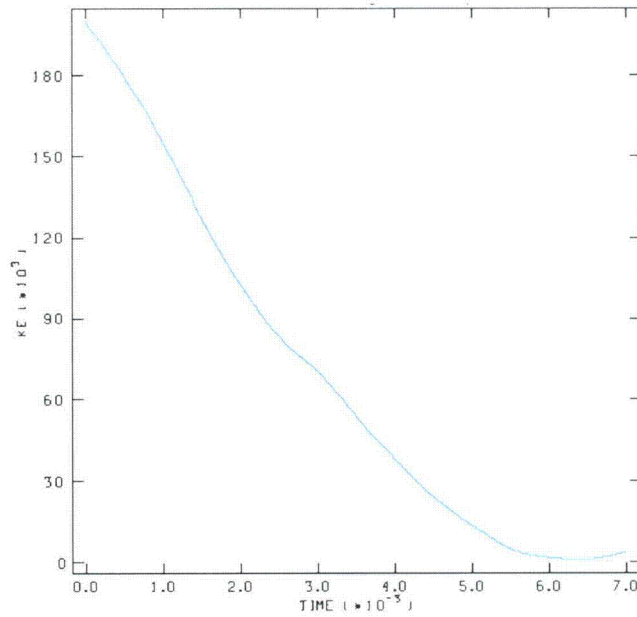
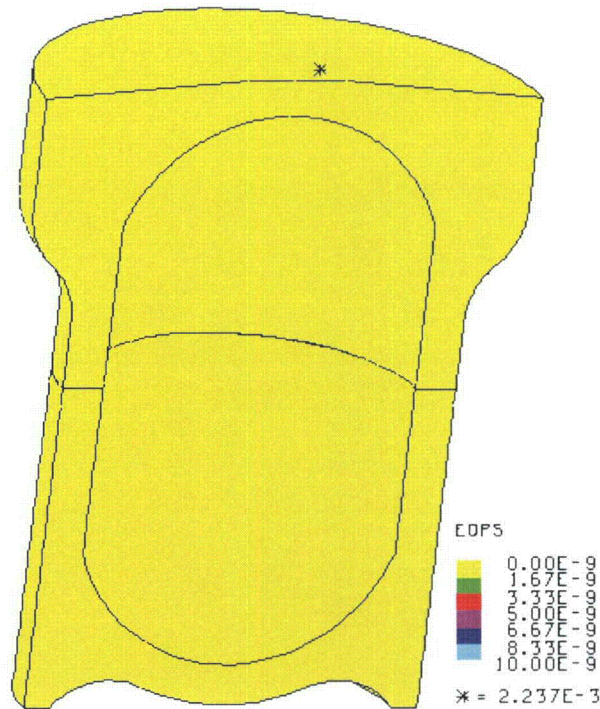


Figure 2-453. Finite Element Mesh for HAC Run 16, 731 g Plutonium Metal Hollow Cylinder, End Impact – Final Displacement



**Figure 2-454. Kinetic Energy Time History for HAC Run 16, 731 g Plutonium Metal Hollow Cylinder, End Impact**



**Figure 2-455. Plot of EQPS in the TB-1 for HAC Run 16, 731 g Plutonium Metal Hollow Cylinder, End Impact**

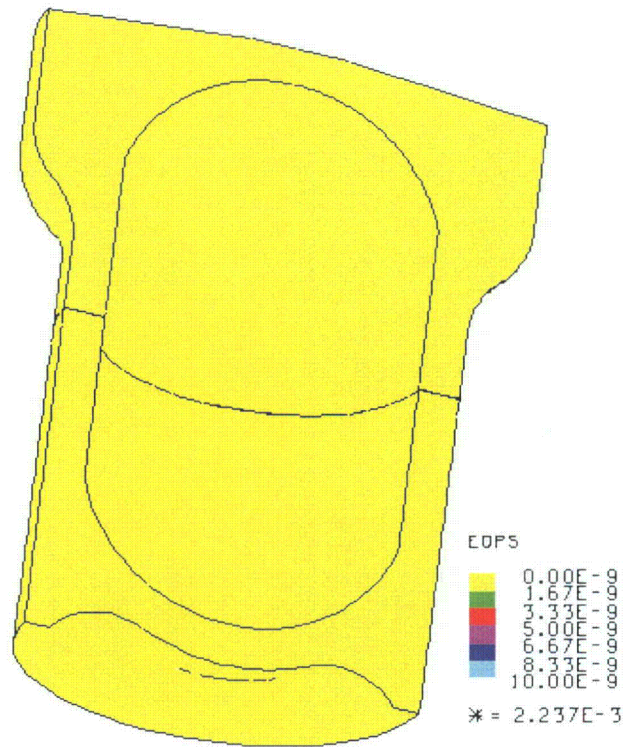


Figure 2-456. Plot of EQPS in the TB-1 for HAC Run 16, 731 g Plutonium Metal Hollow Cylinder, End Impact

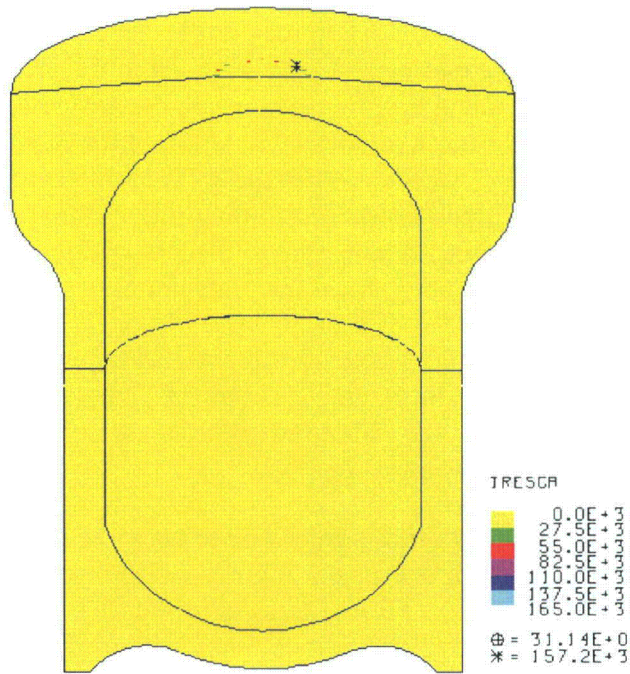
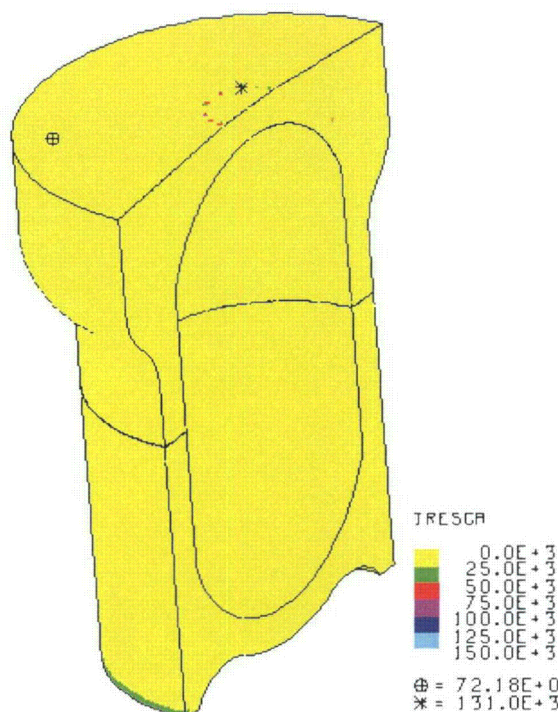


Figure 2-457. Plot of Tresca Stress in the TB-1 for HAC Run 16, 731 g Plutonium Metal Hollow Cylinder, End Impact



**Figure 2-458. Plot of Tresca Stress in the TB-1 for HAC Run 16, 731 g Plutonium Metal Hollow Cylinder, End Impact when Plate Velocity Reaches Zero**

*2.12.5.6.17 HAC- Run 17, 731 g Plutonium Metal Hollow Cylinder, Side Impact*

The dynamic crush side impact HAC analysis run for the 731 g angled plutonium metal hollow cylinder uses the same model for the overpack as the one used in the previous 16 runs. The TB-1, T-Ampoule, and plutonium metal hollow cylinder are the same model as that used in the aircraft analysis. The finite element mesh and initial position of the model are shown in Figure 2-459. The plutonium metal hollow cylinder within the T-Ampoule is positioned at the bottom of the model because it was considered to be at rest at the time of impact. The plate was positioned between the flanges to be most damaging to the TB-1 and contents by preventing the flanges from absorbing energy and slowing down the plate before it hits the overpack.

The post-impact deformation is shown in Figure 2-460 and its kinetic energy history in Figure 2-461. The flanges on the overpack deform, and the cylinder bounces due to the impact of the plate. Zero elements extended beyond the tested Bao-Wierzbicki strain locus. The maximum Tearing Parameter value for this analysis was 0.

Peak EQPS in the TB-1 vessel is shown in Figure 2-462 to be 45.76-3, and is localized in the outer contact regions with the redwood overpack. Figures 2-463 and 2-464 plot the Tresca stresses within the TB-1. The maximum Tresca stress in the TB-1 is 177.9 ksi, but there are no through thickness stresses exceeding the limit of 106.6 ksi, which can be seen clearly in the figure. Figure 2-465 is a plot of the Tresca stresses at the time when all of the kinetic energy of the plate has been transferred to the package, just as the plate begins to rebound. The maximum through thickness stress at this time is below 20.8 ksi, below the allowable through thickness stress of 106.6 ksi, as seen in the figure.

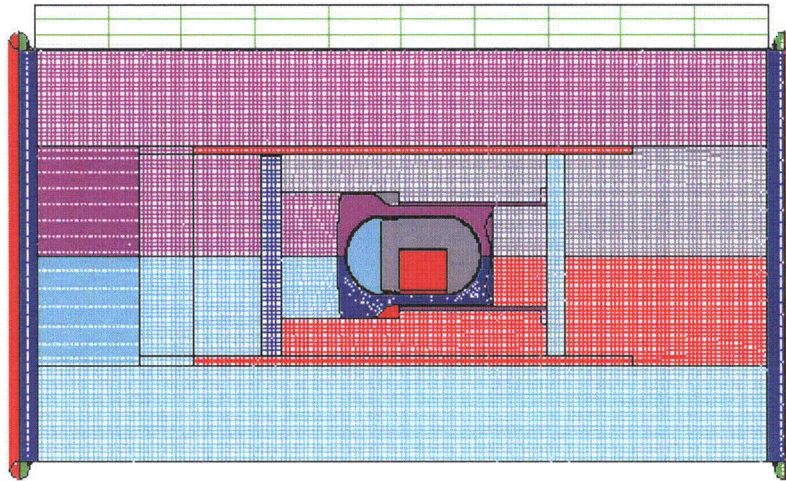


Figure 2-459. Finite Element Mesh for HAC Run 17, 731 g Plutonium Metal Hollow Cylinder, Side Impact

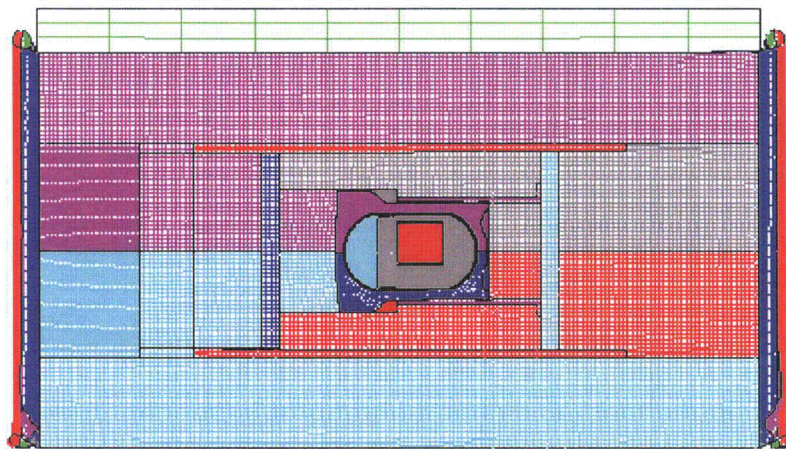


Figure 2-460. Finite Element Mesh for HAC Run 17, 731 g Plutonium Metal Hollow Cylinder, Side Impact – Final Displacement

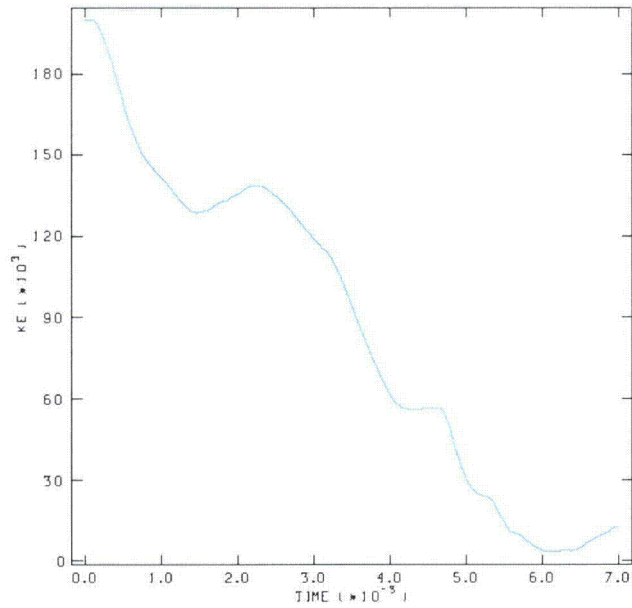
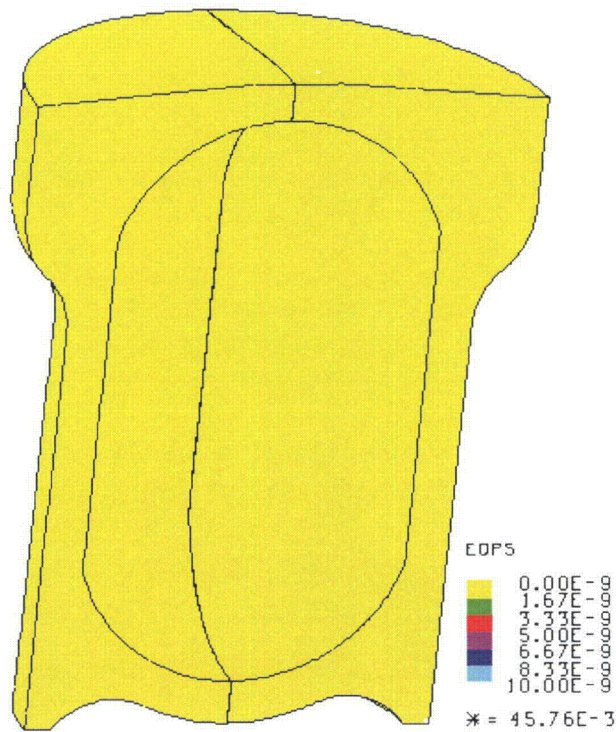


Figure 2-461. Kinetic Energy Time History for HAC Run 17, 731 g Plutonium Metal Hollow Cylinder, Side Impact



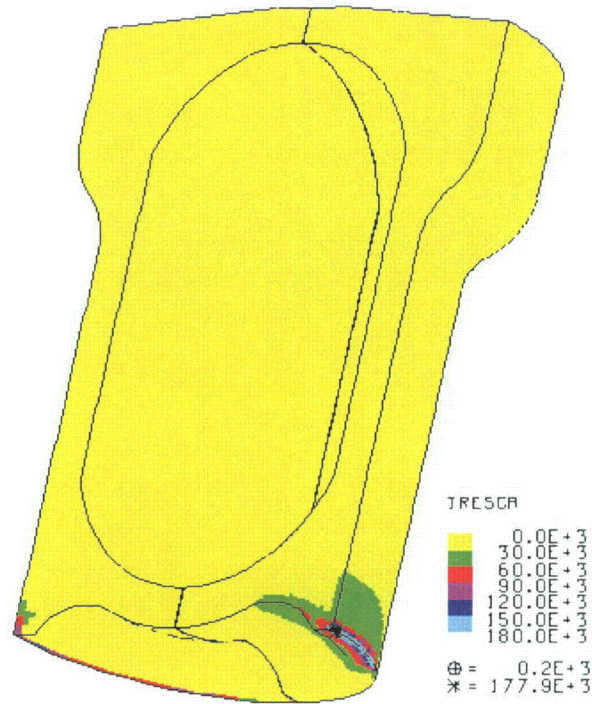


Figure 2-463. Plot of Tresca Stress in the TB-1 for HAC Run 17, 731 g Plutonium Metal Hollow Cylinder, Side Impact

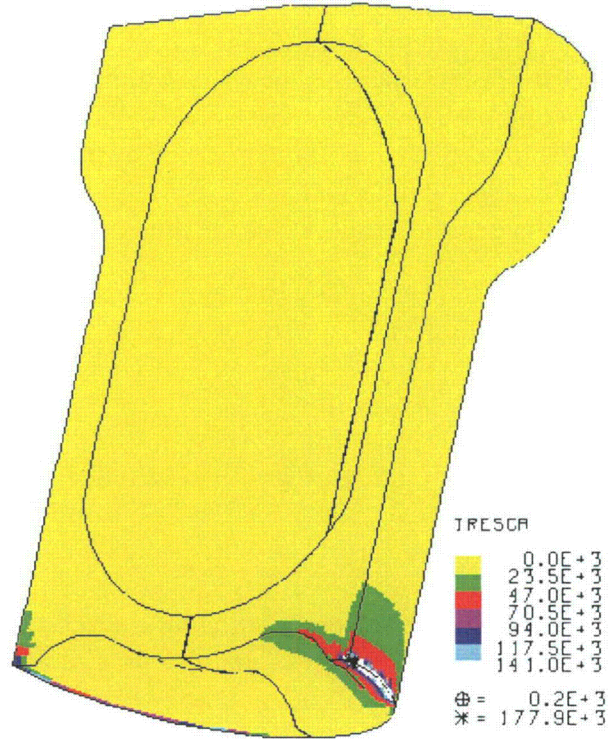


Figure 2-464. Plot of Tresca Stress in the TB-1 for HAC Run 17, 731 g Plutonium Metal Hollow Cylinder, Side Impact



**Figure 2-465. Plot of Tresca Stress in the TB-1 for HAC Run 17, 731 g Plutonium Metal Hollow Cylinder, Side Impact when Plate Velocity Reaches Zero**

*2.12.5.6.18 HAC- Run 18, 731 g Angled Plutonium Metal Hollow Cylinder, End Impact*

The dynamic crush end impact HAC analysis run for the 731 g angled plutonium metal hollow cylinder uses the same model for the overpack as the one used in the previous 17 runs. The TB-1, T-Ampoule, and plutonium metal hollow cylinder are the same model as that used in the aircraft analysis. The finite element mesh and initial position of the model are shown in Figure 2-466. The plutonium metal hollow cylinder within the T-Ampoule is positioned at the bottom of the model because it was considered to be at rest at the time of impact.

The post-impact deformation is shown in Figure 2-467 and its kinetic energy history in Figure 2-468. The flanges on the overpack deform, and the cylinder bounces due to the impact of the plate. Zero elements extended beyond the tested Bao-Wierzbicki strain locus. The maximum Tearing Parameter value for this analysis was 0.

Peak EQPS in the TB-1 vessel is shown in Figure 2-469 to be 0.2813e-3, and is localized in the outer contact regions with the redwood overpack. Figures 2-470 and 2-471 plot the Tresca stresses within the TB-1. The maximum Tresca stress in the TB-1 is 157.3 ksi, but there are no through thickness stresses exceeding the limit of 106.6 ksi, which can be seen clearly in the figure. Figure 2-472 is a plot of the Tresca stresses at the time when all of the kinetic energy of the plate has been transferred to the package, just as the plate begins to rebound. The maximum through thickness stress at this time is below 20.8 ksi, below the allowable through thickness stress of 106.6 ksi, as seen in the figure.

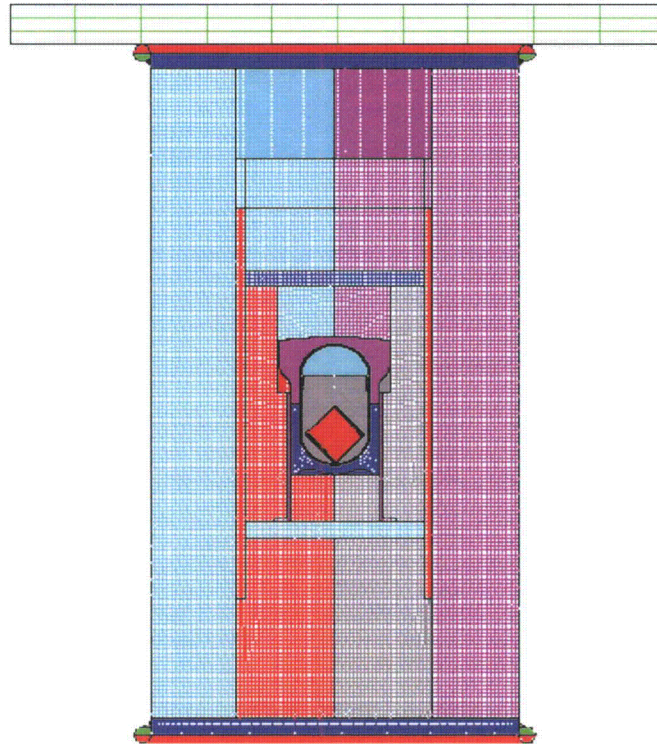


**Figure 2-466. Finite Element Mesh for HAC Run 18, 731 g Angled Plutonium Metal Hollow Cylinder, End Impact**

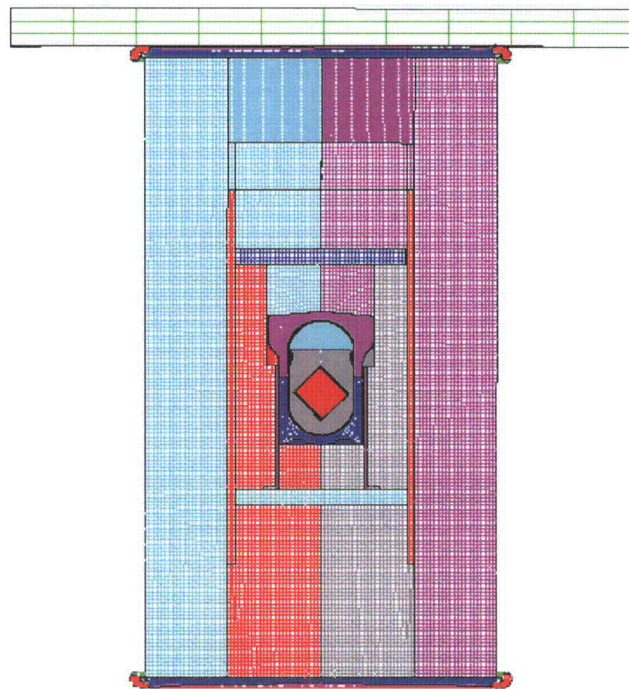


**Figure 2-467. Finite Element Mesh for HAC Run 18, 731 g Angled Plutonium Metal Hollow Cylinder, End Impact – Final Displacement**

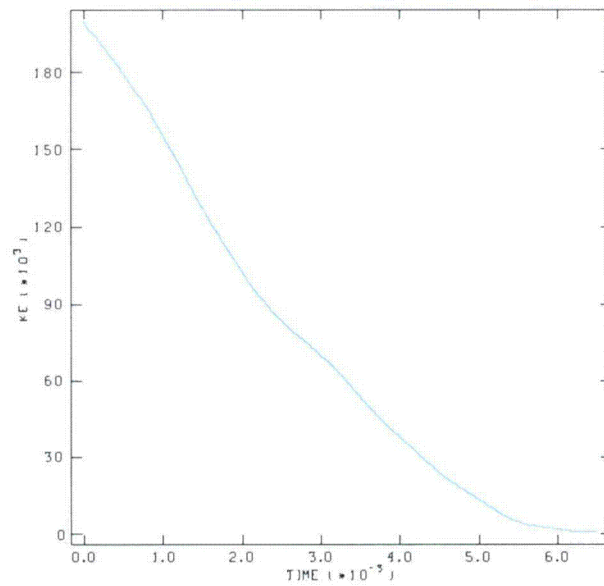


**Figure 2-468. Kinetic Energy Time History for HAC Run 18, 731 g Angled Plutonium Metal Hollow Cylinder, End Impact**

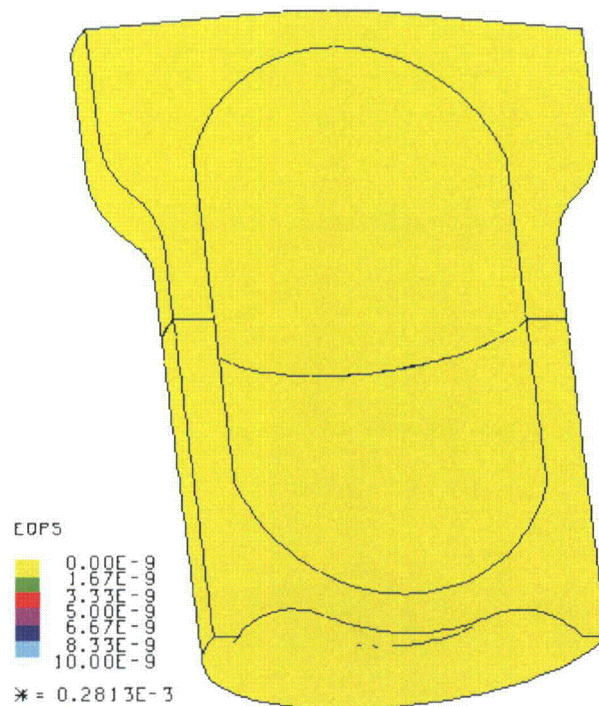


**Figure 2-469. Plot of EQPS in the TB-1 for HAC Run 18, 731 g Angled Plutonium Metal Hollow Cylinder, End Impact**

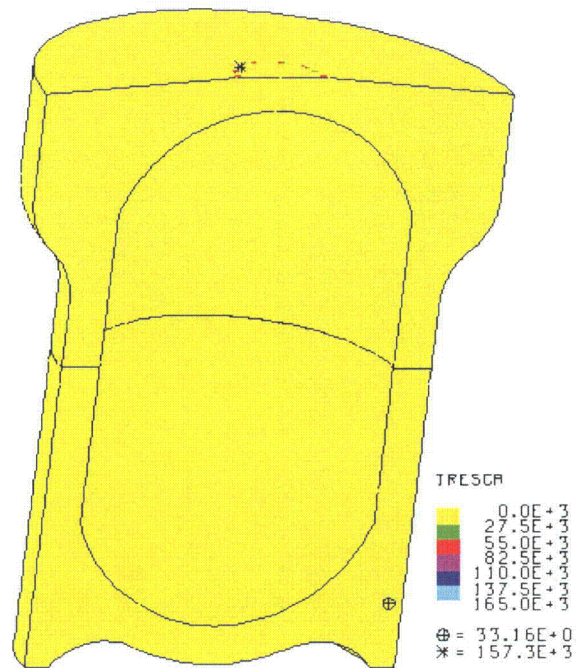


Figure 2-470. Plot of Tresca Stress in the TB-1 for HAC Run 18, 731 g Angled Plutonium Metal Hollow Cylinder, End Impact

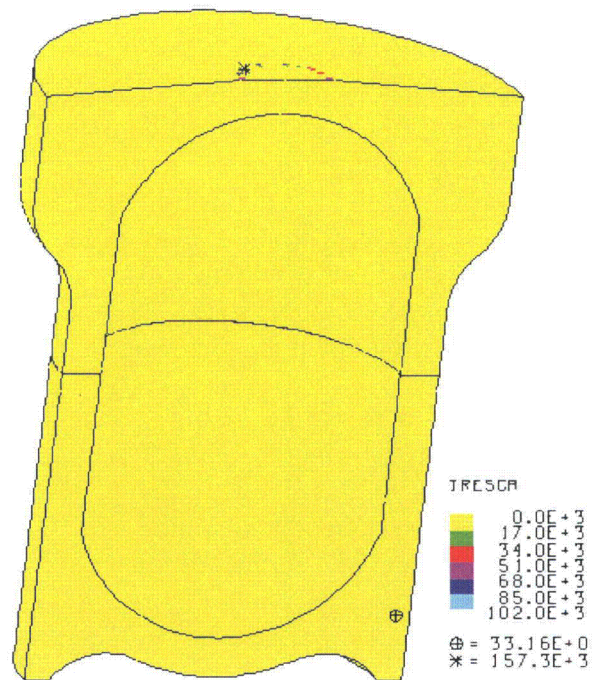
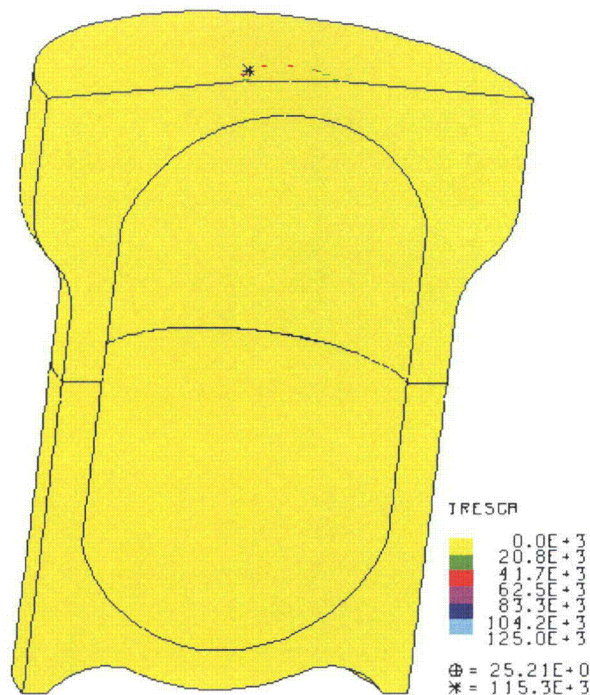


Figure 2-471. Plot of Tresca Stress in the TB-1 for HAC Run 18, 731 g Angled Plutonium Metal Hollow Cylinder, End Impact



**Figure 2-472. Plot of Tresca Stress in the TB-1 for HAC Run 18, 731 g Angled Plutonium Metal Hollow Cylinder, End Impact when Plate Velocity Reaches Zero**

*2.12.5.6.19 HAC- Run 19, 731 g Angled Plutonium Metal Hollow Cylinder, Side Impact*

The dynamic crush side impact HAC analysis run for the 731 g angled plutonium metal hollow cylinder uses the same model for the overpack as the one used in the previous 18 runs. The TB-1, T-Ampoule, and plutonium metal hollow cylinder are the same model as that used in the aircraft analysis. The finite element mesh and initial position of the model are shown in Figure 2-473. The plutonium metal hollow cylinder within the T-Ampoule is positioned at the bottom of the model because it was considered to be at rest at the time of impact. The plate was positioned between the flanges to be most damaging to the TB-1 and contents by preventing the flanges from absorbing energy and slowing down the plate before it hits the overpack.

The post-impact deformation is shown in Figure 2-474 and its kinetic energy history in Figure 2-475. The flanges on the overpack deform, and the cylinder bounces due to the impact of the plate. Average stress-triaxiality versus EQPS is shown in Figures 2-476 and 2-477 for the elements extending beyond the tested Bao-Wierzbicki strain locus. These elements are at high stress triaxiality and low EQPS. The graph of Tearing Parameter versus EQPS for those elements extending beyond the strain locus is shown in Figure 2-478. The elements that exceeded the strain locus are highlighted in red Figure 2-479. The maximum Tearing Parameter value for this analysis was 5.092e-2, and is below the critical Tearing Parameter value of 1.012 for Ti-6Al-4V, thus T-Ampoule integrity is maintained.

Peak EQPS in the TB-1 vessel is shown in Figure 2-480 to be 0.1124, and is localized in the outer contact regions with the redwood overpack. Figures 2-481 and 2-482 plot the Tresca stresses within the TB-1. The maximum Tresca stress in the TB-1 is 201.7 ksi, but there are no through thickness stresses exceeding the limit of 106.6 ksi, which can be seen clearly in the

figures. Figure 2-483 is a plot of the Tresca stresses at the time when all of the kinetic energy of the plate has been transferred to the package, just as the plate begins to rebound. The maximum through thickness stress at this time is below 33.3 ksi, below the allowable through thickness stress of 106.6 ksi, as seen in the figure.

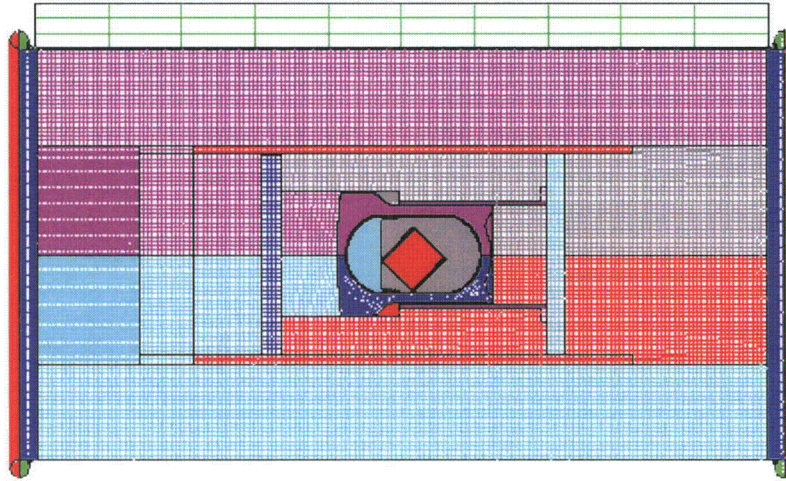


**Figure 2-473. Finite Element Mesh for HAC Run 19, 731 g Angled Plutonium Metal Hollow Cylinder, Side Impact**

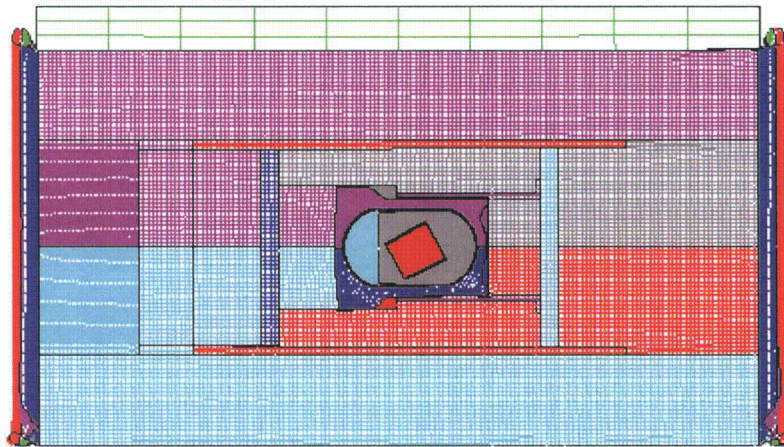


**Figure 2-474. Finite Element Mesh for HAC Run 19, 731 g Angled Plutonium Metal Hollow Cylinder, Side Impact – Final Displacement**

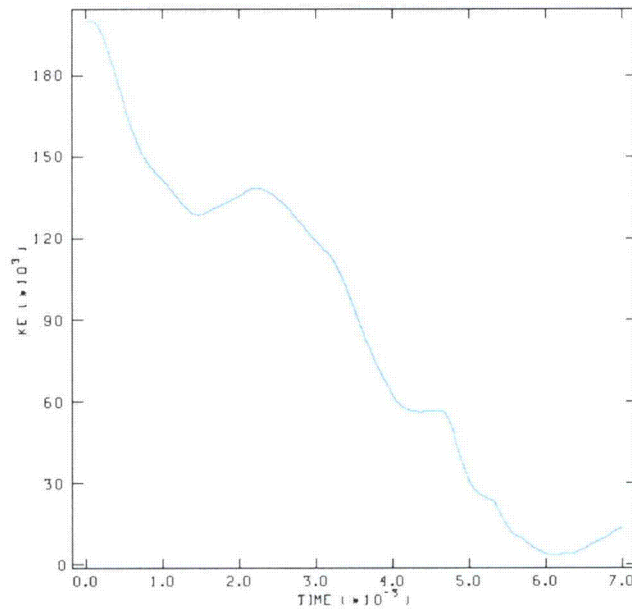


Figure 2-475. Kinetic Energy Time History for HAC Run 19, 731 g Angled Plutonium Metal Hollow Cylinder, Side Impact

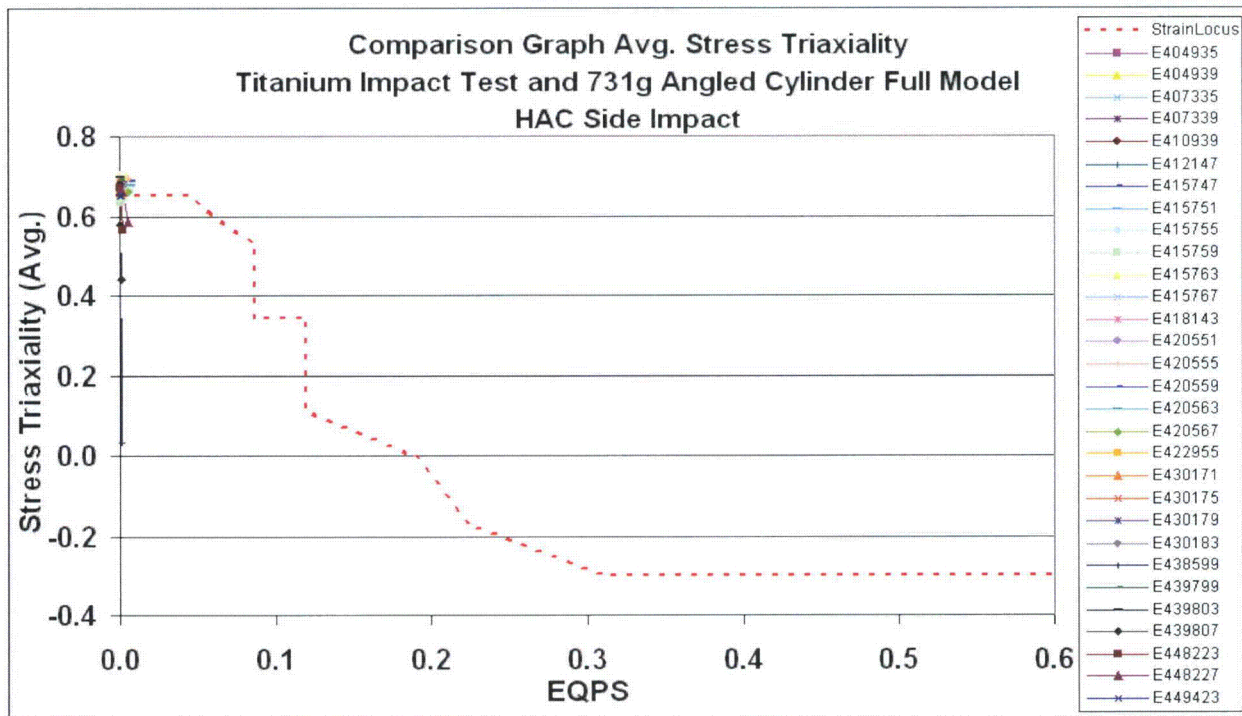
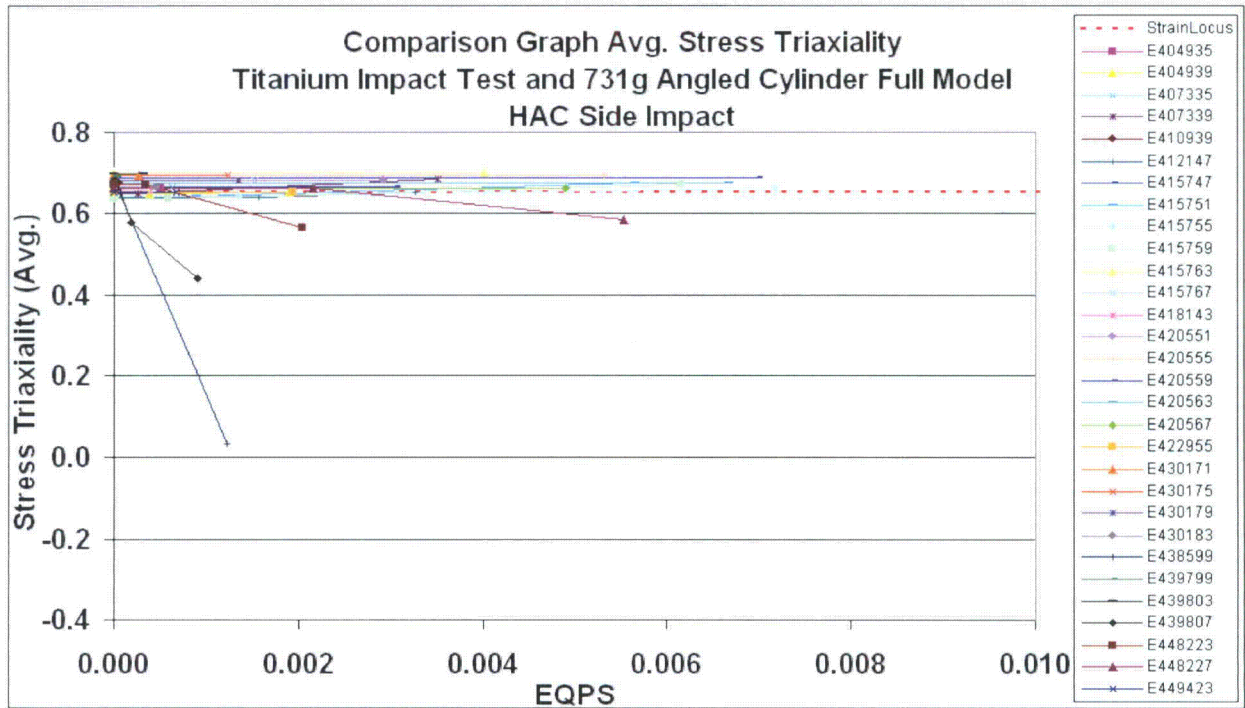
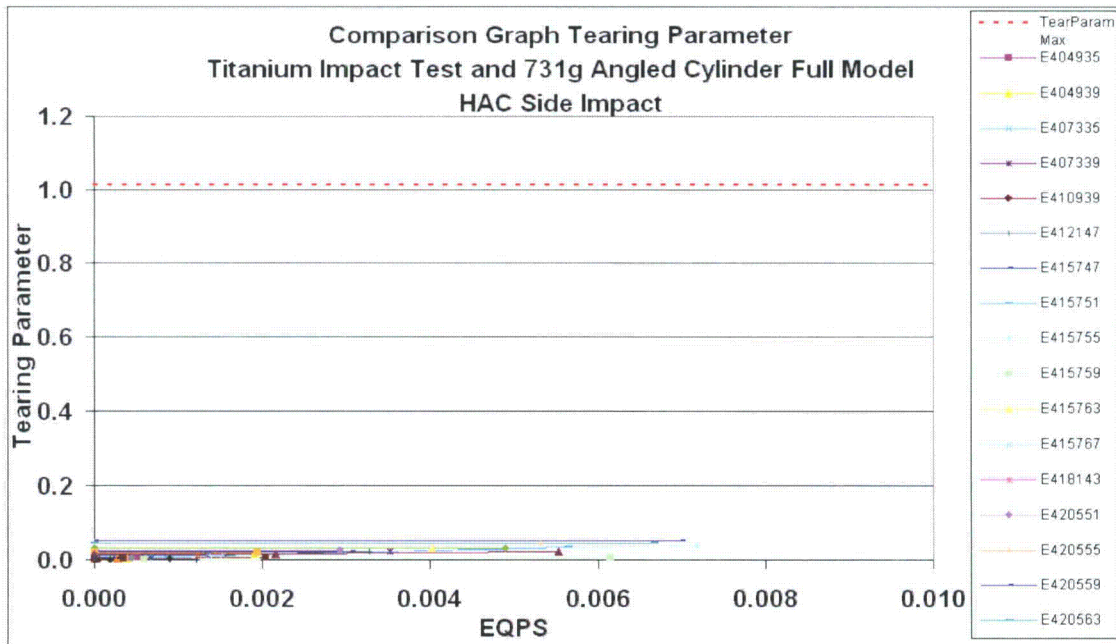


Figure 2-476. Graph of Average Stress Triaxiality versus EQPS for Elements Exceeding the Experimental Strain Locus for HAC Run 19, 731 g Angled Plutonium Metal Hollow Cylinder, Side Impact



**Figure 2-477. Graph of Average Stress Triaxiality versus EQPS for Elements Exceeding the Experimental Strain Locus (Zoomed In) for HAC Run 19, 731 g Angled Plutonium Metal Hollow Cylinder, Side Impact**



**Figure 2-478. Graph of Tearing Parameter versus EQPS for Elements Exceeding the Experimental Strain Locus for HAC Run 19, 731 g Angled Plutonium Metal Hollow Cylinder, Side Impact**

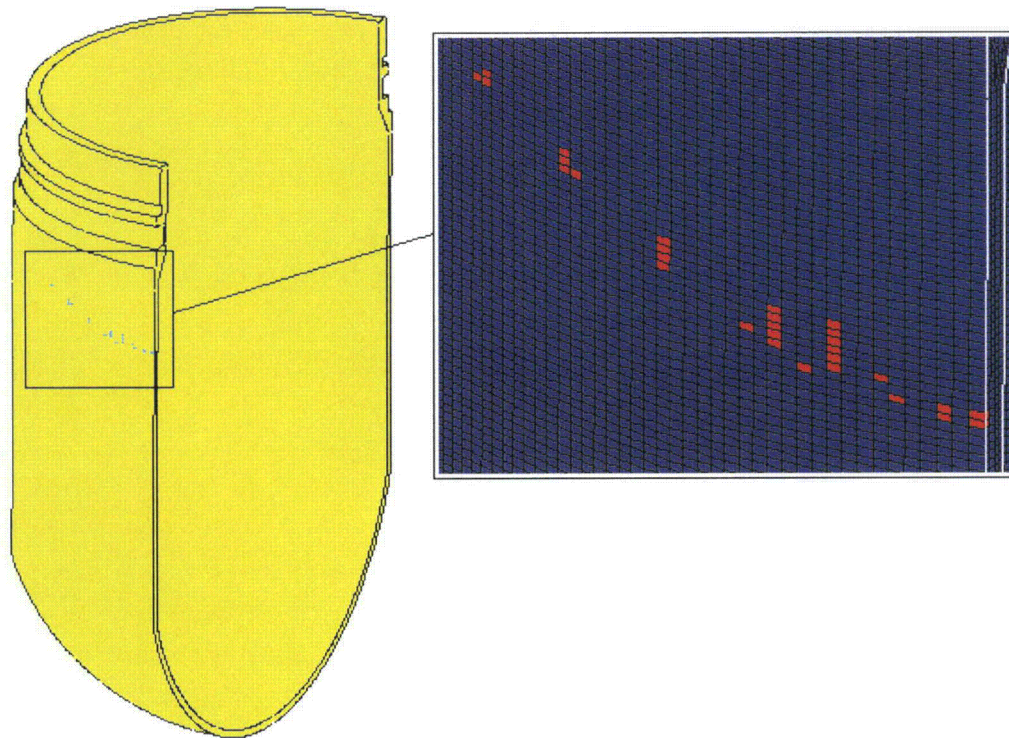


**Figure 2-479. Plot of Elements Exceeding the Experimental Strain Locus for HAC Run 19, 731 g Angled Plutonium Metal Hollow Cylinder, Side Impact**

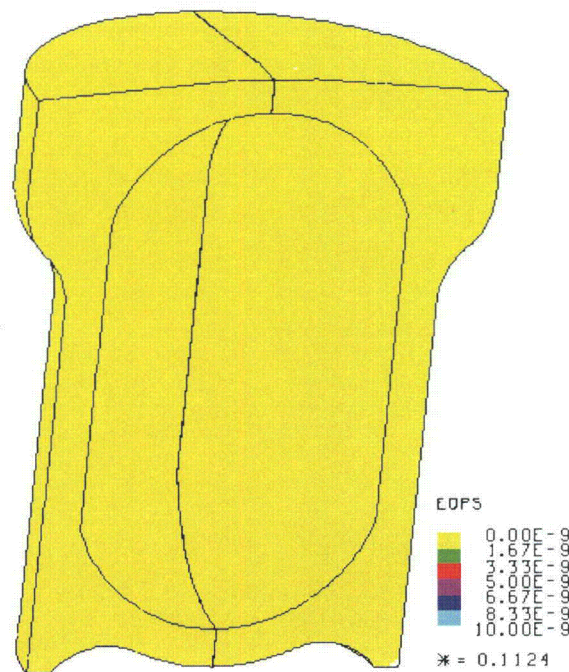


**Figure 2-480. Plot of EQPS in the TB-1 for HAC Run 19, 731 g Angled Plutonium Metal Hollow Cylinder, Side Impact**

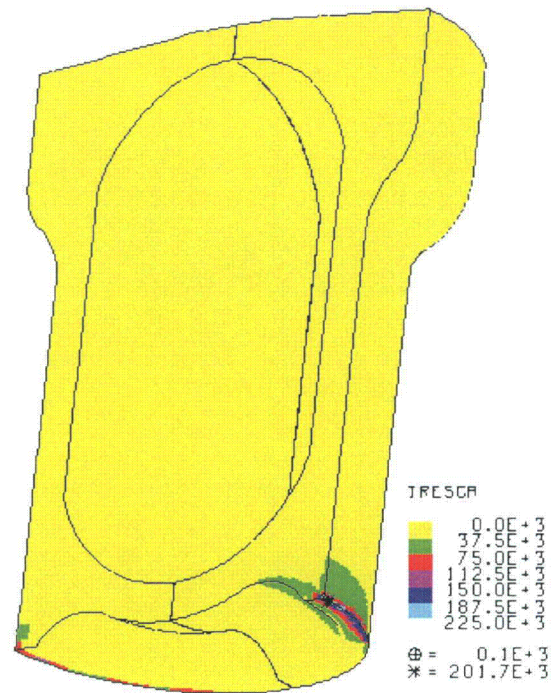


Figure 2-481. Plot of Tresca Stress in the TB-1 for HAC Run 19, 731 g Angled Plutonium Metal Hollow Cylinder, Side Impact

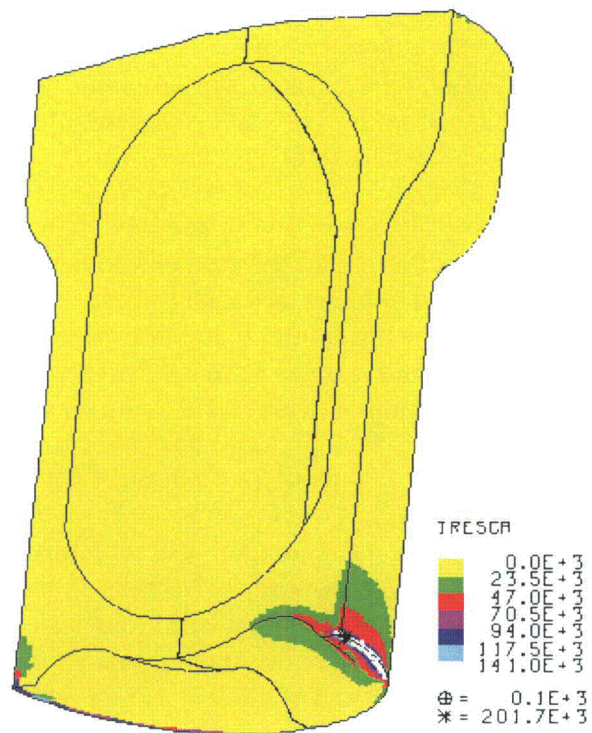
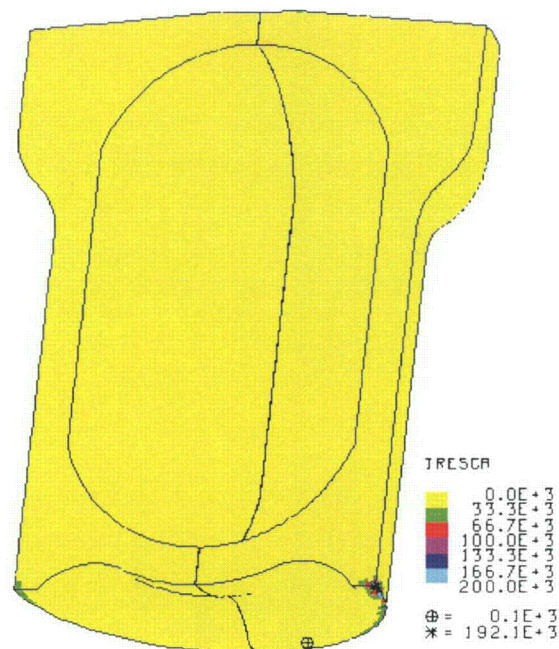


Figure 2-482. Plot of Tresca Stress in the TB-1 for HAC Run 19, 731 g Angled Plutonium Metal Hollow Cylinder, Side Impact



**Figure 2-483. Plot of Tresca Stress in the TB-1 for HAC Run 19, 731 g Angled Plutonium Metal Hollow Cylinder, Side Impact when Plate Velocity Reaches Zero**

*2.12.5.6.20 HAC- Run 20, 731 g Angled Plutonium Metal Hollow Cylinder, CGOC Impact*

The dynamic crush CGOC impact HAC analysis run for the 731 g angled plutonium metal hollow cylinder uses the same overpack model as those used in HAC runs 1 through 19. The finite element mesh and initial position of the model are shown in Figure 2-484. The plutonium metal hollow cylinder within the T-Ampoule is positioned at the bottom of the model because it was considered to be at rest.

The post-impact deformation is shown in Figure 2-485 and its kinetic energy history in Figure 2-486. The flanges on the overpack deform, and the cylinder bounces due to the impact of the plate. The kinetic energy does not drop completely to zero because the plate is still vibrating and internal contents are still in motion. The plutonium metal hollow cylinder has bounced off of the top and bottom surface of the T-Ampoule, and the plate is now rebounding slowly with the package, ensuring that the highest containment vessel and contents loadings have occurred.

There was zero EQPS in the T-Ampoule and nearly zero in the TB-1 (see Figure 2-487), and the maximum Tearing Parameter was 0. Figure 2-488 is a plot of the Tresca stresses within the TB-1. The maximum Tresca stress in the TB-1 is 70.57 ksi, which is below the maximum through thickness allowable stress of 106.6 ksi. Figure 2-489 is a plot of the Tresca stresses at the time when all of the kinetic energy of the plate has been transferred to the package, just as the plate begins to rebound. The maximum through thickness stress at this time is below 16.7 ksi, below the allowable through thickness stress of 106.6 ksi, as seen in the figure.

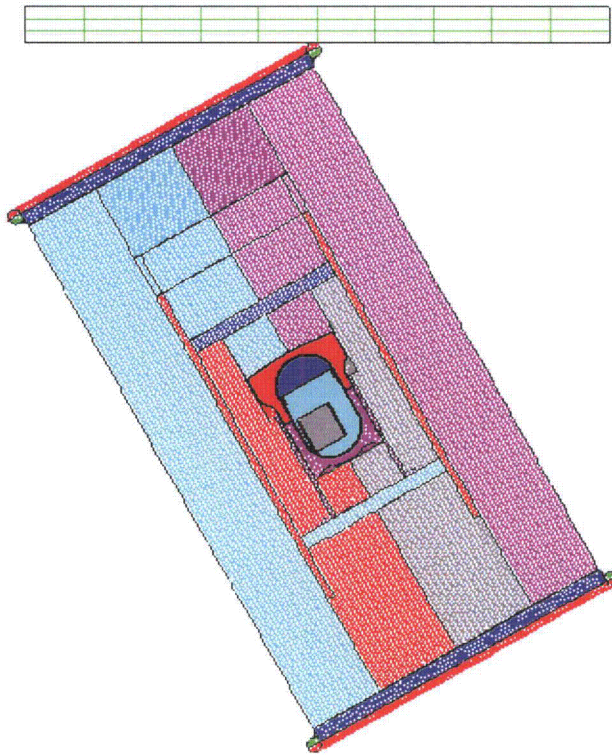


**Figure 2-484. Finite Element Mesh for HAC Run 20, 731 g Angled Plutonium Metal Hollow Cylinder, CGOC Impact**

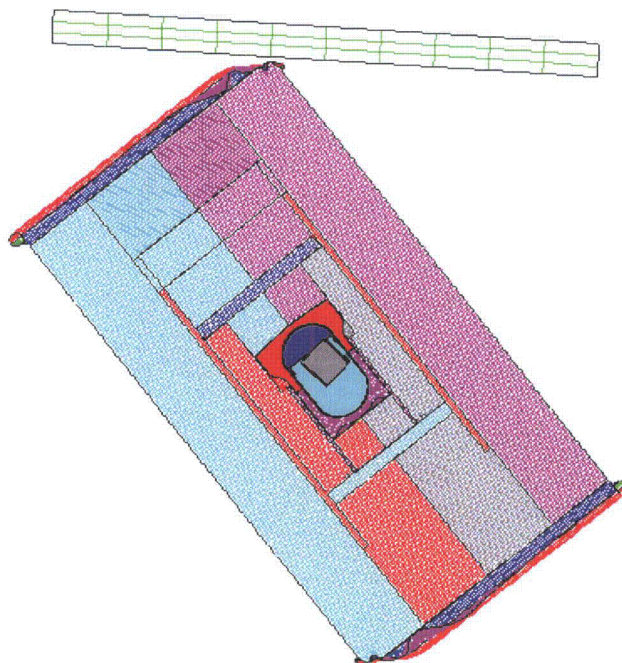


**Figure 2-485. Finite Element Mesh for HAC Run 20, 731 g Angled Plutonium Metal Hollow Cylinder, CGOC Impact – Final Displacement**

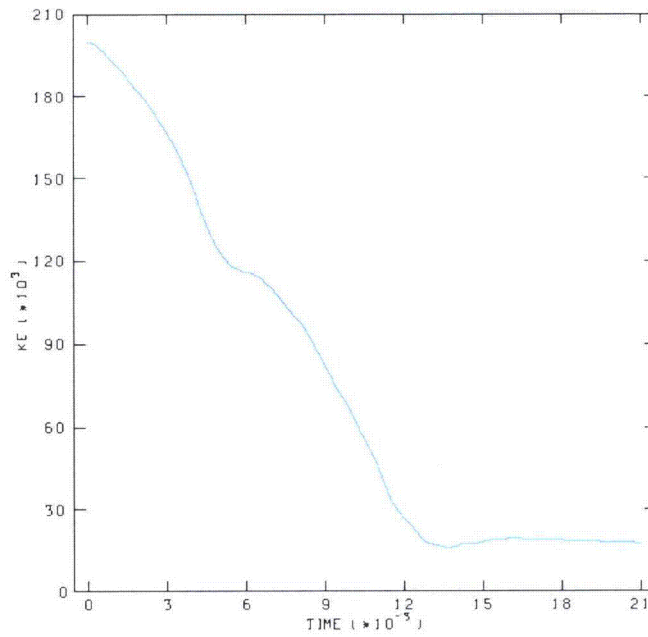


**Figure 2-486. Kinetic Energy Time History for HAC Run 20, 731 g Angled Plutonium Metal Hollow Cylinder, CGOC Impact**

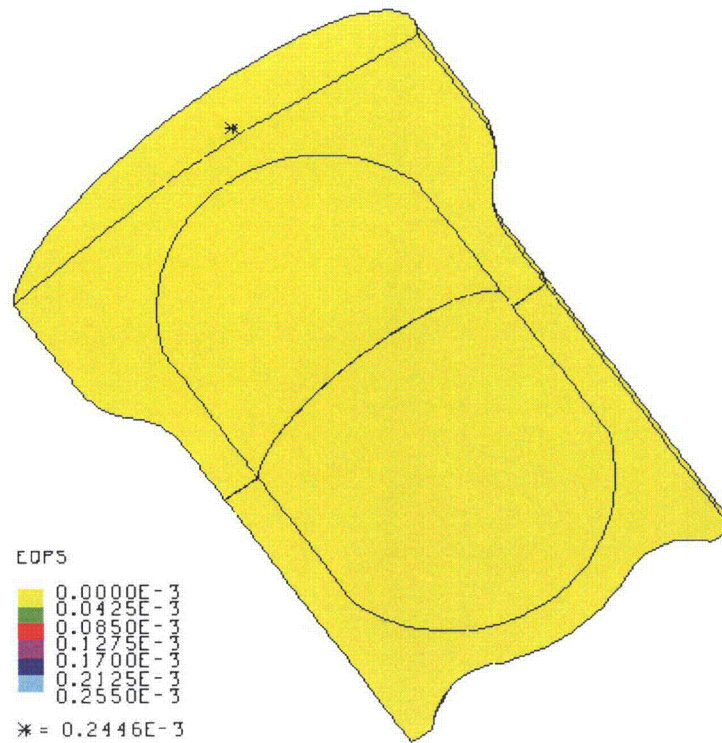


**Figure 2-487. Plot of EQPS in the TB-1 for HAC Run 20, 731 g Angled Plutonium Metal Hollow Cylinder, CGOC Impact**

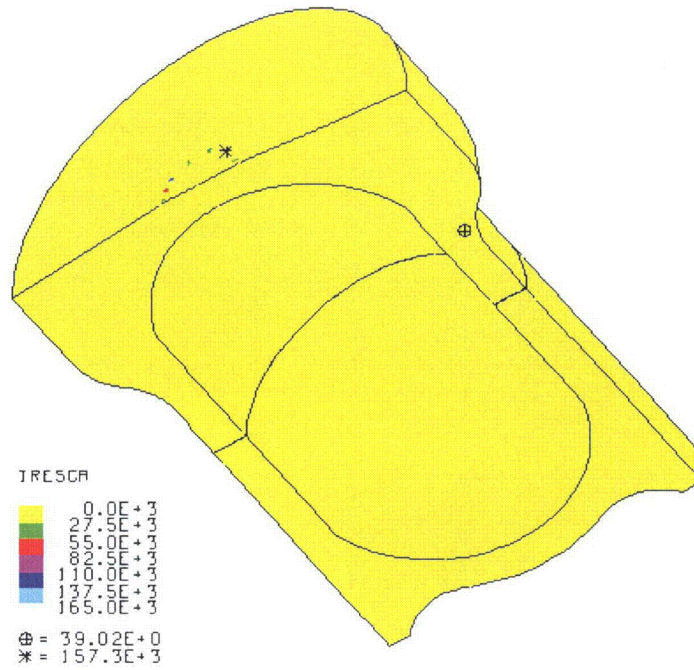


Figure 2-488. Plot of Tresca Stress in the TB-1 for HAC Run 20, 731 g Angled Plutonium Metal Hollow Cylinder, CGOC Impact



Figure 2-489. Plot of Tresca Stress in the TB-1 for HAC Run 20, 731 g Angled Plutonium Metal Hollow Cylinder, CGOC Impact when Plate Velocity Reaches Zero

### 2.12.5.7 30-foot Drop Analyses

Table 2-21 describes the three runs for the 30-foot drop analyses.

**Table 2-21. 30-ft Drop Impact Analyses (3), Components, and Orientations**

Run No.	Component	Submodel Orientation
1	SC-2 - Pu	Far side position, support structure 45°, side impact
2	831 g Plutonium Metal Hollow Cylinder, alpha Pu	Bottom position (angled), top impact
3	831 g Plutonium Metal Hollow Cylinder, alpha Pu	Bottom position (angled), CGOC impact

#### 2.12.5.7.1 SC-2 45 Degree Rotated Support Structure with Side Impact

The two-sample-container 45-degree rotated support structure contents was used for the 30-ft drop with side impact since this case produced the most severe loading of the aircraft side impacts. Pre-impact model geometry shown in Figure 2-490, and the final displacement shown in Figure 2-491. Note that the overall overpack deformation (rolled outer skin end closures, and slight denting of redwood) resulting from the 30-ft side impact analysis (half-symmetric model) compares well with the test result documented in the SAR,<sup>1</sup> shown in Figure 2-492. The kinetic energy history is shown in Figure 2-493 to verify that the analysis ran through the time of rebound. The negligible 0.26% equivalent plastic strain in the T-Ampoule eutectic boundary is shown in Figure 2-494. There were no T-Ampoule elements exceeding the experimental strain locus. Tresca stress in the TB-1 is shown in Figure 2-495, with through-thickness values below even the NCT allowables from Table 2-4.

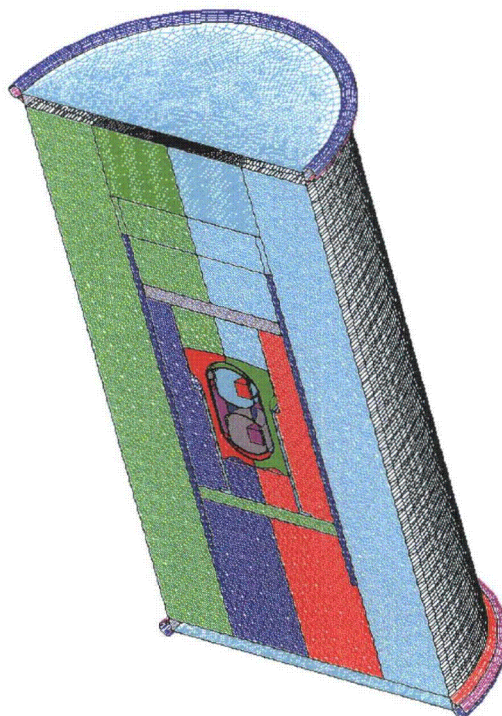


**Figure 2-490. Finite Element Mesh for 30-ft Drop Run 1 – SC-2 with Support Structure Rotated 45 Degrees and Side Impact**

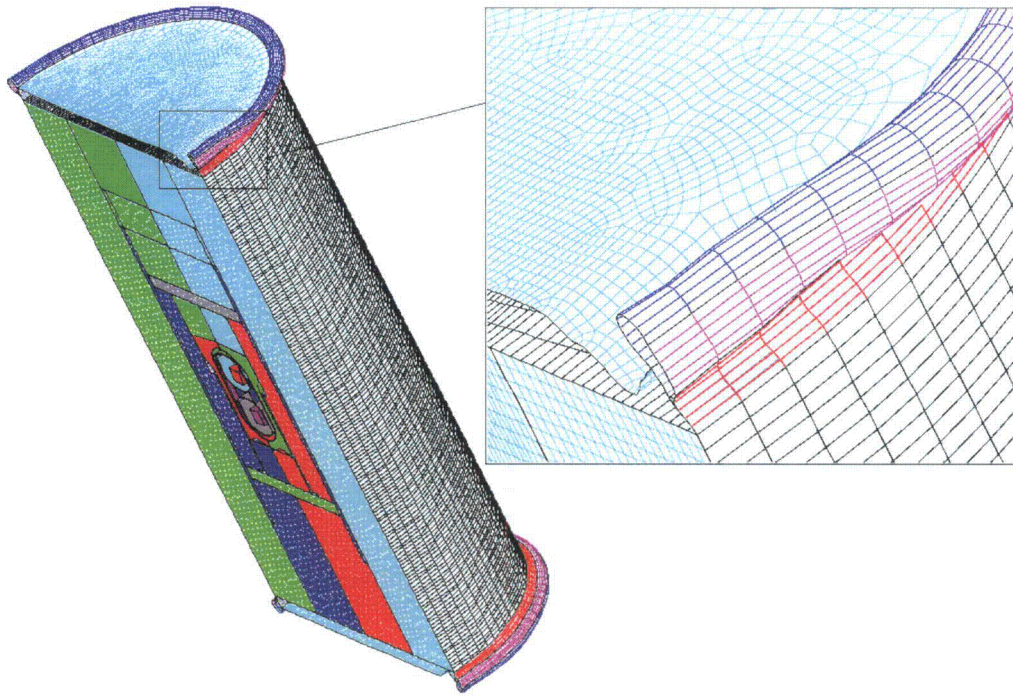


**Figure 2-491. Final Displacement in Finite Element Mesh for 30-ft Drop Run 1 – SC-2 with Support Structure Rotated 45 Degrees and Side Impact**

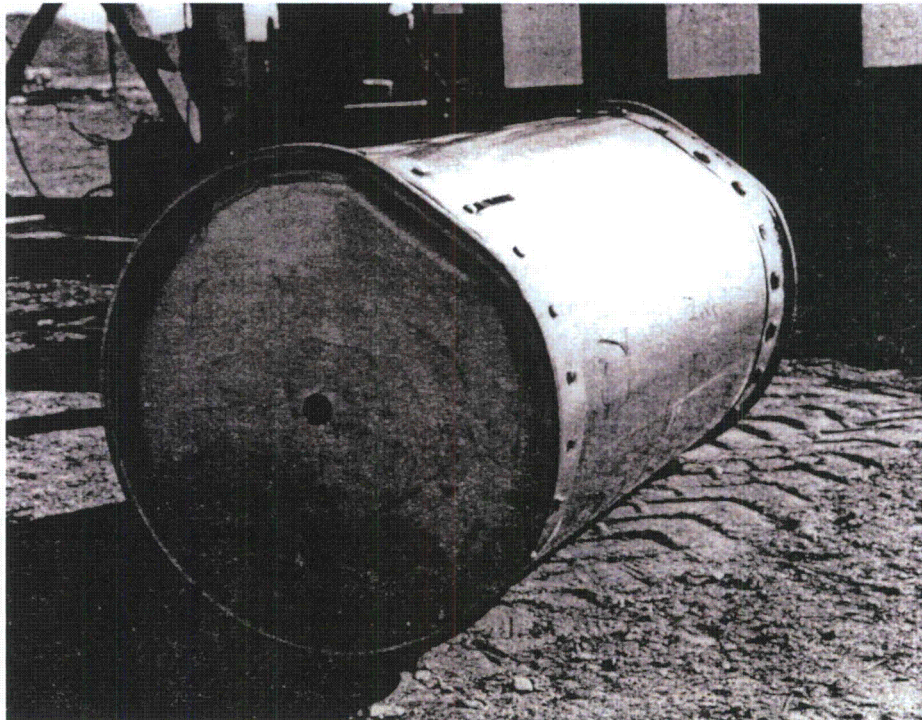


**Figure 2-492. Final Displacement in SAR<sup>1</sup> Test for 30-ft Drop**

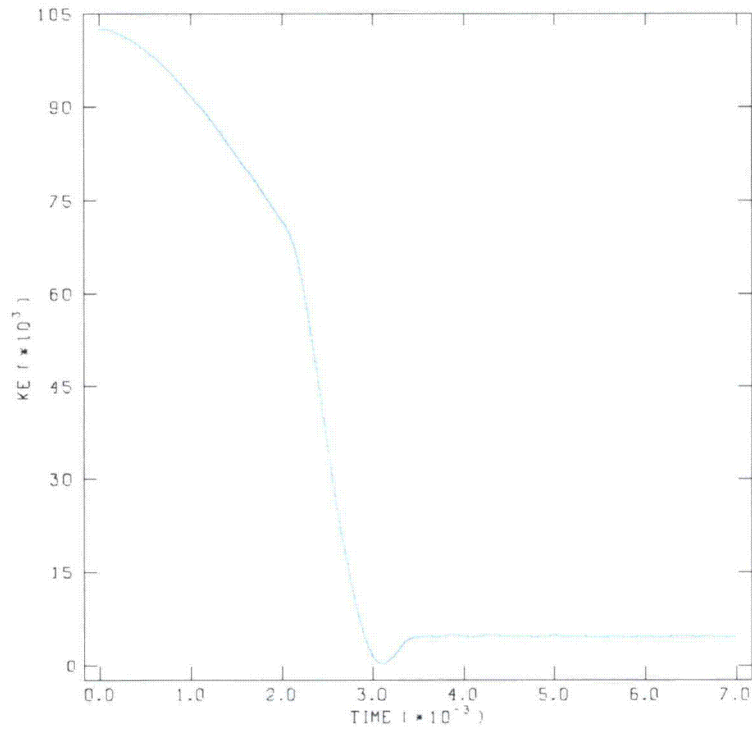


**Figure 2-493. Kinetic Energy for 30-ft Drop Run 1 – SC-2 with Support Structure Rotated 45 Degrees and Side Impact**

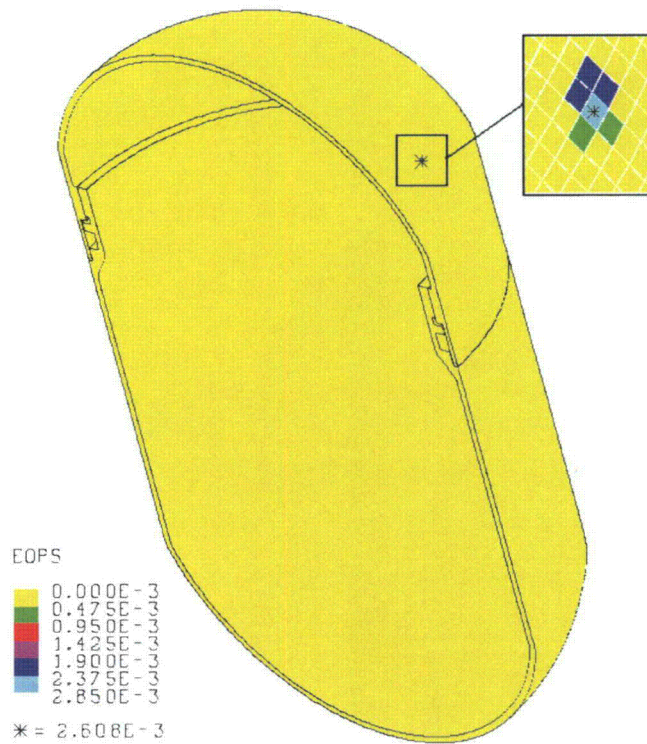


**Figure 2-494. EQPS in the T-Amp for 30-ft Drop Run 1 – SC-2 with Support Structure Rotated 45 Degrees and Side Impact**